UNIVERSIDADE DE LISBOA

FACULDADE DE MEDICINA VETERINÁRIA

FUNCTIONAL CHARACTERIZATION OF UNASSIGNED AFRICAN SWINE FEVER VIRUS PROTEINS PUTATIVELY INVOLVED IN TRANSCRIPTION AND REPLICATION TOWARDS AN EFFICIENT VACCINE DESIGN

Ferdinando Bernardino de Freitas

Orientador(es): Professor Doutor Fernando António da Costa Ferreira

Professor Doutor Carlos Manuel Lopes Vieira Martins

Tese especialmente elaborada para obtenção do grau de Doutor em Ciências Veterinárias na especialidade de Ciências Biológicas e Biomédicas.

2019

UNIVERSIDADE DE LISBOA

FACULDADE DE MEDICINA VETERINÁRIA

FUNCTIONAL CHARACTERIZATION OF UNASSIGNED AFRICAN SWINE FEVER VIRUS PROTEINS PUTATIVELY INVOLVED IN TRANSCRIPTION AND REPLICATION TOWARDS AN EFFICIENT VACCINE DESIGN

Ferdinando Bernardino de Freitas

Orientador(es): Professor Doutor Fernando António da Costa Ferreira

Professor Doutor Carlos Manuel Lopes Vieira Martins

Tese especialmente elaborada para obtenção do grau de Doutor em Ciências Veterinárias na especialidade de Ciências Biológicas e Biomédicas.

Júri:

Presidente: Professor Doutor Luís Filipe Lopes da Costa
Vogais:
- Professor Doutor Luís Manuel Morgado Tavares
- Doutora Yolanda Revilla Novella
- Doutor Robert Michael Evans Parkhouse
- Professor Doutor João Mário Brás da Piedade
- Doutor José Alexandre da Costa Perdigão e Cameira Leitão
- Professor Doutor Fernando António da Costa Ferreira

2019

To my Mother….

ACKNOWLEDGMENTS

This work would not be accomplished without the help of many people. Firstly, I would like to acknowledge my supervisor, Professor Fernando Ferreira for the guidance, critical review and to allow myself to grow as a researcher. I also acknowledge my co-supervisor Professor Carlos Martins for the opportunity to work in the Infectious Disease Laboratory and for his valuable advices and shared expertise in ASFV field.

I would like to thank all the members of Infectious Disease Lab, Gonçalo Frouco, Margarida Simões, João Coelho, Alexandre Leitão, Maria de Jesus Silva, Rui Vieira for their help, friendship and support during my work.

To my friends and colleagues of CIISA, Carla Carneiro, Clara Cartaxeiro, Samuel Francisco, Carla Mottola, Rui Seixas, Inês Delgado, Sara Zúquete, Marta Madeira, Catarina Carvalho, Raquel Portugal, Manuela Oliveira, Solange Gil, Mario Quaresma, Eva Cunha, Cátia Marquês, Ana Rita, Claudia Fernandes, Ana Amaral, Claudia Marquês during these years we had a lot of scientific and non-scientific discussions, fun and good times.

To my former colleagues and supervisors, indeed, without them nothing of this would be possible.

To my friends, Xavier Araújo, Carlos Figueira, Nuno Vieira, Eurico Santos, Gonçalo Castro, Tânia Serrão, Paulo Mota, João Gois, Ricardo Semedo, Marco Rodrigues, Manuel Francisco and Lena for just being here.

To Carolina's parents for their kindness and for offering me a second home.

To my family for their full support, love and education, in particular to my mother Susete, brother Carlos, grandfathers, Nuno and Filomena. "À minha família, pelo apoio incondicional, educação e amor durante todos estes anos, em especial à minha mãe Susete ao meu irmão Carlos e aos meus avós Nuno e Filomena".

A special word of acknowledged to Carolina, for everything we shared, for the help, patience and love during these years.

To my "little" love Filomena, my all day motivation, specially during the writing of this manuscript.

Thank you…

"Alone we go faster, together we go further"

African Proverb, Author unknown

FUNDING

The present work was funded by:

PhD fellowship from FCT, Portugal SFRH/BD/104261/2014.

PTDC/CVT/105630/2008: “Role of African swine fever virus topoisomerase II in viral DNA replication - a possible target for antiviral therapy”. Fundação para a Ciência e a Tecnologia.

European Union Seventh Framework Programme (FP7/2007-2013) under grant agreement n° 311931 – ASFORCE

Project UID/CVT/00276/2013 (CIISA- Center for Interdesciplinary Research in animal Health)

CIISA-2016-06: “Study on the role of African swine fever virus (ASFV) ubiquitin-conjugating e2-like enzyme towards vaccine development against ASF”.

CIISA-2015-04: “New strategies for an efficient vaccine design on African Swine Fever Virus (ASFV) – development of ASFV-A104R-DISC mutants”.

Functional characterization of unassigned African Swine Fever Virus proteins putatively involved in transcription and replication towards an efficient vaccine design

Abstract

African swine fever (ASF) is an infectious disease of domestic pigs and wild boars with mortality rates reaching up to 100% and is endemic in most of the Sub-Saharan countries. In 2007 it was introduced in Georgia and spread to neighbouring countries, reaching the Russian Federation, several European countries and, more recently, China and Vietnam (February 2019). Currently, there is neither a vaccine nor a treatment against ASF and the control of the disease depends strictly on sanitary measures, including stamping out and trade bans of animals and pork products leading to devastating socio-economic losses to affected countries. The etiologic agent of the disease is *African swine fever virus* (ASFV), a large (approx. 190 nm) double-stranded DNA (170 to 193 kbp) enveloped virus. ASFV genome encloses more than 150 open reading frames (ORFs) and to this date most of them lack any known or predictable function. ASFV is quite independent from cellular machinery encoding enzymes required for replication, transcription and virion assembly, including the putative I215L E2 Ubiquitin-conjugating enzyme, QP509L, Q706L RNA Helicases and the P1192R type II topoisomerase. The E2 ubiquitin-conjugating enzymes are part of the essential cellular post-transcriptional regulation ubiquitin-proteasome pathway. In this study, the pI215L binding activity was characterized as being mono and poly-ubiquitinated in the Cys85 at different temperatures and pH values. Moreover, I215L gene is transcribed from 2 hours post infection (hpi), and immunoblot analysis confirmed that pI215L is expressed from 4 hpi being detected all over the cell specially in the viral factories from 8 hpi. Downregulation assays by siRNA suggested that pI215L plays a critical role in the transcription of late viral genes and in viral DNA replication. RNA helicases are described as essential for infections, modulating RNA-RNA and RNA-protein interactions, gene expression, viral egress and host antiviral responses. In the present work, we found that QP509L, Q706L are conserved between ASFV virulent and non-virulent isolates. Furthermore, ASFV-QP509L and Q706L are actively transcribed from 2 hours post infection, and both proteins are localized in the viral factories at 12 hours post infection. However, QP509L was also detected in the cell nucleus. Transcript downregulation uncovered the essential role of these proteins during viral cycle progression, in particular for the late transcription. Type II topoisomerases are involved in resolving DNA tangles and supercoils by cutting the duplex and allowing the DNA replication to proceed. In this study, we report that P1192R is actively transcribed throughout infection, being detected from 2 hpi and reaching a maximum concentration around 16 hpi. P1192R knockdown experiments revealed its critical role for viral infection, given by a reduction in viral transcripts, cytopathic effect, the number of viral factories per cell, and virus yields. We also demonstrated that enrofloxacin exposure during the late phase of infection induces viral genomes fragmentation, whereas, when added at early phase of infection completely abolishes replication. The data obtained from I215L, QP509L. Q706L and P1192R characterization studies opens new venues to the rational design of a mutant virus lacking these genes, and also points new pathways to be targeted by antiviral drugs.

Keywords: African swine fever virus, ASFV, I215L, QP509L, Q706L, P1192R, vaccine, antivirals.

Caracterização funcional de proteínas do vírus da peste suína Africana putativamente envolvidas na transcrição e replicação com o intuito de desenvolvimento de uma vacina.

Resumo

A peste suína africana é uma doença viral infeciosa que afeta os suínos domésticos e os selvagens, com taxas de mortalidade perto dos 100%, originando perdas económicas elevadas nos países afetados. A doença é endémica na maioria dos países subsaarianos, e desde 2007, assistiu-se uma expansão nos países Europeus, incluindo membros da União Europeia, e mais recentemente, na China e Vietname. Atualmente não existe vacina ou tratamento para esta infeção e o controlo da doença baseia-se no diagnóstico rápido, na eliminação compulsiva dos suínos e no bloqueio ao comércio de suínos e produtos derivados. O agente etiológico é o vírus da peste suína africana (VPSA), um vírus composto por uma molécula de ADN de cadeia dupla (170 to 193 kbp) contendo mais de 150 grelhas de leitura. Algumas destas estão devidamente caracterizadas codificando para proteínas estruturais ou regulatórias, contudo, a grande maioria foi identificada por homologia de sequência com outros vírus não se conhecendo, até à data, qual a sua função durante a infeção. Apesar dos inúmeros esforços ao longo dos anos, a complexidade viral, a falta de conhecimento sobre muitos dos aspetos da biologia do vírus e das suas interações com o hospedeiro invalidaram a obtenção de uma vacina segura e eficaz. Por um lado, as abordagens clássicas embora promissoras não garantem proteção contra estirpes heterólogas, enquanto a produção de vacinas de ADN ou proteína, mesmo com adjuvantes, não induzem imunidade contra uma segunda infeção. No entanto, a identificação de suínos previamente infetados e que resistem a novas infeções reforça a ideia da possibilidade de se obter uma imunidade protetora. Dadas as circunstâncias atuais de expansão da doença, estudos recentes apontam a necessidade de se aprofundar o conhecimento sobre os aspetos da biologia do VPSA com vista a identificação de novas estratégias para o desenvolvimento racional de vacinas ou de identificação de novos alvos para o uso de fármacos com vista a controlar a infeção. Neste contexto, os estudos apresentados neste trabalho caracterizam a I215L, QP509L, Q706L e P1192R, identificadas inicialmente, por homologia de sequência com outras proteínas tipicamente envolvidas na replicação e transcrição de outros vírus. A I215L foi identificada por partilhar identidade com as enzimas E2 de conjugação da ubiquitina. Estas enzimas pertencem a uma cadeia de sinalização do sistema de regulação pós-transcricional ubiquitina-proteossoma. Os estudos realizados revelaram que a pI215L tem a capacidade de receber uma ou duas ubiquitinas (mono e di-ubiquitinada) no resíduo Cisteína-85, a diferentes temperaturas e valores de pH, evidenciando a sua plasticidade em participar em diferentes fases da infeção quer no hospedeiro quer no vetor. Além disto, o gene é transcrito precocemente (2 horas após infecção, hpi) e a proteína expressa desde as 4h, sugerindo que esta deverá ser necessária desde o início da infecção. Paralelamente, os nossos estudos por imunofluorescência revelaram uma distribuição da pI215L por toda a célula, e em especial, nas fábricas virais, sugerindo um papel ativo na regulação de vários processos, incluindo replicação de ADN e da transcrição. Os ensaios de ARN de interferência (siRNA) contra o I215L demonstraram um papel essencial desta proteína durante a infeção, originando uma redução dos transcritos tardios, do número de genomas (-63 a -68%) e na libertação de partículas infeciosas (até -94%).

A QP509L e Q706L, identificadas previamente como RNA helicases, estão envolvidas no metabolismo do ADN e do ARN, na replicação, recombinação do ADN, transcrição, síntese ribossomal, processamento e maturação do ARN, entre outros. Os resultados realizados revelaram que as sequências codificantes dos genes QP509L, Q706L apresentam-se conservadas entre os isolados virulentos e não virulentos do VPSA. Além disso, ambos os genes são ativamente transcritos a partir das 2 hpi e as proteínas correspondentes são detetadas nas fábricas virais 12 hpi, no entanto, a pQP509L encontra-se também distribuída pelo núcleo da célula, sugerindo a sua participação em processos distintos durante a infeção. A depleção dos transcritos dos genes QP509L e Q706L, por ARN de interferência, revelou uma redução dos transcritos virais tardios (até -46.2% e -77,7%, respetivamente), do número de cópias de genoma (até -53.4% e -71.4%, respetivamente) e de partículas virais infeciosas (até -99.4 e -98.6%, respetivamente), demostrando o papel crucial destas helicases para a progressão da infeção viral.

Por último, este trabalho contribuiu para a caracterização funcional da pP1192R (topoisomerase do tipo II) durante a infeção. Genericamente estas enzimas estão envolvidas na resolução de constrangimentos e enrolamentos do ADN, sendo responsáveis pelo rearranjo estrutural da molécula através do corte e religação da cadeia dupla de ADN. Neste estudo, verificou-se que o gene viral P1192R é ativamente transcrito ao longo da infeção, sendo detetado a partir de 2 hpi e atingindo um ponto máximo de acumulação pelas 16 hpi. A depleção do transcrito durante a infeção revelou o papel indispensável desta enzima, originando uma redução do efeito citopático (-66%), diminuição dos transcritos virais (-89%), do número de fábricas e da progenia viral (até -99.7%, 2.5 log). Além disto, os nossos estudos clarificaram o mecanismo de ação das fluoroquinolonas contra a pP1192R. Os resultados obtidos mostram que as células infetadas e expostas a enrofloxacina numa fase final do ciclo de infeção (15-16 hpi) apresentavam uma fragmentação dos genomas virais. Por outro lado, quando a exposição foi efetuada desde o início da infeção (2-16 hpi), observou-se um bloqueio total da replicação.

Em suma, os dados obtidos nos estudos aqui apresentados para o I215L, QP509L, Q706L e P1192R abrem novas perspetivas para o desenvolvimento racional de vacinas tendo por base vírus mutantes. Adicionalmente, levantam a possibilidade de recorrer a ferramentas farmacológicas visando diretamente estas proteínas, ou os processos em que estas estão envolvidas, permitindo o eventual bloqueio da infeção viral.

Palavras-Chave: Vírus da peste suína africana, VPSA, I215L, QP509L, Q706L, P1192R, vacina, antivirais.

Table of contents:

ACKNOWLEDGMENTS ..... **II**

FUNDING ..... **III**

ABSTRACT ..... **IV**

RESUMO ..... **V**

CHAPTER I **1**

INTRODUCTION **1**

1. AFRICAN SWINE FEVER **2**

1.1. History and geographic expansion 2
1.2. Hosts and transmission of African swine fever 2
1.3. ASF clinical signs and control strategies 4
1.4. ASF vaccine development 5
1.5. African Swine Fever virus 7
1.5.1. ASFV classification 7
1.5.2. ASFV morphology 7
1.5.3. ASFV genome 8
1.5.4. ASFV infection cycle 9
1.5.4.1. Cell entry and uncoating 9
1.5.4.2 DNA replication 10
1.5.4.3 Temporal regulation of gene expression 11
1.5.4.4 Encapsidation 13
1.5.4.5 Virion egress 13

2. STUDY OF ASFV GENES INVOLVED IN TRANSCRIPTION, REPLICATION AND HOST IMMUNE SYSTEM EVASION, TOWARDS A POTENTIAL VACCINE CANDIDATE OR DRUG TARGET **13**

2.1. ASFV I215L putative E2 ubiquitin-conjugating enzyme 14
2.2. ASFV QP509L and Q706L RNA helicases 16
2.3. ASFV P1192R type II topoisomerase 19

3. OBJECTIVES **22**

CHAPTER II **23**

AFRICAN SWINE FEVER VIRUS ENCODES FOR AN E2-UBIQUITIN CONJUGATING ENZYME THAT IS MONO- AND DI-UBIQUITINATED AND REQUIRED FOR VIRAL REPLICATION CYCLE **23**

1. INTRODUCTION **25**

2. MATERIAL AND METHODS **26**

2.1. Viruses and cells 26
2.2. Cloning, expression and purification of recombinant ASFV-pI215L 26
2.3. In vitro ubiquitination assay 27
2.4. RNA extraction and cDNA synthesis 28
2.5. Recombinant plasmids and standard curves 28
2.6. Quantitative PCR 29
2.7. Antibodies 30
2.8. Immunoblot analysis 31
2.9. Immunofluorescence and microscopy analysis 31
2.10. siRNA assays 31
2.11. Quantification of ASFV genomes by qPCR 32
2.12. Statistical analysis 32

3. RESULTS **33**

3.1. pI215L acts as an E2-ubiquitin conjugating enzyme, binding one or two ubiquitin molecules at the cysteine 85, in an ATP- and Mg^{2+}-dependent manner 33

3.2. ASFV-I215L gene encodes for a very early protein that localizes in viral factories and host cell nucleus ... 36
3.3. Knockdown of pI215L impairs viral infection ... 38

4. DISCUSSION ... 40

CHAPTER III ... 44

THE QP509L AND Q706L SUPERFAMILY II RNA HELICASES OF AFRICAN SWINE FEVER VIRUS ARE REQUIRED FOR VIRAL REPLICATION, HAVING NON-REDUNDANT ACTIVITIES ... 44

1. INTRODUCTION ... 46

2. MATERIAL AND METHODS ... 47

2.1. Phylogenetic analysis ... 47
2.2. Cells and virus ... 47
2.3. RNA extraction and cDNA synthesis ... 48
2.4. Recombinant plasmids ... 48
2.5. Standard curves optimization ... 49
2.6. Quantitative PCR ... 49
2.7. Cloning, expressing and purifying recombinant fragments of ASFV-QP509L and ASFV-Q706L ... 50
2.8. Antibody production ... 51
2.9. Immunofluorescence and microscopy analysis ... 51
2.10. Immunoblot analysis ... 52
2.11. siRNA assays ... 53
2.12. Statistical analysis ... 53

3. RESULTS ... 54

3.1. The ASFV DEAD-box RNA helicases QP509L and Q706L are conserved among virulent and non-virulent isolates, uncovering genotype clustering and showing partial homology with RNA helicases of other NCLDV ... 54
3.2. QP509L and Q706 ASFV genes are transcribed during infection, encoding for two intermediate-late proteins with distinct localization ... 56
3.3. QP509L and Q706L ASFV RNA helicases are required for viral infection showing non-redundant functions ... 57

3. DISCUSSION ... 60

CHAPTER IV ... 64

IN VITRO INHIBITION OF AFRICAN SWINE FEVER VIRUS-TOPOISOMERASE II DISRUPTS VIRAL REPLICATION ... 64

1. INTRODUCTION ... 67

2. MATERIAL AND METHODS ... 69

2.1. Cells and viruses ... 69
2.2. Cytopathic effect (CPE) evaluation ... 69
2.3. RNA extraction and cDNA synthesis ... 69
2.4. Recombinant plasmids ... 70
2.5. Standard curves optimization ... 70
2.6. Quantitative PCR ... 70
2.7. Quantification of ASFV-Topo II, VP32, VP72 mRNA levels ... 71
2.8. siRNA assays ... 71
2.9. Immunofluorescence and microscopy analysis ... 72
2.10. Quantification of ASFV-Topo II, VP32 and VP72 transcripts after the siRNA treatments ... 73
2.11. Comet assay ... 73
2.12. Effect of enrofloxacin on ASFV transcription ... 74

3. RESULTS ... 75

3.1. ASFV-topoisomerase II gene is transcribed from the early phase of infection ... 75

3.2. siRNAs targeting ASFV-Topo II impairs viral infection 75
3.3. Enrofloxacin acts as an ASFV-Topo II poison during infection 78

4. DISCUSSION 80

CHAPTER V 82

DISCUSSION, CONCLUSION AND FUTURE PERSPECTIVES 82

1. DISCUSSION 83

1.1. Characterization of ASFV I215L during the infection 83
1.2. ASFV QP509L and Q706L; phylogenetic analysis and activity characterization during the infection 84
1.3. ASFV-ORF P1192R activity characterization studies during infection 86
1.4. Future perspectives 87
1.5. General conclusion 90

REFERENCES 91

List of Figures

Figure 1. African swine fever transmission routes in Europe. 4
Figure 2. Structure and protein composition of ASFV particle. 8
Figure 3. Ubiquitin proteasome system. 15
Figure 4. Superfamily 2 helicases and SF2 ATP-binding motifs. 17
Figure 5. Schematic representation of the characteristic sequence motifs for SF2 Helicases core proteins. 18
Figure 6. Type IIα topoisomerases structure and mechanism. 20
Figure 7. pI215l acts as an E2-ubiquitin conjugating enzyme. 35
Figure 8. ORF I215L encodes an early viral protein that accumulates in viral factories 37
Figure 9. siRNAs targeting I215L disrupt late viral transcription. 38
Figure 10. Knockdown of I215L mRNA levels inhibits ASFV DNA replication andprogeny production. 39
Figure 11. Proposed working model of the role of pI215L during ASFV infection. 42
Figure 12 The ASFV-QP509L and Q706L RNA helicases are highly conserved among virulent and non-virulent isolates, sharing a distinct ancestor. 54
Figure 13. ASFV-QP509L and ASFV-Q706L RNA helicases show a similar genotype cluster segregation to ASFV-B646L, sharing the same monophyletic groups with other SF2 RNA helicases from NCLDV. 55
Figure 14. ASFV-QP509L and ASFV-Q706L are transcribed from early times of infection. 56
Figure 15. ASFV-pQP509L and ASFV-pQ706L are detected at late times of infection, showing distinct distribution patterns. 57
Figure 16. siRNAs targeting ASFV-QP509L and ASFV-Q706L transcripts disrupt late viral transcription. 58
Figure 17. ASFV-QP509L and ASFV-Q706L downregulation disrupts ASFV DNA replication and progeny production. 59
Figure 18. Proposed working model for ASFV-QP509L and ASFV-Q706L RNA helicases. 62
Figure 19. ASFV-Topo II is a late gene. 75
Figure 20. siRNAs against ASFV-Topo II inhibit ASFV replication. 76
Figure 21. siRNAs anti-ASFV-Topo II inhibit the viral protein synthesis and the formation of viral factories sites. 77
Figure 22. ASFV-Topo II siRNAs disrupt viral transcription. 78
Figure 23. Enrofloxacin induces viral DNA breaks, thus acting as an ASFV-topoisomerase poison. 79
Figure 24. Enrofloxacin disrupts ASFV transcription activity. 79
Figure 25. Schematic diagram representing the generation recombinant ASF viruses expressing GUS reporter gene. 88
Figure 26. Isolation of recombinant virus using the plaque method. 89

List of Tables

Table 1. ASFV genes involved in RNA transcription and transcript. 12
Table 2. Primers used in the present study. 30
Table 3. siRNA sequences to knockdown expression I215L. 32
Table 4. Primers used in the present study. 50
Table 5. siRNA sequences to knockdown ASFV-QP509L and ASFV-Q706L transcripts. 53
Table 6. List of used primers. 71
Table 7. siRNA used in this work. 72
Table 8. Primers used to generate the constructs for viral gene deletion. 90

List of abbreviations

Arac	Cytosine Arabinoside
ASF	African swine fever
ASFV	African swine fever virus
ATP	adenosine triphosphate
AVG ± S.E.	average ± standard error
Bp	Base-pair
BSA	bovine serum albumin
Ca	Capsid
cDNA	complementary DNA
CPE	Cytopathic effect
cs	Core shell
Ct	Threshold cycle
DAPI	4′,6-diamidino-2-phenylindole
DISC	Disabled infectious single cycle
DMEM	Dulbecco's modified Eagle's medium
DNA	deoxyribonucleic acid
dsDNA	double-stranded DNA
DTT	Dithiothreitol
DUBs	deubiquitylating enzymes
ECACC	European Collection of Authenticated Cell Culture
EDTA	ethylenediaminetetraacetic acid
EGTA	ethylene glycol tetraacetic acid
FBS	fetal bovine serum
FITC	fluorescein isothicyanate
GAPDH	Glyceraldehyde 3-phosphate dehydrogenase
Gus	β-glucuronidase
HCV	Hepatitis C virus
HEPES	4-(2-hydroxyethyl)-1-piperazineethanesulfonic acid
hpi	hour(s) post infection
HRP	Horseradish peroxidase

HSV	Herpes simplex virus (só usa por extenso não usa abreviatura)
Ie	Inner envelope
IPP	inorganic pyrophosphatase solution
IPTG	isopropyl-β-D-1-thiogalactopyranoside
kbp	kilo base-pair
kDa	Kilo Dalton
miRNA	micro RNA
MOI	Multiplicity of infection
Mono-Ub	Monoubiquitylation
mRNA	messenger RNA
Multi-Ub	multiple monoubiquitylation
NCLDV	nucleo-cytoplasmic large DNA virus
nt	nucleotides
OD	optical density
Oe	Outer envelop
OIE	Office International des Épizooties - World Animal Health Organization
ORF	Open reading frame
PBS	Phosphate-buffered saline
PBST	Phosphate-buffered saline supplemented with Tween-20
PCR	Polymerase chain reaction
PIPES	piperazine-N,N′-bis 2-ethanesulfonic acid
PMSF	phenylmethylsulphonyl fluoride
poly-Ub	polyubiquitylation
qPCR	quantitative PCR
RNA	ribonucleic acid
ROS	Reactive oxygen species
rpm	rotations per minute
RT	Room temperature
SDS	Sodium dodecylsulphate
SDS-PAGE	Sodium dodecylsulphate-polyacrylamide gel electrophoresis
SE	Standard error
SF2	Superfamily 2

siRNA	Small interfering RNA
Topo	Topoisomerase
Tx	Triton X-100
UBA	Ubiquitin-activating
v/v	volume per volume
w/v	weight per volume
wt	wild-type
X-Gluc	5-bromo-4-chloro-3-indolyl-beta-D-glucuronic acid

CHAPTER I

INTRODUCTION

1. African Swine Fever

1.1. History and geographic expansion

African swine fever (ASF) is considered a highly threatening disease for pig husbandry and was firstly described in Kenya (Montgomery, 1921). The etiologic agent is the African swine fever virus (ASFV), against which there is neither an effective vaccine nor a treatment and whose control relays, exclusively, on strict sanitary measures (Costard, Mur, Lubroth, Sánchez-Vizcaíno, & Pfeiffer, 2013). The disease is historically endemic in most of the sub-Saharan countries, having reached Europe through Portugal in 1957 via contaminated waste from airline flights, which was used to feed pigs nearby the Lisbon airport. This first outbreak was successfully controlled and eradicated in the following years. However, a second introduction was reported in 1960 (Manso Ribeiro & Azevedo, 1961) spreading to neighbouring countries and throughout Europe (France, Italy, Malta, Belgium and the Netherlands). Infection crossed the Atlantic Ocean reaching Cuba (1971 and 1980), Dominican Republic Brazil (1978) and Haiti (1979). Fortunately, the disease was eradicated from almost all of the above-mentioned countries, remaining endemic in the Italian island of Sardinia, since 1978 (Costard et al., 2009, 2013; Sánchez-Vizcaíno et al., 2012). More recently, in 2007, the disease was reported in Georgia (Sánchez-Vizcaíno et al., 2012) and quickly spread to the Transcaucasian countries and to the Russian Federation (Costard et al., 2013; Gogin, Gerasimov, Malogolovkin, & Kolbasov, 2013). ASF dramatic expansion continued to Ukraine (2012), Belarus (2013) (Gallardo et al., 2015) and reached the EU through Lithuania (2014). Further outbreaks were reported in Poland, Latvia, Estonia, Czech Republic, Moldova and Romania (Gallardo et al., 2015) and during the latest months of 2018 in Belgium and China and during more recently to Vietnam and Cambodia (WAHID. 2019).

1.2. Hosts and transmission of African swine fever

African swine fever virus infects all members of the family Suidae and soft ticks (genus *Ornithodoros*). ASFV is transmitted by direct contact among pigs, pig meat and other contaminated materials (e.g. blood secretions, excretions, faeces, urine or saliva) or by tick bite (Penrith & Vosloo, 2009). In susceptible pigs, ASFV enters the body via the tonsils or pharyngeal mucosa, heading to the mandibular or retropharyngeal lymph nodes, from where the virus spreads through viraemia (Sánchez-Vizcaíno et al., 2009). In Africa, the warthog (*Phacochoerus africanus*), the bushpigs (*Potamochoerus larvatus*), the red river hogs (*Potamochoerus porcus*) and the giant forest hogs (*Hylochoerus meinertzhageni*) are known as asymptomatic carriers of the virus. In contrast, in domestic pigs the acute form of the disease is characterized by massive apoptosis of lymphocytes and haemorrhage with disseminated intravascular coagulation leading to death in few days (Blome, Gabriel, & Beer,

2013; Oura, Powell, Anderson, & Parkhouse, 1998). The extent of lymphocyte apoptosis is correlated with the level of ASFV replication and with the virulence of the isolate (Galindo-Cardiel et al., 2013; Portugal, Leitão, & Martins, 2009). In Africa, the warthog is considered the original vertebrate host of ASFV and the most important reservoir of disease, being involved in the sylvatic cycle of transmission with soft ticks of the genus *Ornithodoros*. Although the low viremia in adult animals seems to be unable to infect ticks, the high viremia presented by young animals, bitten in the burrows by naive ticks, are an important vehicle of dissemination (Thomson, 1985). The role of the remaining groups in transmission remains unclear due to low population density, geographic distribution and degree of isolation from susceptible domestic pigs and also distinct ecology since they have nocturnal habits and do not use burrows, reducing the potential contact with soft ticks (Jori & Bastos, 2009). The role of *Ornithodoros moubata* in ASFV transmission, in domestic and wild pigs, is very well documented in Southern regions of Africa and Madagascar, but it is almost absent in Central and West Africa (Costard et al., 2013; Jori & Bastos, 2009). Nevertheless, other species of ticks may be involved in ASF transmission, since they have been confirmed in laboratory conditions to be susceptible to ASFV infection (*O. coriaceus, O. turicata, O. parkeri, O. puertoricensis* from North America and Caribbean; *O. savignyi* from North Africa; and *O. sonrai* from West Africa) as previously reviewed (Vial et al., 2007). ASFV can persist in ticks for long periods of time, being important for the maintenance of ASF despite the absence of the natural host (pigs).

In Europe, a similar scenario was observed with *O. erraticus* showing an important role in ASFV persistence and recurrence of the disease across the Iberian Peninsula (Boinas, Wilson, Hutchings, Martins, & Dixon, 2011; Louza, Boinas, Caiado, Vigario, & Hess, 1989; Wilkinson, 1984). Although ticks seemed to play an important role in the previous epidemic of ASFV in Europe, their contribution for the current spread of the disease in the Caucasus, Russia and Eastern Europe is unlikely (Guinat et al., 2016; Jori & Bastos, 2009). Nowadays, the main dissemination routes in Europe include the transmission from infected wild boars to non-infected domestic pigs and direct contact between infected and naive domestic pigs, together with intense movement and/or trade of pigs and the lack of biosecurity measures (e.g. contaminated clothes and footwear, vehicles, equipment, bedding) (Gabriel et al., 2011; Gallardo et al., 2015). This scenario is also aggravated by the resistance of ASFV to inactivation and its lengthy persistence in pork products (Costard et al., 2013). A schematic representation of ASFV transmission routes, in Europe, is represented in Figure 1.

Figure 1. African swine fever transmission routes in Europe.

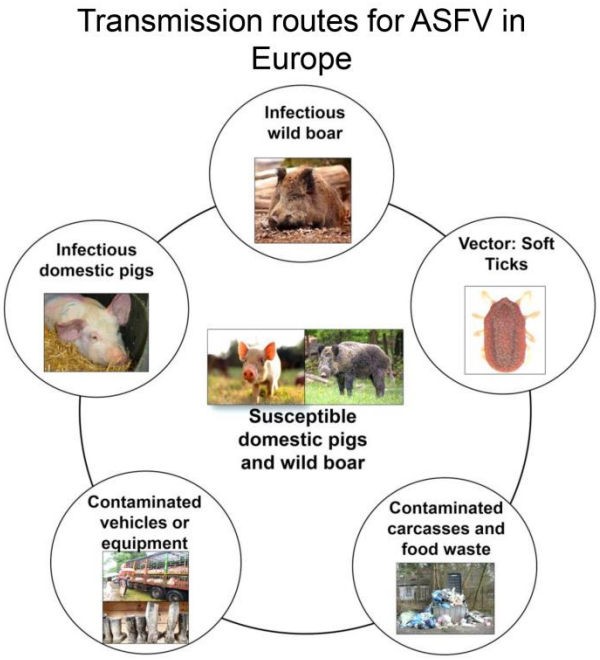

ASF can be transmitted to susceptible domestic and wild boars via direct contact with infected animals, indirectly through the consumption of contaminated pork products and contaminated objects (fomites) such as animal bedding or feed, vehicles, clothes, footwear and equipment. Wild boar contaminated carcasses are also thought to be relevant in transmission, as well as ticks (in particular European regions) as disease vectors.

1.3. ASF clinical signs and control strategies

The clinical and pathological signs of ASF in domestic and wild pigs vary considerably depending on the virulence of the ASFV strain and host factors. The highly virulent strains are usually responsible for more acute forms of the disease, characterized by febrile syndrome with erythema and cyanosis of the skin, multifunctional failure of internal organs, vomiting and haemorrhagic diarrhoea leading to mortality rates up to 100% in 1-9 days post-infection. In subacute forms, the mortality rates decrease from 30 to 70%, with pigs showing a persistent or fluctuating fever that can persist for up to 20 days. In the chronic forms, clinical signs and lesions are not specific, inducing a delayed growth, emaciation, skin ulcers, arthritis and pneumonia that can persist for several months (Blome et al., 2013; Gallardo et al., 2015; Sánchez-Vizcaíno et al., 2015). Despite the research efforts along the last 50 years there is neither a vaccine nor a treatment for the infection (Costard et al., 2009; Penrith & Vosloo, 2009). The control of ASFV relies on rapid laboratory diagnosis and the implementation of strict sanitary measures, such as culling of all infected and susceptible animals, movement restrictions and notification (EFSA Panel, 2014; Wieland, Dhollander, Salman, & Koenen, 2011). Due to ASF complex epidemiology and transmission, together with increasing global

travelling and the international economic scenario, the World Organisation for Animal Health (OIE) was compelled to classify ASF as an obligatory notifiable disease (Costard et al., 2013; Mur, Martínez-López, & Sánchez-Vizcaíno, 2012; Sánchez-Vizcaíno et al., 2009).

1.4. ASF vaccine development

The recent dissemination to Europe and Asia, the endemic occurrence in Africa and the lack of vaccines or treatments to control African swine fever emphasize the need for the development of a safe and effective vaccine against this major threat for global pig husbandry. The huge efforts on vaccine development are in part supported by the fact that pigs surviving ASFV infection have been reported to resist challenge by parental viruses (Detray, 1957; Malmquist, 1963). However, experiments with inactivated vaccines, such as extracts of infected cells, supernatants of infected pig peripheral blood leukocytes, purified and inactivated ASFV virions and detergent-treated infected alveolar macrophage cell cultures, failed to induce protection (Forman, Wardley, & Wilkinson, 1982; Mebus et al., 1978; Stone & Hess, 1967). More recently, it was shown that some adjuvants do not enhance the protection (Blome, Gabriel, & Beer, 2014). Previous studies showed that pigs became protected from highly virulent isolates after being exposed to natural occurring ASFV isolates (ASFV/NH/P68), and when infected with virus attenuated by passage in tissue culture or by deletion of genes involved in virulence (Boinas, Hutchings, Dixon, & Wilkinson, 2004; Leitão et al., 2001). Protection induced by the non-virulent OURT88/3 isolate seems to be mediated by CD8+ T cells as the depletion of these cells was shown to retract this protection (Oura, Denyer, Takamatsu, & Parkhouse, 2005). Moreover some ASFV neutralization was reported, however, the effect of specific antibodies had not been clearly demonstrated (Onisk et al., 1994).

Although these studies report an effective protection, there are safety issues that preclude the release of attenuated live vaccines. For example, during the first ASFV introduction in Europe, via Portugal (1960) a field isolate was serially passed through primary bone marrow cell cultures and then used to vaccinate about half a million pigs in Portugal. A substantial percentage of these vaccinated pigs developed undesirable post-vaccination reactions, including death. In addition, these vaccination campaigns lead to the generation of a large number of carrier animals, hampering subsequent efforts to eradicate the disease (Manso Ribeiro, 1962; Manso Ribeiro, Nunes Petisca, Lopes Frazao, & Sobral, 1963). Despite this early incident, the current prospect of developing attenuated vaccines has improved due to the progress made in the identification of ASFV genes involved in virulence and immune evasion. Besides this, the availability of complete genome sequences for several ASFV isolates has also contributed for a better understanding of the differences between virulent and non-virulent isolates (Bishop et al., 2015; Chapman, Tcherepanov, Upton, & Dixon, 2008; De Villiers et al.,

2010; Tulman, Delhon, Ku, & Rock, 2009). Further studies identified some of the antigens involved in protective immunity (Takamatsu et al., 2013) and the viral proteins involved in host immune evasion (Correia, Ventura, & Parkhouse, 2013), thus providing a path to the rational construction of attenuated ASFV vaccines. In the last years several studies presented candidates for attenuated live vaccines by deletion of genes linked to virulence (Abrams et al., 2013; Gallardo et al., 2018). However, there are still issues related with cross protection against non-related viruses. On the other hand, several ASF subunit vaccines have been tested and induced a certain degree of protection (Lokhandwala et al., 2016, 2017), but to date none was able to induce sufficient protective immunity in pigs (Argilaguet et al., 2013; Neilan et al., 2004; Rock, 2016). Under this scenario, there is a need to improve previous strategies or to develop new approaches, such as the generation of self-limited replication mutant viruses. ASFV and other related viruses are quite independent of the host cell in terms of replication and transcriptional machineries (Dixon, Chapman, Netherton, & Upton, 2013; Salas & Andrés, 2013) and the deletion of genes involved in these processes may allow the production of an ASFV-disabled infectious single cycle (DISC) virus. These approaches have been developed, with promising results, in other viruses (e.g. human immunodeficiency virus, the herpes simplex virus, bluetongue virus) for which the traditional strategies to produce a vaccine did not succeed (Dudek & Knipe, 2006; Matsuo et al., 2011; Moussa et al., 2015). These mutant viruses are expected to infect the host cells and express most of the early proteins as does the wild type virus. However, replication will be blocked due to the lack of an essential protein, although still triggering an immune response (Dudek & Knipe, 2006). Depending on the deleted gene, one or more functions essential to viral genome replication, viral protein synthesis or to the assembly of viral particles are compromised. This methodology combines safety advantages (when compared with inactivated virus) with the ability to simultaneously allow the expression and the presentation of viral antigens via host MHC class I and II (Morrison & Knipe, 1996).

The deletion of crucial genes and the incapacity to generate infective viral progeny demands the generation of a complementing/helper cell line in order to fully rescue the target gene function and produce these viral particles on a large scale. Therefore, the generation of a vaccine or treatment against ASFV has proved to be very challenging, due to virus complexity, mostly related with host immune response evasion, genotype variability and lack of knowledge on ASFV gene function and immunity (Rock, 2016). Most of the studies agree that a vaccine against ASFV must induce antibody response and cytotoxic activity by T cells. They also highlight the need to deepen the knowledge in ASFV putative genes involved in evasion, replication and transcription in order to identify potential candidates to be deleted and used as mutant vaccines or as drug target (Arias et al., 2017; Arias, Jurado, Gallardo, Fernández-Pinero, & Sánchez-Vizcaíno, 2018).

1.5. African swine fever virus

1.5.1. ASFV classification

African swine fever virus is the only member of the family *Asfarviridae*, genus *Asfivirus* (Dixon et al., 2012), belonging to the nucleocytoplasmic large DNA virus (NCLDV) clade. The phylogenetic analysis of NCLDV group revealed that these viruses share several conserved proteins, including DNA polymerases, DNA helicases and ATPase pumps for DNA packaging, Topoisomerase II, RNA polymerase, that contribute for the autonomy of these viruses from host cells. This clade shares a common ancestor and is constituted by Mimivirus and Mamavirus (*Mimiviridae* family), Marseillevirus and Lausannevirus (*Marseilleviridae* family), some members of the *Ascoviridae* family, *Vaccinia virus* (*Poxviridae* family), Iridoviruses, Phycodnaviruses and *Asfivirus* (Colson et al., 2013; Koonin & Yutin, 2010; Yutin & Koonin, 2012).

1.5.2. ASFV morphology

The African swine fever virus particle has an icosahedral morphology with an average diameter of 200 nm, organized in a complex multi-layered structure composed by capsid, inner envelope, inner core shell and nucleoid (Fig.2). The extracellular virions also contain an external membrane acquired by budding from the cytoplasmic membrane of the infected cell. Although the outer membrane could have an important role in the infection progression, intracellular virions also remain infectious (Andrés, García-Escudero, Viñuela, Salas, & Rodríguez, 2001). The viral capsid is formed by 1892 - 2172 hexagonal capsomers, each with 13 nm in diameter, being mainly constituted by the structural p72, encoded by the gene B646L. The protein pE120R is also present in the capsid, being involved in the transport of viral particles from the viral factory to the plasma membrane (Andrés et al., 2001; Epifano, Krijnse-Locker, Salas, Salas, & Rodríguez, 2006). Besides this, the pB602L is a non-structural protein that acts as a chaperone promoting the correct folding of the capsid (Cobbold, Windsor, & Wileman, 2001; Epifano et al., 2006), whereas pB438L has been proposed to be an integral part of the capsid due to its role for the correct acquisition of the icosahedral structure (Epifano et al., 2006). The inner envelope layer is composed by the p54, p17 and pE248R and is derived from the endoplasmic reticulum (Rodríguez, Nogal, Redrejo-Rodríguez, Bustos, & Salas, 2009; Rodríguez, García-Escudero, Salas, & Andrés, 2004; Rouiller, Brookes, Hyatt, Windsor, & Wileman, 1998; Suárez, Gutiérrez-Berzal, Andrés, Salas, & Rodríguez, 2010) The presence of vp12, a transmembranar protein (Alcamí et al., 1992) both in outer and inner membranes, may be due to its involvement in the pathway that directs proteins to the plasma membrane (Zanetti, Pahuja, Studer, Shim, & Schekman, 2011). The particle core shell is a thick protein layer composed mainly by proteins produced from the proteolytic processing of viral

polyproteins pp220 (vp150, vp37, vp34, vp14), pp62 (vp35 and vp15) and pS273R (Andrés, Alejo, Salas, & Salas, 2002; Andrés et al., 2001). The nucleoid is the last structure to be formed and contains the viral genome and several DNA binding nucleoproteins such as the DNA-binding protein p10 and the histone-like protein pA104R (Borca et al., 1996; Munoz, Freije, Salas, Vinuela, & Lopez-Otin, 1993) This structure also comprises the transcriptional machinery for the synthesis and modification of early RNAs (Salas & Andrés, 2013).

Figure 2. Structure and protein composition of ASFV particle.

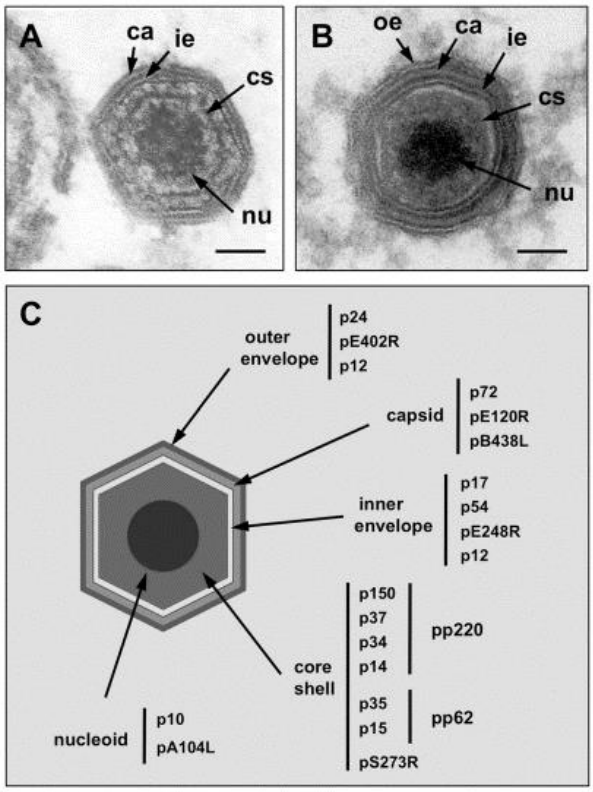

ASFV particle: (A) Electron micrograph of an intracellular full ASFV particle. (B) Electron micrograph of an extracellular mature ASF virion. (C) Schematic representation of the localization of ASFV structural proteins. Outer envelope (oe), capsid (ca), inner envelope (ie), core shell (cs) and nucleoid (nu). Figure and legend were adapted from Salas and Andrés (2013).

1.5.3. ASFV genome

The ASFV genome consists of a linear double-stranded DNA molecule flanked by inverted terminal repeats and closed by hairpin loops, with a length ranging between 170 and 193 kbp, depending of the isolate (Chapman et al., 2008; Dixon et al., 2013; Yáñez et al., 1995). ASFV genome encloses more than 150 open reading frames (ORFs) and most of them lack any known or predictable function (Chapman et al., 2008; Yáñez et al., 1995). These ORFs are closely spaced and are found on both DNA strands, comprising several genes involved in nucleotide metabolism, transcription, replication, repair, immune evasion and modulation of host cell apoptosis (Dixon et al., 2013). In the upstream region of each gene, a short

sequence rich in A/T content acts as a promotor being recognised by the viral RNA polymerase complex and by the transcription factors conducting to distinct temporal phases (early, intermediate and late) of viral gene expression (Dixon et al., 2013).

1.5.4. ASFV infection cycle

1.5.4.1. Cell entry and uncoating

ASFV infects preferentially cells of the mononuclear–phagocytic system, including macrophages and monocytes. Like many other viruses, ASFV enters the cell by endocytosis, in order to overcome the physical barrier of the cytoplasmic membrane. In the last years, different hypotheses have been proposed for viral entry in the host cell including phagocytosis (Basta, Gerber, Schaub, Summerfield, & McCullough, 2010), macropinocytosis (Sánchez et al., 2012), micropinocytosis and receptor-mediated endocytosis (Alcamí, Carrascosa, & Viñuela, 1989; Galindo et al., 2015; Hernaez & Alonso, 2010). This event was recently reviewed and based on several studies it was reported that ASFV is internalized via two distinct endocytic pathways: macropinocytosis and clathrin-mediated endocytosis in a temperature, energy and pH-depended manner (Sánchez, Pérez-Núñez, & Revilla, 2017). Several viral proteins are important for viral attachment and internalization such as p30, p12 and p54 (Angulo, Viñuela, & Alcamí, 1993; Gómez-Puertas et al., 1998). However, CD163, whose expression is restricted to cells of the monocyte/macrophage lineage, is postulated as the main receptor to virus binding (Sánchez-Torres et al., 2003). After internalization, ASFV particle traffics throughout the entire endolysosomal system and depends of late endosomal maturation by a process of acidification allowing the capsid disassembly from 35 to 45min post infection (Alonso et al., 2013; Cuesta-Geijo et al., 2012). Afterwards, the inner membrane becomes exposed and fused with the endosomal membrane, allowing the viral core egress into the cytosol to promote the replication (Hernáez, Guerra, Salas, & Andrés, 2016). Finally, the virion is transported to perinuclear relying on the host microtube motor of dynein with interaction with p54 (Alonso et al., 2013), enabling the start of replication. Recent studies showed that ubiquitin–proteasome system is involved in final degradation of the viral cores, enabling the release of the viral DNA in order to start replication and transcription (Barrado-Gil, Galindo, Martínez-Alonso, Viedma, & Alonso, 2017). However, pathways and proteins involved in this mechanism are still unknown.

1.5.4.2 DNA replication

During the initial phase of DNA replication, in the nucleus, short viral DNA fragments are synthesized in the proximity of the nuclear membrane and then exported to the cytoplasmic space (García-Beato, Salas, Viñuela, & Salas, 1992). It was also shown that ASFV requires intact nuclei for early DNA replication (Dixon et al., 2013; García-Beato, Salas, et al., 1992; Ortin & Viñuela, 1977; Tabares & Sánchez Botija, 1979). Surprisingly, the DNA found in mature viral particles is composed both by nuclear and cytoplasmic fragments (Ortin, Enjuanes, & Vinuela, 1979; Rojo, García-Beato, Viñuela, Salas, & Salas, 1999), highlighting the essential role of nucleus in viral DNA replication. Recently, it was also shown that the early intranuclear replication disrupts nuclear structures and modifies the landscape of the host cell nucleus (Ballester et al., 2011; Simões, Martins, & Ferreira, 2015; Simões, Rino, Pinheiro, Martins, & Ferreira, 2015). Nevertheless, the viral DNA replication is predominantly cytoplasmic, occurring in defined perinuclear factories previously identified (Breese & DeBoer, 1966). One of the initially proposed hypothesis was that cellular topoisomerases could trap the DNA to this perinuclear region (Käs & Laemmli, 1992). Later studies showed that ASFV encodes its own topoisomerase II (ORF P1192R) that might be also involved in this process (García-Beato, et al., 1992). Several aspects of ASFV replication are inferred from poxvirus as both virus share a common ancestor and show several similarities, including their genomic structure, core genes, and the presence of replication intermediates consisting in head to head genome concatemer (Koonin & Yutin, 2010; Yutin & Koonin, 2012). In Vaccinia virus, replication starts with the introduction of a single strand nick in the genome near to one or both termini. From here the exposed 3′-OH group is targeted by the DNA polymerase which initiates the DNA synthesis towards the genome termini. This event generates a self-complementary intermediate resulting in a self-priming hairpin structure. The ASFV genome encodes for a DNA polymerase type B (G1211R) that could be involved in this process, and for a PCNA-like protein (E301R) which may increase the processability of the viral DNA polymerase (Iyer, Balaji, Koonin, & Aravind, 2006; Yáñez et al., 1995). In *Vaccinia virus* another crucial enzyme to initiate this process is the DNA primase (D5), (De Silva, Lewis, Berglund, Koonin, & Moss, 2007), suggesting that its counterpart in ASFV, the putative DNA primase (C962R), may also be important for the initiation of the DNA replication. Other studies showed that large ASFV DNA fragments synthesised in the cytoplasm are chased into mature cross-linked DNA, providing some clues about the dynamics of the viral DNA replication event. It is suggested that mature head to head intermediates concatemers are resolved in single length cross-linked genomes within the viral factories, in order to be packed in the mature virions (Rojo et al., 1999). Some of the ASFV enzymes that may be important to resolve this intermediate concatemers are the viral ERCC4-like nuclease (EP364R), that shares high homology with the cellular Mus81 and the

exonuclease lambda type D345L (Iyer et al., 2006). Replication in macrophages implies a strong DNA repair mechanism adaptation due to the production of reactive oxygen species (ROS) that intend to induce DNA lesions in the microbe genomes. ASFV encodes for three enzymes that may be involved in this process; the DNA polymerase type X (O174L), the adenosine triphosphate (ATP)-dependent-DNA ligase (NP419L) and a class II apurinic/apyrimidinic (AP) endonuclease (E296R) (Dixon et al., 2013). Although the DNA polymerase X is involved in the base excision repair pathway it was suggested that the error prone activity of this polymerase might contribute to increase of mutation frequency, leading to the generation of antigenic variants and thereby facilitating virus survival (Showalter, Byeon, Su, & Tsai, 2001).

1.5.4.3 Temporal regulation of gene expression

Temporal regulation of ASFV gene expression is characterized by a tight control of transcription initiation followed by a fast rate of mRNA degradation. The late promotors are located between −36 and +5 relative to the transcription initiation site expression and point deletion in the TATA box in these promotor regions strongly reduce their activities (García-Escudero & Viñuela, 2000). The early phase is set before the onset of DNA replication and a late phase after the beginning of DNA replication (Rodríguez & Salas, 2013). Early transcription or pre-replicative starts almost immediately after the virus enters the cell and depends on viral factors present in the viral particle (Almazán et al., 1992; Almazán, Rodríguez, Angulo, Viñuela, & Rodriguez, 1993;. Salas, Rey-Campos, Almendral, Talavera, & Viñuela, 1986; Salas, Kuznar, & Viñuela, 1981) and continues until the initiation of DNA replication. Similarly to what is described for poxvirus, after DNA replication step the transcription is divided into two stages: the intermediate transcription, the transcripts are synthesized immediately after DNA replication, and the late transcription, occurring just after the intermediate ones (Broyles, 2003). In terms of gene expression control, the regulatory factors for each phase are expressed in the subsequent stage with the exception of the early factors that are expressed in the late phase of infection and are packaged into the viral particles (Salas & Andrés, 2013). The late transcription starts following the onset of DNA replication in the cytoplasm at about 6h post-infection were a shift in the pattern of virus gene transcription occurs (Salas et al., 1986). More than 20 genes (Table 1) are involved in transcription and in transcript modification and, similarly to *Vaccinia virus,* an accurate temporal control of viral gene expression is required (Rodríguez & Salas, 2013). Although experimental data on the role of the above-mentioned proteins in viral transcription is very limited, studies have identified a viral mRNA capping enzyme (NP868R) with three catalytic activities (triphosphatase, guanyl transferase and methyltransferase) required for

modification of ASFV transcripts by promoting the addition of a 5′ cap and 3′ polyA tail (Pena, Yáñez, Revilla, Viñuela, & Salas, 1993) and a mRNA decapping activity on protein pD250R (Parrish, Hurchalla, Liu, & Moss, 2009). Most of the information regarding proteins function relay only in the degree of homology between ASFV and other members of the NCLDV clade (Table 1) (Koonin & Yutin, 2010; Rodríguez & Salas, 2013). Among these genes, ASFV encodes six putative members of helicase superfamily II (A859L, F105L, B92L, D1133L, QP509L, Q706L) (Dixon et al., 2013). Furthermore, putative polyadenylation enzyme (C475L) has been also identified by comparison with *Vaccinia virus* (Iyer et al., 2006), and a recent study showed that a *Vaccinia virus* core polyadenylation enzyme also adenylates the 3′ end of micro RNAs (miRNA) resulting in their destabilisation (Backes et al., 2012). However, it remains to be determined if the ASFV counterpart has a similar function.

Table 1. ASFV genes involved in replication, transcription and transcript modification.

Similarity/activity	ASFV gene
RPB1	NP1450L
RPB2	EP1242L
RPB3	H359L
RPB5	D205R
RPB6	C147L
RPB7	D339L
RPB10	CP80R
TFIIB	C315R
TFIIS	I243L
D6/D11-like	D1133L/Q706L
A7-like	G1340L
I8-like	B962L
A1-like	B175L
A2-like	B385R
A18-like	QP509L/A859L
Poly(A) polymerase	C475L
Capping enzyme	NP868R
mRNA decapping enzyme	D250R
DNA topoisomerase II	P1192R
RNA ligase	M448R

ASFV genes involved in replication and transcription (right) in comparison with other member of the Nucleocytoplasmic Large DNA Virus or with experimental data available (left). Table and legend were adapted from Rodríguez and Salas (2013).

1.5.4.4 Encapsidation

The mechanisms for genome encapsidation have not been elucidated for ASFV. Data from electron microscopy suggest that viral genome begins to condense into a pronucleoid and then inserted, at a single vertex, into an “empty” particle. The maturation of the viral particle starts with closure of the narrow opening in the icosahedron and gives rise to “intermediate” particles, where the nucleoprotein core undergoes additional consolidation to produce the characteristic mature or “full” virions (Brookes, Hyatt, Wise, & Parkhouse, 1998;. Salas & Andrés, 2013). Repressing expression for the gene encoding the pp220 polyprotein, which encodes the major components of the virus core shell, results in formation and egress of empty virus particles (Andrés et al., 2002).

1.5.4.5 Virion egress

The mature viral particles assembled in the viral factories are transported along microtubules to the cell surface, depending on the kinesin family of motor proteins and on the capsid protein ASFV-pE120R (Andrés et al., 2001; Jouvenet, Monaghan, Way, & Wileman, 2004). ASFV particles are released by budding giving rise to extracellular enveloped virions (Breese & DeBoer, 1966). Although both extracellular or intracellular viral particles are infectious, different structural and antigenic features are recognised leading to important changes in the host immune response against ASFV (Andrés et al., 2001; Jouvenet et al., 2006).

2. Study of ASFV genes involved in transcription, replication and host immune system evasion, towards a potential vaccine candidate or drug target

African swine fever virus is currently spreading in Russia, in several European countries and Asia. The infection is characterized by the absence of clear neutralizing immune response, which has so far impaired the development of a conventional vaccine (Sánchez et al., 2017). ASFV genome enclosures more than 150 ORFs, enabling a high degree of independence from the cell and complex viral-host interaction. Facing this uncontrolled global dissemination it is urgent to deep the knowledge in the basic aspects of the virus biology and look for new tools towards an effective protection. Several studies highlighted the need to better characterize the viral proteins involved in canonical mechanisms of DNA replication, gene expression and host immune evasion to search for new potential therapies or candidates to vaccine development (Arias et al., 2017; Galindo & Alonso, 2017). Among others, four viral ORFS have been previously identified by sequence homology as being putatively involved in replication and transcription.

2.1. ASFV I215L putative E2 ubiquitin-conjugating enzyme

The ubiquitin-proteasome system is a major pathway in the cell, regulating a diversity of cellular processes such as transcription, translation, regulation of the immune response, control of cell division (Mosesson et al., 2003), development, endocytosis (Haglund & Dikic, 2005), cellular trafficking (Hoeller et al., 2006) and cell survival control (Hershko & Ciechanover, 1998; Nandi, Tahiliani, Kumar, & Chandu, 2006). This pathway is constituted by three main components: the proteasome holoenzymes, several ubiquitin ligases and a large variety of deubiquitinating enzymes. In the ubiquitination reaction three main steps are recognized: first, the ubiquitin-activating enzyme (E1) that promotes the establishment of a thiol ester bond with the C-terminal Gly of free ubiquitin, becoming active for nucleophilic attack. Then, the pre-activated ubiquitin is transferred to an ubiquitin conjugating enzyme (E2) binding to its catalytic cysteine residue by transesterification. The E2 primary function is to determine which types of polyubiquitin chains are catalysed (Fig.3A). Finally, the ubiquitin is attached, usually by an isopeptide bond, to the target protein by the action of an ubiquitin ligase (E3), which is substract specific (Fig.3B). Ubiquitination is a reversible modification and proteolytic removal of covalently attached ubiquitin is catalysed by deubiquitylating enzymes (DUBs) which play an import role in the regulation of the system (Randow & Lehner, 2009). The ubiquitin molecule is a small (76 amino acids) and highly conserved protein present in almost all eukaryotic cells. The binding of ubiquitin chains signalises the target protein to participate in many regulatory functions, or serves as a signal for proteasome degradation (Fig.3C). On the other hand, Lys 63-linked polyubiquitin chains will trigger the protein to participate in the oxidative response and the regulation of innate immunity signalling pathways (Deng et al., 2000; Silva, Finley, & Vogel, 2015; Weissman, 2001). The eukaryotic genome encodes only two E1 enzymes, about 40 E2 ubiquitine-conjugating enzymes, more than 400 putative E3 ligases and at least 90 DUBs. This multistep signalling cascade reaction ensures the highly specificity of the ubiquitination pathway (Randow & Lehner, 2009).

Figure 3. Ubiquitin proteasome system.

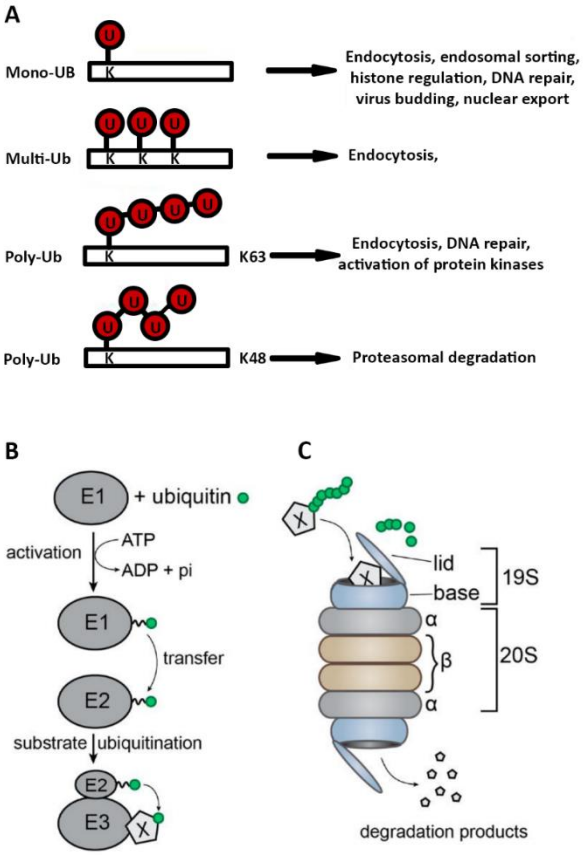

The Ubiquitin proteasome system (A) Schematic representation of Ub modifications and their cellular functions. Monoubiquitylation (mono-Ub), given by the attachment of single Ub molecule to a single Lys (K) residue leads to protein involvement in several process (e.g virus budding, DNA repair). Multiple monoubiquitylation (multi-Ub), is the addition of several single Ub molecules to different Lys residues (e.g. endocytosis, endosomal sorting). Polyubiquitylation (poly-Ub) consists in the attachment of a chain of Ub molecules to one or more Lys residues. When Ub chains are formed via Lys48 (K48) of Ub, target-modified proteins are signalized for proteasomal degradation, whereas when chains are linked via Lys63 (K63) are implicated in DNA repair and activation of protein kinases. Figure and legend were adapted from Haglund and Dikic (2005). (B) Transfer of free ubiquitin from the ubiquitin-activating enzyme E1 to the E2 ubiquitin-conjugating enzyme followed by its transfer onto the target protein X by the substrate specific ubiquitin ligase E3. (C) Schematic representation of protein X degradation in the proteasome, composed of the 20S barrel and two 19S lids. Figure and legend were adapted from Seissler, Marquet, and Paillart (2017).

As obligatory parasites, viruses have evolved to subvert the host ubiquitin-proteasome pathway to overcome the cell innate immune defences (González-Santamaría et al., 2011; Gustin, Moses, Früh, & Douglas, 2011). Nowadays, it is very well documented that viruses modulate the ubiquitin-proteasome system of cells, through different mechanisms, such as encoding ubiquitin-related enzymes (Isaacson & Ploegh, 2009; Randow & Lehner, 2009) or recruiting the endogenous cellular ligases to regulate several aspects of the infection cycle (Randow & Lehner, 2009). Back in the early 90s, a study identified an ASFV protein (UBCv1) showing high homology with E2 ubiquitin-conjugating enzymes (Hingamp, Arnold, Mayer, & Dixon, 1992). This protein was detected in the extracellular viral particle suggesting that the ubiquitin-proteasome pathway could play an important role at early stages of infection

(Hingamp et al., 1995). Corroborating this theory, a recent study demonstrated that the ubiquitin-proteasome pathway is crucial for ASFV replication. The authors found that inhibition of the final stage of the ubiquitin-proteasome pathway leads to a post-internalization step blockage with severe consequences for ASFV genome replication, late gene expression and viral progeny production (Barrado-Gil et al., 2017). ASFV just by coding its own E2´s enzyme reveals that the ubiquitination pathway maybe essential to viral cycle progression like reported for many other virus. Indeed dengue virus make use of the host UBE2J1 (E2 conjugating enzyme) to degrade the transcription factor IRF3, thereby negatively regulating the type one IFN expression and promoting RNA virus infection (Feng et al., 2018). In human cytomegalovirus infection, several E2 ubiquitin-conjugating enzymes regulate US2-mediated immunoreceptor downregulation (Van de Weijer et al., 2017). Thus, further characterization studies on ASFV putative E2 ubiquitin-conjugating could reveal new insights about virus host interactions pointing new pathways to control the infection aiming the development of a vaccine or as target for ubiquitin inhibitors as an potential antiviral approach (Randow & Lehner, 2009).

2.2. ASFV QP509L and Q706L RNA helicases

Approximately 20% of ASFV´s genome contains 20 genes that are considered to be involved in the transcription and modification of its mRNA (Poly (A) polymerase, capping enzyme, mRNA decapping enzyme, topoisomerase II, RNA ligase) (Rodríguez & Salas, 2013). Unfortunately, only a few characterization studies were performed on the functional role of these genes, and most of the information is gathered taking in consideration the role of similar proteins in other virus (e.g. vaccinia virus, orthopoxvirus). Nevertheless, it is known that ASFV gene transcription is quite independent from cellular transcription machinery and does not require the host RNA polymerase II and it is therefore presumed that the virus encodes all the enzymes and factors needed to transcribe and process mRNAs. Besides other critical putative enzymes, ASFV encodes several putative RNA helicases including the QP509L (58.103 kDa) and Q706L (80.376 kDa). *In silico* analysis revealed that QP509L is orthologous to the vaccinia *virus* A18R helicase (Baylis, Twigg, Vydelingum, Dixon, & Smith, 1993; Roberts, Lu, Kutish, & Rock, 1993; Rodríguez & Salas, 2013) and Q706L to the vaccinia virus D6/D11 helicase (Rodríguez & Salas, 2013; Yáñez, Rodríguez, Boursnell, Rodriguez, & Viñuela, 1993). These two vaccinia virus enzymes are involved in transcription, being essential for the elongation, termination and release of the viral transcripts. Based on the high homology between ASFV QP509L/Q706L RNA helicases and vaccinia virus counterparts a similar essential role for these two enzymes can be predicted. ASFV QP509L and Q706L RNA helicases are classified as superfamily 2 (SF2) members, due to the ATP-binding motif (Gorbalenya & Koonin, 1993). Superfamily 2 has been further divided into 10 families including

RecQ-like, RecG-like, Rad3/XPD, Ski2-like, type I restriction enzyme, RIG-I-like, NS3/NPH-II, DEAH/RHA, DEAD-box and Swi/Snf based on their sequence homology (Fig.4A). Both ASFV QP509L and Q706L display DEAH motifs, however some studies joint this family with the DEAD-box family into a large DExH/D family (Jankowsky, 2000; Jankowsky & Bowers, 2006) based on their sequence homology (Fig.4B).

Figure 4. Superfamily 2 helicases and SF2 ATP-binding motifs.

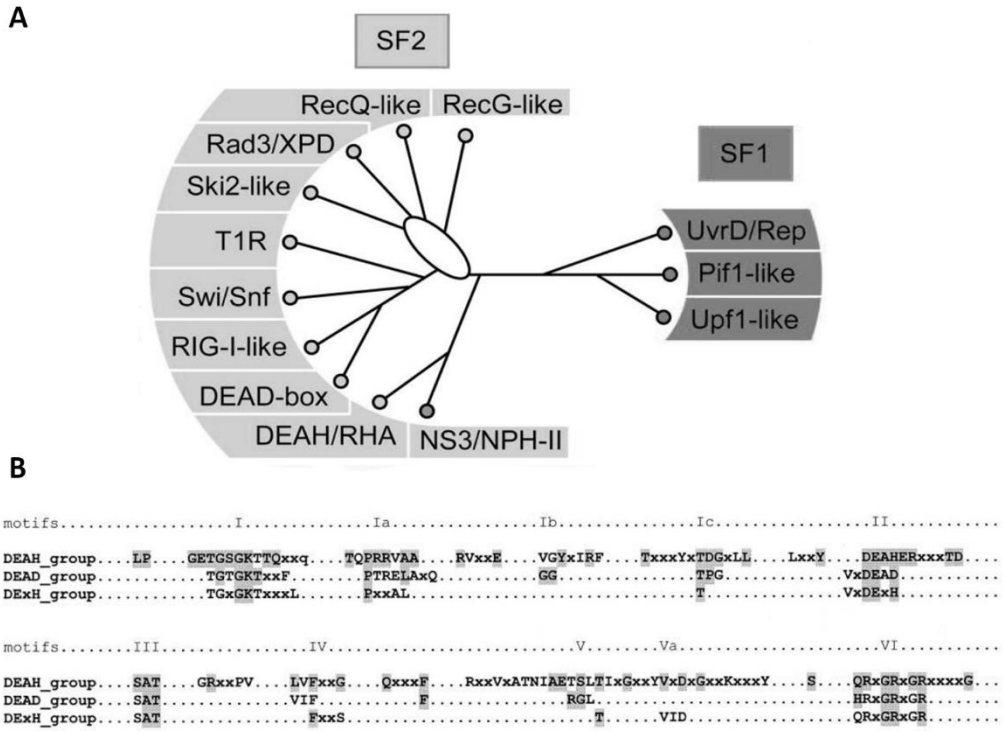

Superfamily 2 helicases and SF2 ATP-binding motifs. (A) Schematic cladogram showing SF2 families (left) vs the three families of the SF1 (right). Family clusters were identified by a combination of phylogenetic analysis of the alignment of all SF1 and SF2 proteins from human, *S. cerevisiae*, *E. coli*, and selected viruses. Branch lengths are not in scale. Figure and legend were adapted from Fairman-Williams, Guenther, and Jankowsky (2010). (B) Sequence motifs of DEAH, DEAD and DExH proteins. Within each group, identical amino acids are represented in gray blocks, conservative substitutions are shown in regular letters, and x represents variable residues. The points separating the conserved motifs do not reflect the exact spacing between the motifs, however, aligned amino acids from the different groups have comparable distance. Figure and legend were adapted from Jankowsky (2000).

The central region of these helicases are formed by the two RecA-like domains, harboring conserved motifs which are crucial for these NTPase-dependent RNA helicases to achieve their function. The I, II, V and VI motifs are necessary for nucleoside triphosphate binding and hydrolysis, whereas Ia, Ib and IV motifs are involved in RNA binding and the motif III participates in coupling the NTPase and the unwinding activity (Caruthers & McKay, 2002; Cordin & Beggs, 2013; Cordin, Hahn, & Beggs, 2012). The C-terminal region is highly conserved in DEAH-box helicases and is composed by three domains: a winged helix (WH), a

ratchet and an oligosaccharide binding (OB) fold (Andersen, & Nielsen, 2010). The N-terminal region is distinctly more variable and the length differs between the members of this subfamily. The N-terminal region is involved in the pre-mRNA processing and in the targeting to the nucleus (Fouraux et al., 2002; Schneider & Schwert, 2001). A schematic representation of a SF2 RNA helicase is displayed in figure 5.

Figure 5. Schematic representation of the characteristic sequence motifs for SF2 Helicases core proteins.

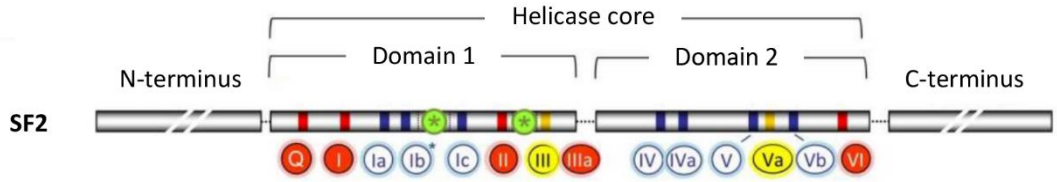

SF2 RNA helicases. Motifs were colored accordingly to their predominant biochemical function: red, ATP binding and hydrolysis; yellow, coordination between nucleic acid and NTP binding sites; blue, nucleic acid binding. Green circled asterisks mark insertions of additional domains. Motifs were numbered consecutively. The Motif IVa in SF2 proteins is frequently marked QxxR and motif Ic often TPGR. The asterisk on motif Ib indicates that in some proteins this motif is replaced by an additional domain (distance/length in not to scale). Figure and legend were adapted from Fairman-Williams et al., 2010.

Helicases are ubiquitous in all the kingdoms of life and are involved in essentially every step in DNA and RNA metabolism, including replication, DNA repair, recombination, transcription, translation, chromatin rearrangement, ribosome synthesis, RNA maturation and splicing, nuclear export, Holliday junction movement, displacement of proteins from DNA and RNA replication (Jankowsky, 2011; Jeang & Yedavalli, 2006). In eukaryotes, this type of enzymes is known to unwind duplexes formed during RNA mechanism in an ATP-dependent fashion (Bizebard, Ferlenghi, Iost, & Dreyfus, 2004; Yang, Del Campo, Lambowitz, & Jankowsky, 2007; Yang & Jankowsky, 2006) and also recognized to be important in the anti-viral immune response either as sensor, by identifying foreign viral nucleic acids, and/or as effectors that directly participate in viral clearance (Ahmad & Hur, 2015). However, viruses evolve rapidly to evade immune system and some hijack cellular RNA helicases for their own proposes (Jeang & Yedavalli, 2006). For example, the cellular DDX3 (DEAD-box) is recruited by human immunodeficiency virus (HIV) -1, by binding to CRM1 (nuclear export receptor) and to HIV-1 Rev leading to an increase of Gag protein production. In vaccinia virus DDX3 is essential during infection by interacting with vaccinia virus K7 protein, which blocks transcriptional

activation of the interferon responsive genes (Ranji & Boris-Lawrie, 2010). However, other viruses encode their own helicases like ASFV (*Asfaviridae*) (Utama et al., 2000), members of *Herpesviridae* (Chattopadhyay, Chen, & Weller, 2006), *Poxviridae* (Jankowsky, Gross, Shuman, & Pyle, 2000), *Parvoviridae* (Christensen & Tattersall, 2002) and *Flaviviridae* (Utama et al., 2000). In hepatitis C virus (HCV), the NS3 (DExH box protein) is required to unwind the double-stranded RNA intermediate, which may enable movement of HCV NS5b polymerase (Belon & Frick, 2009; Dumont et al., 2006; Piccininni et al., 2002). Moreover, the NS3 assists in virus assembly and is likely to act as a scaffold for interaction with viral or cellular cofactors (Ma, Yates, Liang, Lemon, & Yi, 2008). Thus, more knowledge about the basic aspects of RNA helicases and identifying their specific role during viral infections by modulating RNA-RNA and RNA-protein interactions, gene expression, viral egress and host antiviral responses (Frick & Lam, 2006; Ranji & Boris-Lawrie, 2010) raised an opportunity to explore new molecular targets for the development of selective inhibitors (Briguglio, Piras, Corona, & Carta, 2011; Ranji & Boris-Lawrie, 2010; Shuman, 1992). The study of ASFV RNA helicases is fundamental for understanding the viral-host interface. Given the role of other viral RNA helicases, these studies may also uncover ways to control gene expression that results in proper utilization of the viral RNA in translation and viral assembly.

2.3. ASFV P1192R type II topoisomerase

Topoisomerases are ubiquitous and responsible for altering DNA topology, also being important targets of antibacterial and anticancer drugs (Drlica et al., 2009; Nitiss, 2009a; Vos, Tretter, Schmidt, & Berger, 2011). Topoisomerases have a relevant role in DNA replication being responsible for relieving torsional stress ahead of the replication fork, in particular the topoisomerase IV, that reveals an effective decatenating activity essential for *de novo* separation of genomes (Drlica & Malik, 2003; Drlica, Malik, Kerns, & Zhao, 2008; Malik, Hussain, & Drlica, 2007). In prokaryotes, two highly conserved type IIA topoisomerases can be found: the topoisomerase (topo) IV and the DNA gyrase involved, respectively, in chromosome relaxation/segregation and DNA supercoiling (Gellert, Mizuuchi, O'Dea, & Nash, 1976; Zechiedrich & Cozzarelli, 1995). The topo IV is a tetramer constituted by two subunits, ParC and ParE, that form an active E2C2 complex; in a similar way gyrases are formed by GyrA and GyrB subunits, as schematic described in figure 6A (Corbett & Berger, 2004). These enzymes transiently cleave both strands of DNA in an ATP-dependent fashion and pass a second DNA duplex through the break which is then resealed (Corbett, Schoeffler, Thomsen, & Berger, 2005; Mizuuchi, Fisher, O'Dea, & Gellert, 1980). The DNA is captured by closure of the N gate implying adenosine triphosphate (ATP)-dependent dimerization of the topoisomerase/gyrase (ParE/GyrB) ATPase domains and allowing the DNA presentation to the cleavage core of the enzyme, passage through the G (gate) DNA bound at the DNA

cleavage gate and subsequent release through the protein C gate (Roca, 2004; Roca, Berger, Harrison, & Wang, 1996). A schematic representation of the mechanism is illustrated in Figure 6B and C. Some antibacterial drugs such as novobiocin target the ATPase gate, whereas clinically important fluoroquinolones such as levofloxacin interfere with DNA resealing at the DNA cleavage gate (Bax et al., 2010; Chan et al., 2015; Laponogov et al., 2009, 2010). Eukaryotic cells express topoisomerase IIA and IIB isoforms and rely in a close related mechanism of action, sharing a similar double-strand break process using the sequential operation of N (ATPase), DNA and protein C gates (Nitiss, 2009b; Vos et al., 2011). The cleavage gates are inhibited by clinically important anticancer drugs such as doxorubicin and etoposide (Wu et al., 2011; Wu, Li, Wang, Li, & Chan, 2013). These two cellular topoisomerases (Topoisomerase-IIA and IIB) share a high sequence homology (Gadelle, Filée, Buhler, & Forterre, 2003), except in their degenerate C-terminal region containing nuclear localization signals (Mirski, Gerlach, & Cole, 1999), in their regulatory sites (Isaacs et al., 1998) and in their biologic function (Nitiss, 2009a).

Figure 6. Type IIα topoisomerases structure and mechanism.

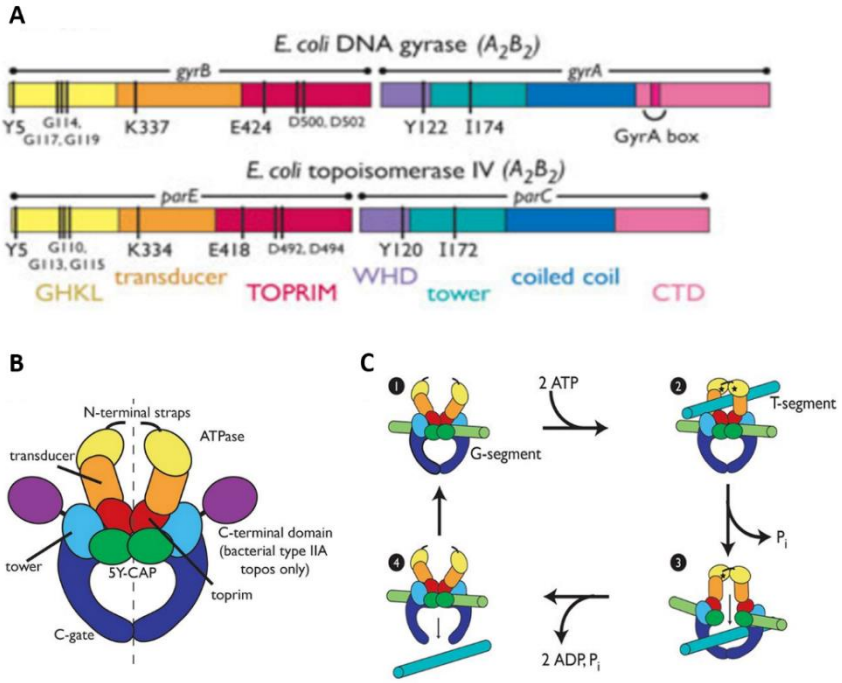

Type II α topoisomerases (A) Primary domain structures of representative bacterial type II topoisomerases (topoisomerase IV and gyrase). Domains are indicated by color and important residues are indicated by black bars. Gene names are shown above each primary structure along with the subunit compositions of the holoenzymes. Figure and legend were adapted from Allyn J. Schoeffler & Berger, 2008. (B) Schematic model for type IIα topoisomerase elements. ATPase domains are shown in yellow (the GHKL subdomain) and orange (the transducer subdomain), with the N-terminal straps represented by black lines. The DNA gate is formed by two 5Y-CAP domains (green); a pair of toprim folds (red) assists with the catalysis of DNA cleavage. The tower domains are coloured light blue, the C-gate dark blue and the CTD purple. Bacterial GyrB/ParE subunits encompass the ATPase, transducer and toprim folds, while the GyrA and ParC subunits comprise the other elements. (C) Schematic representation of the type IIα topo catalytic cycle. Domains are coloured as in B. The G-segment (pale green) first binds to the DNA gate (step 1). A T-segment (teal) is captured by dimerization of the ATPase domains upon ATP (black star) binding (step 2). ATP hydrolysis followed by Pi release triggers DNA gate opening and

T-segment passage (step 3). C-gate opening allows escape of the T-segment (step 4), while re-ligation of the G-segment and release of hydrolysis products lead to opening of the ATP gate, thus resetting the enzyme for another round of catalysis (step 1). Figure and legend were adapted from Schoeffler e Berger, 2005.

Topo-IIA is involved in positive supercoils relaxation and is considered a key enzyme in DNA replication and chromosome segregation being highly expressed in actively-dividing cells. In the other hand, Topo-IIβ is mostly expressed in quiescent cells and does not have a special affinity to positive supercoils, while being crucial for transcription (Grue et al., 1998; McClendon, Rodriguez, & Osheroff, 2005; Nitiss, 2009a). In viruses, type IIA topoisomerases have been identified in several NCLDV families, such as *Iridoviridae*, *Asfarviridae*, *Mimiviridae* and *Phycodnaviridae* (Iyer, Aravind, & Koonin, 2001; Yutin, Colson, Raoult, & Koonin, 2013), as well as in bacteriophages of the T4 superfamily (Kreuzer, 1998). ASFV is the only known virus that infects mammals encoding for a type II topoisomerase (ASFV-Topo II, ORF P1192R). Surprisingly, phylogenetic studies revealed that this viral protein do not cluster with cellular topoisomerases (Gadelle et al., 2003), being more closely related with the bacterial DNA gyrases and topoisomerase IV (Liu, 1994), raising the possibility of targeting this protein with specific anti-bacterial topoisomerase/gyrase drugs (fluoroquinolones). Although the specific role of this enzyme during infection remains unclear, recent studies showed that anti-topoisomerase bacterial inhibitors induced a viral genome fragmentation and a delay in late protein synthesis in ASFV infected cells. These results suggest a similar mechanism of action of these drugs between ASFV and prokaryotes (Mottola et al., 2013). Moreover, it was also shown that ASFV topoisomerase II is functional in complementation assays and is localized at late times post infection in the viral factories where most of the viral DNA replication takes place (Coelho, Martins, Ferreira, & Leitão, 2015). As expected, phylogenetic analysis also revealed that this protein is conserved between ASFV isolates (Coelho et al., 2015). It was also demonstrated that recombinant ASFV-Topo II is active under conditions similar for other type II topoisomerases and is capable to catenate, decatenate and relax DNA. The same authors also showed that ASFV-Topo II was inhibited by common topoisomerase II poisons and inhibitors, namely by doxorubicin, coumermycin A1 and m-AMSA (Coelho, Ferreira, Martins, & Leitão, 2016). It is very likely that ASFV-topo II can also be essential for viral DNA replication, however, further studies are needed to uncover the essential role of this putative enzyme during the infection, and thus explore the possibility to target this enzyme in order to control the infection.

3. Objectives

In the last years, research developed at the Laboratório de Doenças Infecciosas (LDI) FMV/ULisboa has been dedicated at improving knowledge on ASFV biology towards the identification of new strategies for the development of effective and safe vaccine(s) and potential use of drugs. According to this strategy, the central objective of the research herein presented is to increase our understanding on basic molecular mechanisms of ASFV replication, transcription and host immune evasion. The main objectives of this work were as follows:

- To characterize the putative pI215L E2 ubiquitin-conjugating enzymatic activity *in vitro*, evaluate I215L transcription pattern, pI215L protein expression and distribution in infected cells. The effects of downregulating I215L were also studied in order to better understand the relevance of pI215L for viral replication (chapter II).
- To investigate the phylogenetic relation of QP509L and Q706L among different ASFV isolates and with other SF2 ATP-dependent RNA helicases belonging to nucleocytoplasmic large DNA viruses; to assess the transcript dynamics, protein expression patterns and cellular localization of ASFV-QP509L and Q706L RNA helicases during the infection; and to clarify the importance of these two RNA helicases for ASFV infection cycle by siRNA-mediated silencing (chapter III).
- To characterize the role of the putative ASFV P1192R type II topoisomerase in replication by investigating its transcription pattern and assess the effects of transcript downregulating during the infection; and finally to uncover the mechanism of action behind the antiviral effects of fluoroquinolones against this viral protein (chapter IV).

It is expected that the results obtained during this work will contribute to the rational development of novel approaches to precisely control the infection, allowing the use of anti-viral drugs or the generation of mutants lacking in these proteins (e.g. defective infectious single cell cycle particle) to be used as vaccines.

CHAPTER II

African swine fever virus encodes for an E2-ubiquitin conjugating enzyme that is mono- and di-ubiquitinated and required for viral replication cycle

Ferdinando B. Freitas, Gonçalo Frouco, Carlos Martins, Fernando Ferreira (2018) Scientific Reports. 134:34-41 http://doi.org/10.1038/s41598-018-21872-2

Abstract

African swine fever virus is the etiological agent of a contagious and fatal acute haemorrhagic viral disease for which there are no vaccines or therapeutic options. The ASFV encodes for a putative E2 ubiquitin conjugating enzyme (ORF I215L) that shows sequence homology with eukaryotic counterparts. In the present study, we showed that pI215L acts as an E2-ubiquitin like enzyme in a large range of pH values and temperatures, after short incubation times. Further experiments revealed that pI215L is polyubiquitinated instead of multi-mono-ubiquitinated and Cys85 residue plays an essential role in the transthioesterification reaction. In infected cells, I215L gene is transcribed from 2 hours post infection and immunoblot analysis confirmed that pI215L is expressed from 4 hpi. Immunofluorescence studies revealed that pI215L is recruited to viral factories from 8 hpi and a diffuse distribution pattern throughout the nucleus and cytoplasm. siRNA studies suggested that pI215L plays a critical role in the transcription of late viral genes and viral DNA replication. Altogether, our results emphasize the potential use of this enzyme as target for drug and vaccine development against ASF.

1. Introduction

African swine fever (ASF) is a contagious haemorrhagic disease of domestic and wild suids, associated with mortality rates close to 100% and devastating socio-economic implications on affected regions (Costard et al., 2009; Penrith & Vosloo, 2009). Despite all the efforts applied to control the disease, the disease is solely controlled through the application of strict sanitary measures including among others, slaughtering of infected and exposed animals and trade restrictions (Costard et al., 2009, 2013). Currently, ASF is endemic in most of sub-Saharan Africa, in Sardinia and since its introduction in Georgia via contaminated food in 2007, has been spreading through the Caucasus (Georgia, Armenia and Azerbaijan), Eastern Europe (Belarus, Moldova, Poland, Russia and Ukraine) and the Baltic countries (Estonia, Latvia and Lithuania), (Sánchez-Vizcaíno et al., 2015). Caused by a large (≈200nm) lipoprotein-enveloped, icosahedral, double-stranded DNA virus (170 to 190kbp) and being the only member of family *Asfarviridae*, the African swine fever virus (ASFV) infects different species of soft ticks, wild and domestic pigs (Tulman et al., 2009). ASFV genome encloses between 151 and 167 open reading frames (ORFs), with half of them lacking any known function (Costard et al., 2013; Dixon et al., 2013; Tulman et al., 2009). As reported for other viruses (González-Santamaría et al., 2011; Gustin et al., 2011), ASFV must evade the cellular antiviral defenses and modulate gene expression to establish a productive infection, probably by disrupting the ubiquitination and SUMOylation status of host proteins. The ubiquitin pathway is a major cellular system consisting of enzymes that conjugate the 76-amino-acid protein tag ubiquitin to and deconjugate it from host target proteins for proteasomal degradation, thereby regulating signaling cascades and cell cycle. Interestingly, ASFV encodes for a putative ubiquitin-conjugating E2-like enzyme (pI215L, ASFV-UBCv1), (Hingamp et al., 1992) found within the virion, suggesting that pI215L may be involved in the early steps of infection (Hingamp et al., 1995). As previously described, ASFV-infected cells tightly regulate ubiquitin mRNA levels when compared to mock-infected cells, strengthening the idea that ASFV perverts the ubiquitin pathway to its own benefit (Bulimo, Miskin, & Dixon, 2000). Although the exploitation of ubiquitin system by viruses is emerging as a central theme and several studies highlight the use of ubiquitin inhibitors as an antiviral approach (Randow & Lehner, 2009), few data is available on the ASFV ubiquitin-conjugating E2-like enzyme and its role during infection. Thus, this study aims to characterize the pI215L E2 ubiquitin-conjugating enzymatic activity in vitro and to evaluate the transcription pattern of the ASFV-I215L gene, as well as its expression and its distribution in infected cells. To better understand the importance of pI215L during infection, the transcription activity of early and late viral genes, the number of ASFV genomes and the viral progeny were analyzed and compared between I215L-knockdown cells and mock-transfected cells. Finally, the biological role of the pI215L in a cellular context was

schematically illustrated, suggesting that pI215L can be a good candidate for the development of a vaccine against ASF or used as a target for antiviral therapy.

2. Material and methods

2.1. Viruses and cells

The Vero-adapted ASFV isolate Ba71V was used to infect cells and was propagated as described (Carrascosa, Bustos, & de Leon, 2011). Infections were carried out at the indicated multiplicities of infection (MOI), and at the end of the adsorption period (1h), the inoculum was removed and cells were washed twice with serum-free medium. The virus titration was performed on sub-confluent Vero cells grown in 96-well plates inoculated with ten-fold viral dilutions of viral suspensions. Viral infection was assessed by CPE observation and calculated by using the Spearman-Kärber method (Kärber, 1931). All experimental infections were conducted with the non-pathogenic ASFV-Ba71V strain (Rodríguez et al., 2015) and performed in a BSL-3-like containment laboratory.

Vero E6 cells (kidney epithelial cells of African green monkey *Cholorocebus aethiops*) were obtained from the European Cell Culture Collection (ECACC, Salisbury, UK) and maintained as previously reported (Freitas, Frouco, Martins, Leitão, & Ferreira, 2016). All experiments were conducted on actively replicating sub confluent cells.

2.2. Cloning, expression and purification of recombinant ASFV-pI215L

The complete ORF I215L, lacking the stop codon, was PCR-amplified from Ba71V genomic DNA, using the 215Fw and 215Rv primers (Table 2), which include at their 5´and 3´ ends, NheI and XhoI restriction endonuclease sites to facilitate vector insertion. The PCR reactions were performed as follow: 98 °C for 2 min., 30 cycles at 98 °C for 30 seconds, 65 °C for 30 seconds, 72 °C for 30 seconds plus one extension step at 72 °C for 10 min. After confirmation of correct fragment size by electrophoresis on a 1% agarose gel, the DNA fragments were purified and quantified in the NanoDrop 2000c. Then, these fragments were inserted in a cloning vector (pET24a, Novagen) to add a 6xHis-tag at the tag C-terminal, in order to facilitate the purification step. Two clones were sequenced to avoid mutations generated from Taq polymerase errors. Confirmed plasmids were then transformed into the *E.coli* strain BL21(DE3)-pLysS (Novagen) and grown in LB medium (10 g tryptone, 5 g yeast extract, 5 g NaCl, pH 7.2) supplemented with kanamycin (30 µg/ml) plus chloramphenicol (34 µg/ml), at 37 °C, with shaking at 200 rpm, until the OD_{600} reached 0.1-0.2. Induction of protein expression was carried out by adding isopropyl-β-D-1-thiogalactopyranoside (IPTG) at a final concentration of 1 mM during 5 hours.

After this step, bacterial cells were harvested by centrifugation (10,000 g for 10 min, 4 °C), and washed with sterile water. The pellet was resuspended in binding buffer (20 mM sodium phosphate, 500 mM NaCl, 20 mM imidazole, pH 7.4) and cells were lysed by a lysis solution (0.2 mg/ml lysozyme, 20 µg/ml DNAse and 1mM PMSF) and sonicated for 5x5 minutes on ice (5 cycles, 70% amplitude). Lysates were then centrifuged at 3000g for 15 minutes and pellets were discarded. The extracts were thereafter filtered (0.45 µm syringe filter Rotilabo®, CarlRoth) and incubated with Ni Sepharose 6 Fast Flow slurry (GE Healthcare) for 1 hour. The mixture was loaded onto a PD-10 column (GE Healthcare), washed with binding buffer solution (20 mM sodium phosphate, 500 mM NaCl, pH 7.4) containing increasing concentrations of imidazole (40, 60 and 80 mM), and the recombinant pI215L was eluted with an elution buffer (20 mM sodium phosphate, 500 mM NaCl, 500 mM imidazole, pH 7.4). Fractions were collected in low-binding tubes (Maxymum Recovery® TM tubes, Axygen, Corning Life Sciences, Amsterdam, The Netherlands), analyzed by SDS-PAGE and the recombinant pI215L, purified under native conditions, was stored at -80 °C until further use. The three single point mutants (pI215L^{C85A}, pI215L^{C162A}, pI215L^{C189A}) were generated using the QuikChange II XL Site-Directed Mutagenesis Kit (Agilent Technologies), following the manufacturer's instructions and using the primers indicated in Table 2.

2.3. In vitro ubiquitination assay

To determine if the ASFV-pI215L has a catalytic activity similar to an E2 ubiquitin conjugating enzyme, a commercial kit was used (E2-Ubiquitin Conjugation Kit, ab139472, Abcam) and the manufacturer's instructions were followed. Reactions were performed in a 50 µl mixture containing 5 µl of ubiquitination buffer (50 mM Tris-HCl, pH 7.4, 5 mM MgCl2, 15 µM ZnCl2, 0.3 mM dithiothreitol (DTT,) 0.006% DTT, 2 mM ATP, 10 U creatine phosphokinase, and 10 mM phosphocreatine), 2.5 µl of biotinylated ubiquitin (2.5 µM) or with a mutant biotinylated ubiquitin lacking the seven acceptor lysine residues (Ub^{NOK}, Boston Biochem), 2.5 µl of an E1-enzyme (recombinant UBA1 at 100 nM), 5 µl of an E2-enzyme at 2.5 µM (recombinant pI215L or recombinant UbcH5b provided by the kit) and 10 µl of an inorganic pyrophosphatase solution (IPP, 100 U/mL). To investigate whether pI215L-ubiquitin conjugates were mediated by thioester bond formation, samples were incubated at 95 °C with 5% 2-mercaptoethanol (Sigma) during 10 min. Additionally, the reactions were performed in the presence and absence of ATP-Mg^{2+} (2.5 µl at 5 mM) and incubated at 37 ºC during 120 min, except when indicated. To further characterize the E2-ubiquitin conjugating activity of pI215L, the assay was also performed at different incubation temperatures (4, 24, 37 and 42°C) and pH values (4, 7.5, 9 and 14), and different incubation times (1, 5, 15, 30 and 120 min).

Soluble and insoluble protein fractions were prepared from mock infected and Ba71V-infected Vero cells, harvested at 6 and 16 hpi. Initially, cells were washed with phosphate-buffered

saline (PBS) and incubated with a buffer containing 50 mM HEPES (pH 7.6), 100 mM NaCl, 2 mM Ethylenediaminetetraacetic acid (EDTA), 250 mM sucrose, 0.1% Tx-100, supplemented with protease (cOmplete, Mini, EDTA-free from Roche) and phosphatase inhibitors (PhosStop, Roche). After a centrifugation step (10000 x g for 10 min, 4ºC), the supernatant was collected (soluble fraction) and the pellet containing insoluble proteins was lysed in RIPA buffer [25 mM Tris, 150 mM NaCl, 0.5% (v/v) NP40, 0.5% (w/v) sodium deoxycolate, 0.1% (w/v) SDS, pH 8.2] supplemented with protease-inhibitor cocktail (cOmplete, Mini, EDTA-free, Roche) and phosphatase-inhibitor cocktail (PhosStop, Roche). pI215L activity in protein fractions was investigated by incubating the reaction mixtures at 37 ºC during 120 min. Reactions were quenched by adding 50 µl of 2x non-reducing gel loading buffer. Reaction products were resolved by SDS-PAGE using 8-16% (w/v) polyacrylamide separating gels and transferred to a 0.2 µm pore diameter nitrocellulose membrane (Whatman Schleider & Schuell) by electroblotting. Finally, membranes were incubated with a streptavidin-Horseradish peroxidase (HRP) antibody (RPM 1231, GE Heathcare, 1:10,000 dilution in 3% TBST- bovine serum albumin -BSA solution) or with the anti-pI215L antibody.

2.4. RNA extraction and cDNA synthesis

Total RNA was extracted using the RNeasy Mini Kit (Qiagen, Courtaboeuf, France) and treated with DNAse I (Qiagen) to remove contaminant genomic DNA. RNA concentrations and purity were measured using a spectrophotometer (NanoDrop 2000c, Thermo Fisher Scientific, Waltham, USA). 200 ng of each RNA sample was reverse transcribed into complementary DNA (cDNA) using the Transcriptor First Strand cDNA Synthesis Kit (Roche, Basel, Switzerland). The obtained cDNA was diluted (1/20) in ultra-pure water and stored at -20°C until further use.

2.5. Recombinant plasmids and standard curves

The amplified fragments corresponding to the viral genes (ASFV-I215L, B646L, and CP204L) and the housekeeping gene (Cyclophilin A) were cloned into a pGEM-T Easy Vector System II (Promega, Madison, USA). Each plasmid was used to transform *E. coli* DH5α competent cells, followed by an incubation step at 37 °C, under selective antibiotic pressure. Recombinant plasmids were isolated from bacteria using the Roche High Pure Plasmid Isolation Kit (Roche Applied Science, Germany) and quantified by spectrophotometric absorbance (NanoDrop 2000c). Their corresponding copy number was calculated using the equation: pmol (dsDNA) = µg (dsDNA) x 1515 / DNA length in pb (pmol = picomoles, dsDNA = double-strand DNA, DNA length in pb = number of base pairs from the amplified fragment; 1 mol = 6,022 x 1023

molecules). Finally, the cloned fragments were amplified by PCR and the sequence confirmed by DNA sequencing. For each amplification plate, a standard calibration curve was obtained for viral genes and for Cyclophilin A to insure the accuracy of the results. Standart curves were plotted by following a previously described protocol (Pfaffl, 2001).

2.6. Quantitative PCR

Quantification of ASFV-I215L, B646L and CP204L transcripts was performed by qPCR using Maxima SYBR Green PCR Master Mix (Thermo Fisher) according to the manufacturer's instructions [12.5 µl of master mix, 2.5 µl of forward and reverse primers (50 nM each), 5 µl of Milli-Q water and 2.5 µl of cDNA)]. All qPCR reactions were performed in the Applied Biosystems 7300 Real Time PCR system (Thermo Fisher), and with the following thermal profile: initial denaturation at 95°C for 10 min followed by 40 cycles of 15 s at 95°C, 60°C for 60 s, and a final denaturation step at 65°C for 5 s with a 20°C/s ramp rate and subsequent heating of the samples at 95°C with a ramp rate of 0.1°C/s. Quantification of ASFV-I215L, B646L, CP204L and Cyclophilin A mRNA levels was determined by the intersection between the fluorescence amplification curve and the threshold line. The crossing point values of each plasmid obtained from different known concentrations were plotted in a standard curve used to determine the copy number of each transcript. The values were determined using the comparative threshold cycle method, which compares the expression of a viral gene normalized to the housekeeping gene (Cyclophilin A). The validation of the housekeeping gene was confirmed using the ANOVA test, whereas the specificity of the qPCR assays was confirmed by the melting curve analysis. The sequences of all primers used in this study are shown in Table 2. To quantify viral gene expression, Vero cells seeded onto 30 mm dishes were infected with a MOI of 1,5. After 1 hour of adsorption, the virus inoculum was washed off with DMEM, and every 2 hours (from 0 to 20 hpi), total RNA extraction was performed from one culture dish. Results were expressed as the mean standard error of the mean and were obtained from three independent experiments performed in different days, to ensure the biological relevance of the results.

Table 2. Primers used in the present study.

Target	Primer designation	Sequence (5´- 3´)	Coordinates*	Orientation
ASFV-I215L	215FwE	AGACACCTGATAGAGAACCC	157562-157581	Foward
ASFV-I215L	215Fwl	TCCAATGTTCCACCAATACCC	157069-157089	Foward
ASFV-I215L	215Rvl	TCATCCATCTCTTCATCCTCCTC	156971-156993	Reverse
Cyclophilin A	CycloFw1	AGACAAGGTTCCAAAGACAGCAG	-	Foward
Cyclophilin A	CycloRev	AGACTGAGTGGTTGGATGGCA	-	Reverse
Cyclophilin A	CycloFw2	TGCCATCCAACCACTCAGTCT	-	Foward
VP72	VP72Fw	ACGGCGCCCTCTAAAGGT	88273-88290	Foward
VP72	VP72Rev	CATGGTCAGCTTCAAACGTTTC	88322-88343	Reverse
VP32	VP32Rev	TCTTTTGTGCAAGCATATACAGCTT	108162-108186	Foward
VP32	VP32Fw	TGCACATCCTCCTTTGAAACAT	108228-108249	Reverse
ASFV-I215L	215Fw	ACTAGCTAGCATGGTTTCCAGGTTTTTAATAGCAGAG	157562-157581	Foward
ASFV-I215L	215Rv	TCCGCTCGAGCTCATCATCCATCTCTTCATCCTC	157069-157089	Reverse
ASFV-I215L	C85AFW	TATTTACCCTGATGGAAGACTAGCTATCTCTATCTTACACGGAGAC	157336-157381	Foward
ASFV-I215L	C85ARV	GTCTCCGTGTAAGATAGAGATAGCTAGTCTTCCATCAGGGTAAATA	157336-157381	Reverse
ASFV-I215L	C162AFW	ATTTTTAAAATATTCTATGTCTTCTGGTGAAGCCTCATCTAATGATTTTTTGACAGTCTTTTTA	157336-157381	Foward
ASFV-I215L	C162ARV	TAAAAAGACTGTCAAAAAATCATTAGATGAGGCTTCACCAGAAGACATAGAATATTTTAAAAAT	157096-157159	Reverse
ASFV-I215L	C189AFW	ATACCCAGTGATGCTTATGAAGATGAAGCTGAAGAAATGGAGGATG	157029-157029	Foward
ASFV-I215L	C189ARV	CATCCTCCATTTCTTCAGCTTCATCTTCATAAGCATCACTGGGTAT	157029-157029	Reverse

*Primer coordinates are relative to Ba71V sequence used has template for primer design.

2.7. Antibodies

The purified recombinant pI215L was used to produce a mouse polyclonal antiserum. Briefly, young female mice (BALB/c, 4 to 6-week-old) were injected subcutaneously with 100 µg of purified pI215L in a mixture with Freund's complete adjuvant. Following the primary injection, two booster injections were administered at 2-week intervals. Finally, the total blood was collected 10 days after the second booster injection and sera were aliquoted and stored at -20 °C until further use for immunoblotting and immunofluorescence studies. The specificity of the polyclonal antiserum was tested against purified recombinant ASFV-pI215L and whole infected-cells extracts. The immunostaining of pI215L and ASFV-infected cells was achieved by incubation with two in-house primary antibodies: mouse anti-pI215L [1:10 in PBST (Phosphate Buffered Saline with Tween 20 0.01% v/v), overnight at 4ºC] and swine anti-ASFV polyclonal antibody (1:100, 1h, RT). Two secondary fluorescent-conjugated antibodies were used as follows: anti-mouse FITC (1:300, sc-2099, Santa Cruz Biotechnology) and anti-swine Texas Red (1:500, ab6775, Abcam). Between each antibody incubation, cells were wash twice with PBS (5 min) and once with PBST (0.1% v/v, 5 min). All incubations were performed in a dark humidified chamber to prevent fluorochrome fading and a mounting medium with DAPI

(4′,6-diamidino-2-phenylindole) was used to detect the cell nucleus and viral factories (Vectashield, Vector Laboratories, Peterborough, UK).

For immunoblot analysis, two primary antibodies (anti-pI215L, 1:100; anti-α-tubulin, 1:1250, #2125, Cell Signalling Technology) and two HRP-conjugated secondary antibodies were used (anti-rabbit IgG, 1:10000, 4010-05; anti-mouse IgG, 1:30000, 1010-05; both from SouthernBiotech). All antibody dilutions were performed in blocking solution and incubated according to the manufacturers' recommendations.

2.8. Immunoblot analysis

Vero cells grown in 30 mm dishes were infected with ASFV-Ba71V isolate (MOI of 5) and when indicated, exposed to cytosine arabinoside (50 µg/ml, AraC; Sigma-Aldrich), after the adsorption period (1h). Cells were washed twice with PBS and then lysed in ice-cold modified RIPA buffer supplemented with protease-inhibitor cocktail (cOmplete, Mini, EDTA-free, Roche) and phosphatase-inhibitor cocktail (PhosStop, Roche). Clarified whole-cell lysates harvested at 4, 8, 12, 14, 16, 18 and 20 hpi, were then analyzed by western blot technique as previous described (Freitas et al., 2016), using the above mentioned antibodies. α–Tubulin was used as a loading control.

2.9. Immunofluorescence and microscopy analysis

Vero cells seeded on glass coverslips ($1x10^5/cm^2$) were infected with the ASFV Ba71V isolate (MOI of 10). At 4, 8, 12, and 16 hpi, cells were fixed and subsequently processed as previously described (Freitas et al., 2016). Fluorescence images were acquired using an epifluorescence microscope equipped with a 40X objective (Leica DMR HC model, Wetzlar, Germany) and data sets were acquired with the Adobe Photoshop CS5 software (Adobe Systems, Inc., San Jose, USA).

2.10. siRNA assays

Two double-stranded siRNAs (I215L siRNA_I and I215L siRNA_II; ON-TARGETplus, Thermo Fisher Scientific, USA) targeting different regions of ASFV-I215L mRNA were designed (siDESIGN Center, Thermo Fisher Scientific, USA), based on the full genome sequence of ASFV Ba71V isolate (GenBank/EMBL, accession number: ASU18466). One siRNA against the GAPDH gene (siRNA-GAPDH; Silencer™ GAPDH siRNA human control number 4605; Ambion/Thermo Fisher Scientific) was used as a control. The siRNA sequences targeting

ASFV-I215L are shown in Table 3. All siRNAs duplexes were diluted at different final concentrations (10, 50 and 100 nM) in serum-free Opti-MEM (Gibco, Life Technology, Karlsruhe, Germany) and using 8 µl HiPerfect Transfection reagent (Qiagen, Courtaboeuf, France). Mixtures were incubated at room temperature for 20 min to allow the formation of transfection complexes, and thereafter, 100 µl of the transfection solution was incubated with $2x10^4$ Vero cells cultured in 500 µl of DMEM supplemented with 10 % fetal bovine serum (FBS) (24-well plate) for 8 h at 37 °C. One hour after infection, the culture medium was removed and fresh medium was added to allow recovery of the cells. Next, cells were infected with ASFV Ba71V (MOI = 0.1). Then, the virus inoculum was removed one hour after and cells maintained at 37 °C for 72 h. The viability of transfected cells was assessed every 8 hours, until 72 hours, by phase-contrast microscopy. The two different siRNAs were used individually and their antiviral effects were evaluated by the quantification of CP204L and B646L mRNA levels, titration of the ASFV genomes and viral progeny, at 4, 8 and 16 hpi. To ensure high RNA concentrations for qPCR measurements, the siRNA assays were performed in quadruplicated.

Table 3. siRNA sequences to knockdown expression I215L.

Target	**siRNA designation**	**Sequence (5´- 3´)**	Target c**oordinates***	**Orientation**
ASFV-I215L	I215L_I	GUGAAGAAAUGGAGGAUGAUU	565-584	Sense
ASFV-I215L	I215L_II	GCUAAAAGCUACCGUAAAUUU	394-412	Sense

*siRNA coordinates according to the relative position in gene nucleotide sequence (start at position 1, ATG).

2.11. Quantification of ASFV genomes by qPCR

Viral DNA was extracted from Ba71V-infected Vero cells (MOI of 0.1) transfected separately with two siRNAs targeting I215L, at 72 hours post infection (hpi), using the High Pure Viral Nucleic Acid Kit (Roche). The number of viral genomes was determined by quantitative PCR as described by King et al., 2003. Mock-infected and infected cells transfected with siRNA-GAPDH were used as controls.

2.12. Statistical analysis

The Kolmogorov-Smirnov test was used to check the normal distribution of the results from the RNAi assays (mRNA expression, ASFV genome copy number and virus titer). Differences between experimental groups were assessed using the non-parametric Wilcoxon-Mann-Whitney test, because a normal distribution was not obatained. *p*-values less than 0.05 were

considered significant and the GraphPad Prism software (version 7.02) was used to perform statistical analysis.

3. Results

3.1. pI215L acts as an E2-ubiquitin conjugating enzyme, binding one or two ubiquitin molecules at the cysteine 85, in an ATP- and Mg^{2+}-dependent manner

Considering the sequence homology (49% identity) between the ASFV-pI215L (accession number: AJZ77128.1) and human E2-ubiquitin conjugating enzyme G2 (accession number: CBW46807.1), we aimed to confirm previous results which have shown that pI215L has the ability to bind ubiquitin, to determine the optimal conditions required for the formation of the thioester bond, to identify the cysteine residue of pI215L essential for the formation of the Ub-conjugates and to analyze the pI215L-ubiquitin conjugates forms present in detergent insoluble/soluble protein fractions collected from ASFV-infected cells. Immunoblot analysis showed that pI215L only binds to pre-activated ubiquitin (by an E1 enzyme, UBA1) and in the presence of ATP and Mg^{2+}, similarly to the human E2-ubiquitin conjugating enzyme UbcH5b, used as control (Fig.7A). Two distinct biotinylated-ubiquitin conjugates corresponding to mono-ubiquitinated (≈36 KDa, pI215L-Ub_1) and di-ubiquitinated (≈47 KDa, pI215L-Ub_2) species were detected. Since the upper band (pI215L-Ub_2) can result from multi-ubiquitinated pI215L forms (two monoubiquitinations in two different cysteine residues) and/or from poly-ubiquitinated forms of pI215L (di-ubiquitination of one or more cysteine residues), the ubiquitin wild type was substituted by a commercial ubiquitin mutated in the seven acceptor lysine residues (Ub^{NOK}), thus preventing ubiquitin chain elongation (polyubiquitination). The results obtained show a loss of the upper band when the Ub^{NOK} mutant replaces the ubiquitin wild type (Fig.7B), indicating that pI215L has oligoubiquitin chains that contain only two ubiquitin molecules, not being multi-ubiquitinated. Taking in consideration these results, we next investigated if ubiquitin binds to pI215L using the same cysteine or not. Although cysteine residue at position 85 is conserved in all ASFV isolates and in eukaryotic E2-ubiquitin conjugating enzymes, and annotated as the putative catalytic residue of pI215L, its importance in ubiquitin ligation in unknown, as well as the Cys-162 and Cys-189 residues. In order to evaluate if these residues are responsible for the formation of mono- and di-ubiquitinated pI215L conjugates, three single point mutants were generated by site-directed mutagenesis: pI215L^{C85A}, pI215L^{C162A} and pI215L^{C189A}. Immunoblot results showed that replacement of the sulfur containing cysteine at position 85 by a nonpolar amino acid (alanine) totally inhibits the formation of ubiquitin pI215L conjugates contrasting with the pI215L^{wt} and the single point mutants: pI215L^{C162A} and pI215L^{C189A} (Fig.7C). To investigate if a transesterification reaction mediates the transfer of ubiquitin between the E1-ubiquitin activating enzyme and cysteine-85 present at the active site of pI215L, reaction mixtures were incubated with the 2-mercaptoethanol (a reducing

agent) and, as expected, the ubiquitin pI215L conjugates become lost after a short incubation period, indicating that ubiquitin binds to pI215L through a thioester bond (data not shown). Further experiments to characterize the binding activity of pI215L revealed that mono-ubiquitinated and di-ubiquitinated species were detectable in a wide range of temperatures, although their formation seems to be favored at 37 °C (Fig. 7D). When the reaction mixtures were incubated at different pH values, the E2-ubiquitin conjugating activity of pI215L was maximal at a pH value of 7.5, with the mono-ubiquitinated species not being detected at pH values below 4 or above 9. In addition, an upper band corresponding to poly-ubiquitinated forms was detected in acidic conditions and an almost complete absence of ubiquitin-conjugating activity was found at pH values of 14 (Fig.7E). Interestingly, the formation of di-ubiquitinated conjugates was identified after short incubation times (e.g. 1 min), whereas mono-ubiquitinated pI215L forms were only detected at longer incubation times (Fig.7F). Finally, to better characterize the pI215L E2-ubiquitin conjugating activity, reaction mixtures were incubated with soluble and insoluble protein fractions prepared from mock infected and Ba71V-infected cells (6 and 16 hpi). Results revealed that pI215L has two distribution pools, with three species of pI215L-ubiquitin conjugates being detectable in the detergent soluble protein fraction (Fig.7G) and only a faint band corresponding to di-ubiquitinated forms was observed in insoluble protein fractions (Fig. 7G, asterisks).

Figure 7. pI215l acts as an E2-ubiquitin conjugating enzyme.

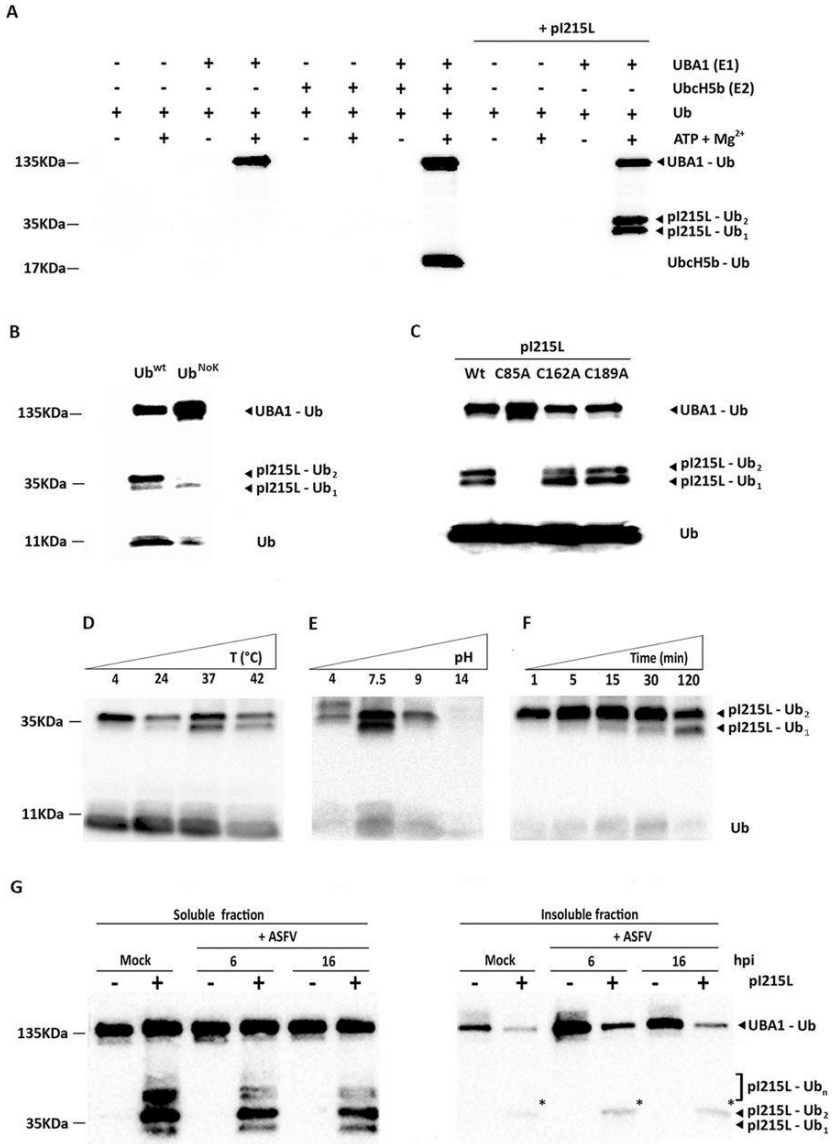

(A) Results from an in vitro ubiquitination assay showed that recombinant pI215L binds one or two ubiquitin molecules, in an ATP- and Mg2+-dependent manner, and in the presence of an E1 ubiquitin-activating enzyme (UBA1). Reaction mixtures were incubated 2 hours at 37 C, quenched with a non-reducing protein loading buffer, and then subjected to polyacrylamide gel electrophoresis. (B) When the ubiquitination assay was performed using an ubiquitin that is mutated in all lysine residues (UbNoK), the di-ubiquitinated forms of pI215L were not detected. (C) The residue cysteine-85 is essential for the E2-like activity of pI215L. Site-directed mutagenesis revealed that replacement of Cys-85 by an alanine residue led to an absence of ubiquitinated species, whereas the substitution of the Cys-162 or Cys-189 residue does not hamper the formation of ubiquitinated forms of pI215L. (D) pI215L forms thioester bonds with ubiquitin in a wide range of temperatures, although mono-ubiquitinated forms of pI215L were less detectable at 4 °C and 24 °C. (E) pI215L binds ubiquitin in a broad range of pH values, with mono-ubiquitinated forms only found at a pH value of 7.5. (F) Poly-ubiquitinated forms of I215L were detected after a short incubation period of 1 min, whereas the mono-ubiquitinated forms were detected later (5 min), showing increased concentrations in longer incubation times (e.g. 30, 60 minutes). (G) Mono- and poly-ubiquitinated forms of pI215L were mainly found in the Triton X-100-soluble fractions harvested at 6 and 16 hpi. In detergent-insoluble fractions, only the di-ubiquitinated form of pI215L was faintly detected (asterisks). Blots of Fig. 1(D to F) were cropped to improve clarity, full-length blots are presented in supplementary Figure S1. Fig. 1(G) is composed by two individual blots obtained from soluble and insoluble fractions.

3.2. ASFV-I215L gene encodes for a very early protein that localizes in viral factories and host cell nucleus

qPCR results revealed that ASFV-I215L gene is actively transcribed from 2hpi onwards (Fig.8A), showing two transcription peaks at early and late infection time points (2 and 16 hpi), suggesting that pI215L is involved in different phases of viral life cycle. However, ASFV-I215L mRNA levels were much lower than the ones found in two viral genes that encode for structural proteins and were used as controls (the early CP204L viral gene and the late B646L viral gene). In order to ensure that normalized mRNA levels of three viral genes are comparable, only qPCR reactions with efficiency values ranged from 90 to 91% and showing R2 values > 0.987 were considered.

The immunoblot analysis showed that pI215L is detectable in ASFV-infected Vero cells from 4 hpi onwards (Fig.8B), increasing its concentration throughout the infection, in accordance with I215L mRNA levels. As expected, pI215L was detected in whole extracts of infected cells exposed to cytosine arabinoside (AraC), an inhibitor of ASFV DNA replication and of late transcription phase, supporting that pI215L is an early viral protein (Fig.8B). In parallel, immunostaining studies revealed that pI215L accumulates in viral cytoplasmic factories, colocalizes with other ASFV proteins and shows a diffuse nuclear pattern (Fig.8C), from 8 hpi onwards.

Figure 8. ORF I215L encodes an early viral protein that accumulates in viral factories

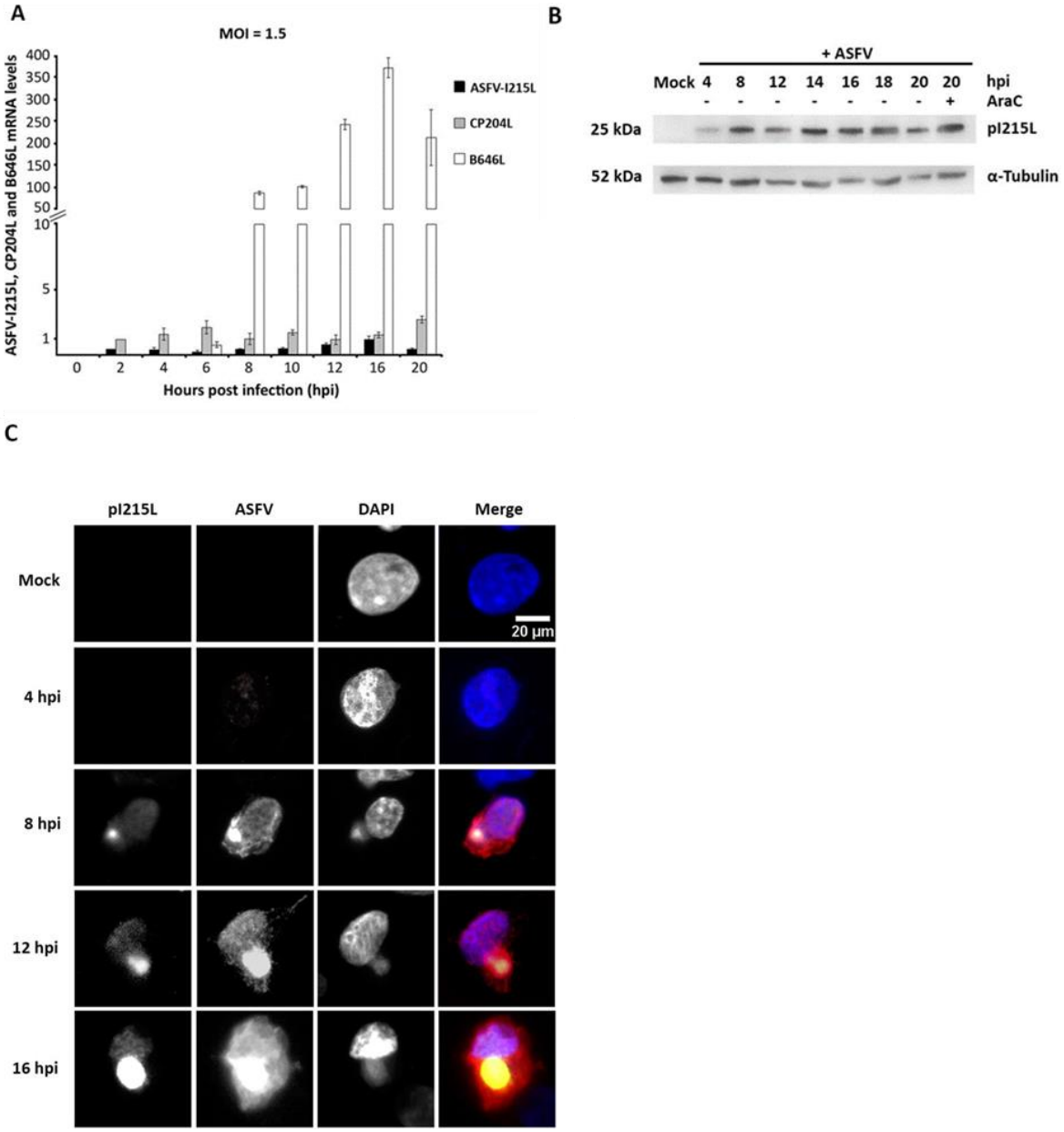

(A) I215L transcripts were detected from 2 hpi onwards showing a maximum peak at 16 hpi. The mRNA levels of CP204L (vp32) and B646L (vp72) were measured in parallel and used as controls of early and late viral gene expression, respectively. Results are shown as mean ± standard error by dividing the number of transcripts of each viral gene by the number of Cyclophilin A mRNA molecules (housekeeping gene), obtained from three independent experiments run in duplicate. (B) ASFV-I215L gene encodes for an early protein detectable from 4hpi onwards, with expressing levels unchanged by the AraC treatment. Vero cells infected with ASFV/Ba71V isolate (MOI of 5) and harvested at the indicated time points. The cytosine arabinoside treatment (AraC, 50 µg/ml) was performed after the initial viral adsorption period (1 hour) and cells were collected at 20 hpi. (C) Vero-infected cells (MOI = 2) were fixed (4, 8, 12 and 16 hpi), immunostained and analyzed by fluorescent microscopy. pI215L was detected from 8 hpi onwards, being recruited to viral factories, co-localizing with other viral proteins (e.g. pA104R and VP72, data not shown) and showing a faint distribution pattern in cell nucleus. In the merged images, pI215L, ASFV and DAPI staining is shown in green, red and blue, respectively. Representative images of at least three independent experiments are shown.

3.3. Knockdown of pI215L impairs viral infection

Considering the in vitro results, and the evidences that ASFV-I215L expression occurs during infection, siRNAs experiments were conducted to further explore the role of pI215L during infection. In order to avoid off-target effects and ensure the biological significance of the results, two siRNAs targeting I215L were used, showing significant knockdown efficiency at 4, 8 and 16 hpi (from −23% to −40%, Fig.9A). The qPCR analysis also revealed that I215L-knockdown cells showed reduced mRNA levels of the late B646L viral gene (up to −57.1%, Fig.9C), when compared to control cells (transfected with siRNA against the housekeeping GAPDH gene), whereas the transcriptional activity of the early CP204L viral gene was unaltered (Fig.9B). In addition, pI215L seems to be involved in ASFV DNA replication, with depleted cells showing lower number of viral genomes (−65.83% for siRNA_1, −64.87% for siRNA_2) and lower viral progeny (from −68.37% to −99.24%) when compared with Vero cells transfected with siRNA against GAPDH ($p \leq 0.05$, Fig.10A and B).

Figure 9. siRNAs targeting I215L disrupt late viral transcription.

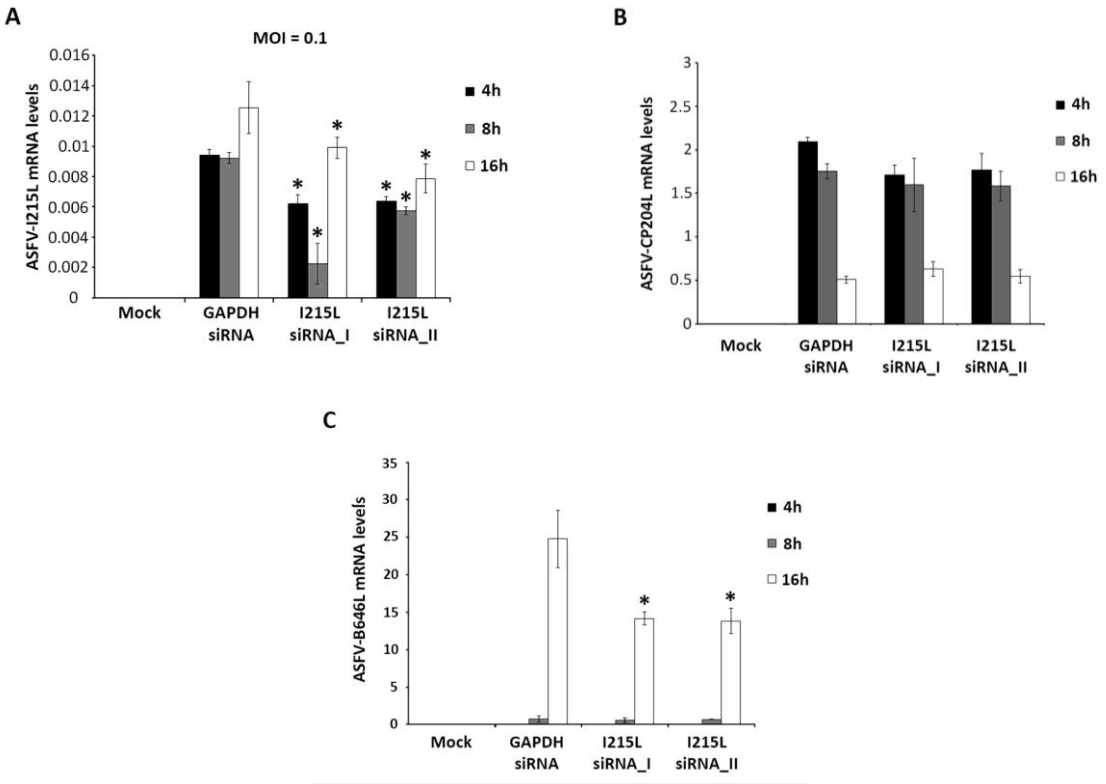

(A) siRNAs against I215L significantly reduced its mRNA levels at 4, 8 and 16 hpi in comparison to the infected control ($p \leq 0.05$). I215L-depleted cells showed significantly lower mRNA levels of the ASFV B646L late gene ($p \leq 0.05$) (C), although the mRNA levels of the early viral gene CP204L (vp32) remained similar to the levels detected in control group (B). Results are shown as average ± standard error (AVG ± S.E.), between the number of molecules of each viral transcript and the number of Cyclophilin A transcripts (housekeeping gene). Data were obtained from three independent experiments run in duplicate.

Figure 10. Knockdown of I215L mRNA levels inhibits ASFV DNA replication andprogeny production.

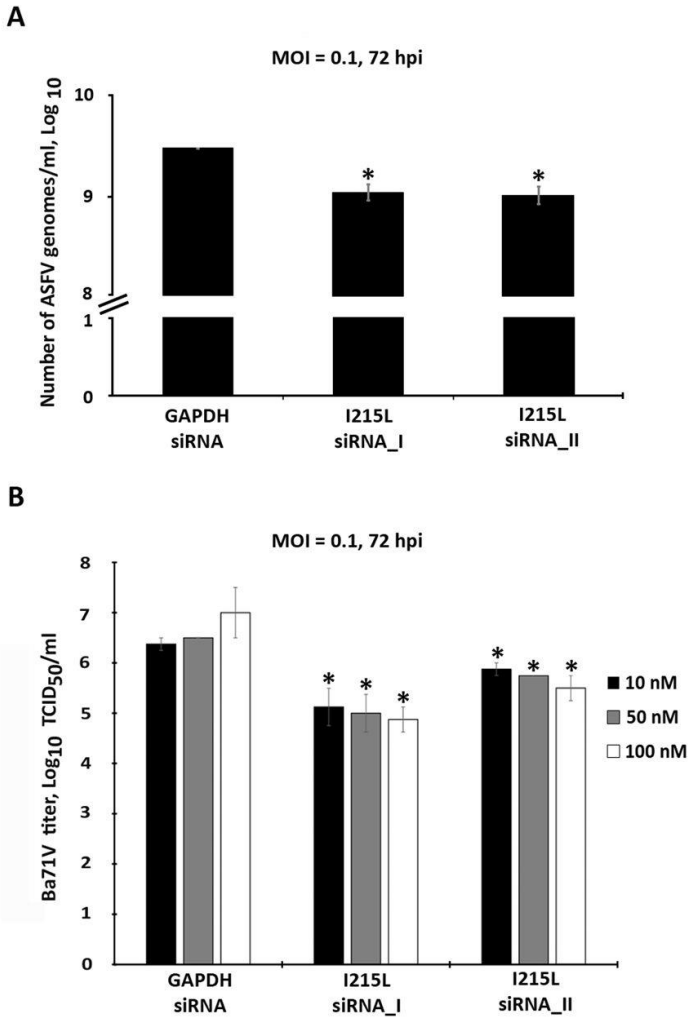

(A) I215L-depleted cells showed a decreased number of ASFV genomes [1.01×10^9 genomes/ml for siRNA_I sequence (−65.83%) and 1.09×10^9 genomes/ml for siRNA_II (−64.87%)] when compared to the control group (2.98×10^9 genomes/ml, $p \leq 0.05$). Results represent the mean of three independent experiments. (B) A statistically significant reduction in viral yield was observed in ASFV-infected Vero cells (MOI of 0.1) transfected with siRNAs against ASFV-I215L (100 nM), in comparison with the GAPDH siRNA-transfected infected cells (between −96.86% and −99.24%; $1 \times 10^{4.88}$ and $1 \times 10^{5.50}$ versus $1 \times 10^{7.00}$ viral particles/ml; $p \leq 0.05$), at 72 hpi. The virus yield of each supernatant was calculated from the average of three independent experiments. Error bars represent standard error (SE) of the mean values.

4. Discussion

For more than 20 years, studies on ASFV have identified the presence a putative E2 Ubiquitin-conjugating enzyme (Dixon et al., 1994; Hingamp et al., 1995; Rodriguez, Salas, & Viñuela, 1992; Yáñez et al., 1995), the first to be described in eukaryotic viruses (Dixon et al., 1994; Hingamp et al., 1995; Rodriguez et al., 1992; Yáñez et al., 1995). Nowadays, it is well known that several viruses modulate the ubiquitin-proteasome system of cells, through different mechanisms, as encoding ubiquitin-related enzymes (Isaacson & Ploegh, 2009; Randow & Lehner, 2009). However, so far the role of the ubiquitination machinery in ASFV infection remains poorly understood, in particular, regarding the function of the viral E2-like protein (pI215L). In this study, we showed that pI215L has the capacity to bind one or two ubiquitin molecules pre-activated by an E1 ubiquitin-activating enzyme, reinforcing the hypothesis that pI215L acts as an E2-like enzyme (Hingamp et al., 1992). This scenario is further supported by the loss of a thioester bond between the carboxyl-terminal of ubiquitin molecules and the conserved catalytic residue of pI215L identified by mutagenesis analysis (Cys 85), when the reducing agent dithiothreitol was added. In addition, the need of ATP and Mg^{2+} as cofactors, mimics the requirements of other E2 ubiquitin-conjugating enzymes (Alonso et al., 2013; Hernáez et al., 2016), strengthening the idea that pI215L acts as an E2 ubiquitin-conjugating enzyme.

Moreover, both ubiquitinated forms of pI215L were detected under a wide range of pH values (4 to 9), suggesting that pI215L found in the viral particles (Hingamp et al., 1995) may remain catalytically active during the cell entry process, which occurs via a low-pH-dependent endosomal pathway (Alonso et al., 2013; Hernáez et al., 2016). This catalytic feature may also contribute to ensure the E2-like activity of pI215L in the midgut epithelial cells of the tick *Ornithodoros* spp., where the pH levels are lower than 7 (Sojka et al., 2013). In parallel, pI215L-ubiquitin conjugates were also observed under a broad range of temperatures (4ºC to 42ºC), further suggesting that pI215L is active in the disease's vector and in infected animals (Lvov, Shchelkanov, Alkhovsky, & Deryabin, 2015). Interestingly, the di-ubiquitinated species were detected earlier (after 1 min of incubation) and in larger amounts than mono-ubiquitinated forms of pI215L (after 5-10 minutes). Although the monoubiquitination is well documented for E2 enzymes (Li et al., 2009; Petroski & Deshaies, 2005), the formation of di-ubiquitinated forms was recently reported in E2 ubiquitin-conjugating enzymes (Hochstrasser, 2006). In this last scenario, the ubiquitin chain pre-generated in the E2 active site may be transferred to a specific E3 ubiquitin ligase and then to the target protein (Li, Tu, Brunger, & Ye, 2007) or be related to a mechanism of E2 autoregulation that may lead to its degradation in the proteasome (David, Ziv, Admon, & Navon, 2010). Moreover, the higher amounts of mono- and di-ubiquitinated forms detected with detergent-soluble protein fractions, as well as poly-ubiquitinated species, suggest that, in cellular context, pI215L may participate in distinct regulation mechanisms,

since the ability to generate diverse substrate-ubiquitin structures is essential to target different host/viral proteins. Indeed, it is reported that monoubiquitination of several nuclear proteins modulates DNA repair and cellular gene expression (Passmore & Barford, 2004; Sadowski & Sarcevic, 2010), whereas the polyubiquitination of a target protein occurs via K48 of ubiquitin can lead to protein degradation through the 26S proteasome pathway or activated phosphatases (Feenstra, Pap, & van Rijn, 2015; Matsuo et al., 2011), or by endocytosis if polyubiquitination occurs via K63 residue of ubiquitin. Also noticeable is the distinct pool of di-ubiquitinated forms detected in detergent-insoluble extracts, probably caused due to the pI215L binding affinity to host proteins containing an ARID DNA-binding domain (Bulimo et al., 2000).

Results obtained from the ASFV-infected Vero cells revealed that I215L viral gene is transcribed throughout infection, showing two transcription peaks (at 2 and 16 hpi), suggesting that pI215L may be required at different stages of the viral life cycle (e.g. viral transcription, genome replication and viral egress), as reported for other viruses (Fukuyo, Horikoshi, Ishov, Silverstein, & Nakajima, 2011). As expected, the pI215L was detected throughout infection (from 4 hpi to 20 hpi), even in the presence of AraC, proving that pI215L is an early viral protein and corroborating the idea that ubiquitin expression must be tightly regulated during ASFV infection (Ferreira, 1996). Immunolocalization studies revealed that pI215L is recruited to viral factories, strengthening the hypothesis that this viral E2 ubiquitin-conjugating enzyme is involved in viral transcription and/or DNA replication, while its diffuse distribution throughout the cytoplasm may be related to its role in ubiquitination of viral proteins and/or host proteins involved in nuclear functions (e.g. antiviral responses, DNA damage responses). Finally, results from siRNA experiments disclosed that pI215L is involved in the late viral transcription with pI215L-knockdown cells showing a lower number of B646L transcripts, while the mRNA levels of the early viral gene CP204L remained unchanged in comparison with mock-transfected Vero cells. Additionally, a decreased number of ASFV genomes (between 63 to 68 %) and a reduced viral progeny (up to -94%) was detected also in pI215L-depleted cells presented, even though siRNAs targeting I215L transcripts exhibited a moderate gene-silencing efficiency (-23 to -40%). Altogether, these results strongly suggest that ASFV genome replication, viral late transcription and progeny production are mediated thought the ubiquitin pathway, as reported for other human and swine viruses (Calistri et al., 2014). These findings are schematically illustrated in the proposed working model for ASFV-pI215L presented as Figure 11.

In summary, our results showed that pI215L plays a key role in ASFV infection, probably by interfering with the ubiquitin machinery and, therefore potentially modulating many viral mechanisms (e.g. transcription, replication and encapsidation) and cellular functions (e.g. antiviral responses, DNA damage responses, apoptosis), raising the hypothesis that an ASFV mutant lacking ORF I215L can be a good candidate for the development of an effective DISC

vaccine, a novel vaccination strategy successfully used in other animal viral disease (Matsuo et al., 2011) Indeed, an ASFV I215L-defective mutant is expected to enter host cell and to express the immediate-early genes products, providing enough antigens to induce a protective response in infected pigs and producing a noninfectious progeny that undergo only one cycle of replication. As vaccines, these defective viral mutants are designed to combine the safety and advantages of inactivated vaccines with the immunogenic activity of live viral vaccines, requiring a complementary cell line that expresses pI215L in order to isolate and propagate the ASFV mutant obtained by homologous recombination.

Figure 11. Proposed working model of the role of pI215L during ASFV infection.

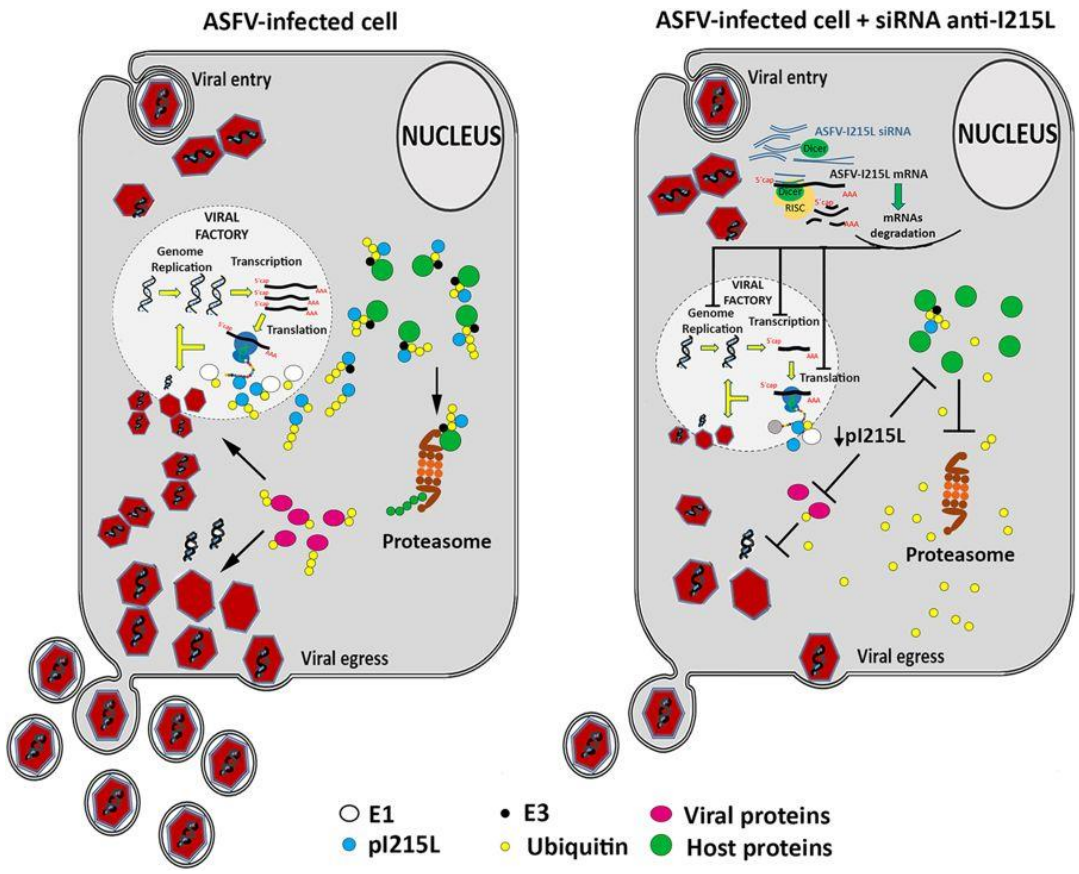

Once ASFV enters the host cell, different host mechanisms are subverted in other to generate a productive infection. By encoding an E2 ubiquitin-conjugating enzyme (pI215L), ASFV hijacks the cellular ubiquitin-proteasome system modulating the function and subcellular localization of host proteins and its own proteins. By controlling the ubiquitination status of the cellular proteins, viruses are able to evade host antiviral responses by targeting proteins to proteasomal degradation and to modulate the activity of viral proteins in different mechanisms. Our model suggests that by downregulating I215L expression, a reduction in the abundance of ubiquitin-tagged proteins occurs and consequently causes an inhibition of several crucial viral processes (e.g. genome replication, gene transcription, translation, egress), as well as host pathways (e.g. antiviral immune response, apoptosis).

Acknowlegments

This work was supported by Fundação para a Ciência e a Tecnologia (CIISA-UID/CVT/00276/2013) and by the European Union's Seventh Framework Programme (FP7/2007-2013, Grant 311931, ASFORCE). FBF and GF were supported by doctoral scholarships from Fundação para a Ciência e a Tecnologia (SFRH/BD/104261/2014, SFRH/BD/89426/2012).

Contributions

F.B.F. and F.F. designed the experiments and the conception of the study. F.B.F. and G.F. carried out the experiments. F.B.F. and F.F. analyzed the data. F.B.F., C.M. and F.F. drafted and review the manuscript.

CHAPTER III

The QP509L and Q706L superfamily II RNA helicases of African swine fever virus are required for viral replication, having non-redundant activities.

Ferdinando B. Freitas, Gonçalo Frouco, Carlos Martins, Fernando Ferreira (2019)
Emerging Microbes & Infections, 8:1, 291-302
https://doi.org/10.1080/22221751.2019.1578624

Abstract

African swine fever virus is complex DNA virus that infects pigs with mortality rates up to 100% leading to devastating socioeconomic effects in the affected countries. There is neither a vaccine nor a treatment to control ASF. African swine fever virus genome encodes two putative SF2 RNA helicases (QP509L and Q706L). In the present study, we found that these two RNA helicases do not share a common ancestral besides sharing a sequence overlap. Although our phylogenetic studies revealed that they are conserved among virulent and non-virulent isolates, it was possible to observe a degree of variation between isolates corresponding to different genotypes occurring in distinct geographic regions. Further experiments showed that QP509L and Q706L are actively transcribed from 2 hours post infection. Immunoblot analysis revealed that both protein co-localized in the viral factories at 12 hours post infection, however, QP509L was also detected in the cell nucleus. Finally, siRNA assays uncover the relevant role of these proteins during viral cycle progression in particular for the late transcription, genome replication and viral progeny (a reduction of infectious particles up to 99.4% when siRNA against QP509L was used and 98.4 % for siRNA against Q706L). Thus, our results suggest that both helicases are essential during viral infection, highlighting the potential use of these enzymes as target for drug and vaccine development against ASF.

1. Introduction

African swine fever (ASF) was first described in 1921 by Montgomery (Montgomery, 1921), being caused by African swine fever virus a large (≈200nm), enveloped, icosahedral double-stranded DNA virus, which belongs to the NCLDV group and family *Asfarviridae* (Tulman et al., 2009). In domestic pigs, the African swine fever virus (ASFV) replicates, preferentially, in cells of the monocyte lineage causing a broad range of symptoms and lesions, ranging from hyperacute to chronic forms of disease, with mortality rates up to 100%. Therefore, ASF leads to devastating effects on pig production and animal trade with high economic and social costs to affected areas (Costard et al., 2009; Penrith & Vosloo, 2009).

Besides being endemic in most sub-Saharan countries and in Sardinia, ASF was introduced in Georgia (2007) spreading to neighboring countries including Armenia, Azerbaijan, Russia (Gulenkin, Korennoy, Karaulov, & Dudnikov, 2011; Sánchez-Vizcaíno et al., 2015) and, Ukraine and Belarus (from 2012 to 2013). In 2014, ASF was reported in Lithuania, making the first arrival of the disease in European Union in decades, before outbreaks in Poland, Estonia and Latvia (Stokstad, 2017). During 2016, ASF was declared in Moldova and last year in Czech Republic, Romania, Hungary and Belgium (August 2018) putting the European Union on high alert. Also during the last months of 2018, and for the first time, ASF was identified in several cities of China, and also in Vietnam during 2019 (WAHID, 2019.). Since neither, a vaccine nor a treatment is available, the control of the disease rely on sanitary measures, including stamping out and trade bans of animals and pork products.

Under this scenario, further studies are needed towards the identification of ASFV genes that regulate viral replication and transcription, in order to develop an efficient vaccine and/or to use as targets for antiviral agents (Arias et al., 2017; Galindo & Alonso, 2017). In other virus, RNA helicases have been described as essential for infection, modulating RNA-RNA and RNA-protein interactions, gene expression, viral egress and host antiviral responses (Frick & Lam, 2006; Ranji & Boris-Lawrie, 2010), being used for novel antiviral strategies (Briguglio et al., 2011; Ranji & Boris-Lawrie, 2010; Shuman, 1992). Interestingly, ASFV encodes for five putative RNA helicases, including the DEAD-box ATP-dependent RNA helicases QP509L and Q706L (Arias et al., 2017; Frick & Lam, 2006; Galindo & Alonso, 2017; Ranji & Boris-Lawrie, 2010). Although *in silico* analysis revealed that QP509L is orthologous to the vaccinia virus A18R helicase (S. A. Baylis et al., 1993; Roberts et al., 1993; Rodríguez & Salas, 2013) and Q706L to the vaccinia virus D6/D11 helicase (Rodríguez & Salas, 2013; Yáñez et al., 1993), no additional information is available on these viral enzymes. Therefore, in this study, we investigated the monophyly of the five RNA helicases encoded by ASFV and explore the phylogenetic relationship of the QP509L and Q706L among different ASFV isolates and with DEAD-box ATP-dependent RNA helicases from other nucleocytoplasmic large DNA viruses (NCLDV), (Yutin & Koonin, 2012). The dynamics of the transcription and expression patterns

of ASFV-QP509L and ASFV-Q706L RNA helicases were evaluated during the infection, as well as their intracellular distribution. Finally, the involvement of each ASFV RNA helicases in viral transcription, genome replication and progeny production was assessed by siRNA-mediated silencing.

2. Material and methods

2.1. Phylogenetic analysis

Amino acid sequences of the five ATP-dependent RNA helicases of ASFV (QP509L, Q706L, A859L, B962L and D1133L) were obtained by in silico translation using genomic sequences of different ASFV isolates available in GenBank (ASFV/Ba71V, NC_001659.1; ASFV/Benin 97/1, AM712239.1; ASFV/L60, KM262844.1; ASFV/OURT 88/3, AM712240.1; ASFV/Mkuzi 1979, AY261362.1; ASFV/Georgia 2007/1, FR682468.1; ASFV/Malawi Lil/20/1, AY261361.1; ASFV/Kenya 1950, AY261360.1; ASFV/NHV 1968, KM262845.1; ASFV/Tengani 62, AY261364.1; ASFV/Warmbaths 2003, AY261365.1; ASFV/Pretorisuskop/96/4, AY261363.1; ASFV/Warthog 2004, AY261366.1). Similarly, the amino acid sequences of other superfamily 2 (SF2) RNA helicases encoded by different NCLDV (*Ranavirus,* ORF55, ASQ42908.1; *Bathycoccus sp*. RCC1105 virus BpV1, BpV1_050, NC_014765.1; *Acanthocystis turfacea Chlorella* virus, TN603.4.2_736L, JX997186.1; *Paramecium bursaria Chlorella* virus CVM-1, CVM-1_251R, JX997163.1; *Vaccinia* virus, A18R, NC_006998.1; *Vaccinia* virus, D11, NC_006998.1; *Marseillevirus marseillevirus*, MAR_ORF241,NC_013756.1; *Ostreococcus tauri* virus, OtV6_066, JN225873.1) and by pig (*Sus scrofa,* DDX58, AAG09428.1) were also retrieved from GeneBank.

MAFFT software (version 7, https://mafft.cbrc.jp/alignment/server/) was used to perform sequence alignments (employing default parameters) (Katoh, Rozewicki, & Yamada, 2017; Kuraku, Zmasek, Nishimura, & Katoh, 2013) and MEGA 7 *software* was used to selected the best model (ML) for phylogenetic tree construction based on amino acid alignments(Kumar, Stecher, & Tamura, 2016; Nei & Kumar, 2000). Maximum likelihood trees were constructed by adopting Le_Gascuel_2008 model with 1000 bootstrap replicates, using MEGA 7 (Kumar et al., 2016; Le & Gascuel, 2008).

2.2. Cells and virus

Vero E6 cells obtained from the European Authenticated Cell Cultures Collection (ECACC, Salisbury, UK) were maintained in DMEM (Dulbecco Modified Eagle's minimal essential medium) supplemented with L-GlutaMax, 10% heat-inactivated fetal calf serum, 1x non-

essential amino acids and penicillin/streptomycin at 100 units/ml (all from Gibco, Life Technology, Karlsruhe, Germany). All experiments were conducted on actively replicating sub confluent cells, grown at 37 °C, under a 5% CO_2 humidified atmosphere (≥95% air). The Vero-adapted ASFV strain (Badajoz 1971, Ba71V) was used in all infections and propagated as previously described (Carrascosa et al., 2011). For viral titration, culture supernatants harvested at 72 hours post infection (hpi) were used to infect new cell monolayers, in 10-fold serial dilutions, during 5 days (Spearman-Kärber endpoint method) using 96-well plates. Cytopathic effect was evaluated and the results were expressed as TCID50/ml.

2.3. RNA extraction and cDNA synthesis

For qPCR analysis, total RNA was extracted from ASFV-infected Vero cells (MOI=1.5) at different time points of infection, using the RNeasy Mini Kit (Qiagen, Courtaboeuf, France) and with possible DNA contaminants degraded by a treatment in column with DNAse I (Qiagen). RNA concentrations and purity were measured using a spectrophotometer (NanoDrop 2000c, Thermo Fisher Scientific, Waltham, USA) and only RNA samples showing high purity (A260/A280 ratio between 1.8 and 2.0) were used. 200 ng of each total RNA sample was reverse transcribed (Transcriptor First Strand cDNA Synthesis Kit, Roche, Basel, Switzerland), according to the manufacturer's instructions. The obtained cDNA was diluted (1/20) in ultra-pure water and stored at -20 °C until further use.

2.4. Recombinant plasmids

The amplified fragments (ASFV-QP509L, ASFV-Q706L, ASFV-CP204L, ASFV-B646L and Cyclophilin A) were cloned into a plasmid vector (pGEM-Teasy Vector System II, Promega, Madison, USA), and used to transform DH5α competent cells. Then, plasmids were isolated from bacteria using the Roche High Pure Plasmid Isolation Kit (Roche Applied Science, Germany), according to the manufacturer's manual. To determine whether the cloned DNA fragments were incorporated into vectors, the inserts were amplified by PCR and their sequences were confirmed. Following this step, the concentration of each plasmid preparation was determined by spectrophotometric absorbance (NanoDrop 2000c). Their corresponding copy number was calculated using the equation: pmol (dsDNA) = µg (dsDNA) x 1515 / DNA length in pb (pmol = picomoles, dsDNA = double-strand DNA, DNA length in pb = number of base pairs from the amplified fragment; 1 mol = 6.022 x 10^{23} molecules).

2.5. Standard curves optimization

Ten-fold serial dilutions of each plasmid (ASFV-QP509L, ASFV-Q706L, ASFV-CP204L, ASFV-B646L and Cyclophilin A), ranging from $1x10^{-1}$ to $1x10^{-9}$ were initially used in duplicate to generate the standard curves in two different days. Threshold cycle (Ct) values obtained from each dilution were plotted against the logarithm of their initial template copy numbers and corresponding standard curves were generated by linear regression of the plotted points. From the slope of each standard curve, PCR amplification efficiency (E) was calculated according to the equation: $E (\%) = (10^{-1}/slope^{-1}) \times 100\%$ (Pfaffl, 2001).

2.6. Quantitative PCR

Quantification of ASFV-QP509L, ASFV-Q706L, ASFV-CP204L and ASFV-B646L transcripts were performed by qPCR using the Maxima SYBR Green PCR Master Mix (Thermo Fisher), according to the manufacturer's instructions [12.5 µl of master mix, 2.5 µl of forward and reverse primers (50 nM each), 5 µl of Milli-Q water and 2.5 µl of cDNA)]. All qPCR reactions were performed in Applied Biosystems 7300 Real Time PCR system (Thermo Fisher), using the following thermal profile: 10 min at 95°C for initial denaturation; 40 cycles of 15 s at 95°C and 60 s at 60°C, followed by a final denaturation step of 5 s at 65°C with a 20°C/s ramp rate and subsequent heating of the samples to 95°C with a ramp rate of 0.1°C/s. Quantification of ASFV-QP509L, ASFV-Q706L, ASFV-CP204L, ASFV-B646L and Cyclophilin A mRNA levels were determined by the intersection between the fluorescence amplification curve and the threshold line. The crossing point values of each plasmid obtained from different known concentrations were plotted in a standard curve used to determine the copy number of each transcript. The values were determined using the comparative threshold cycle method, which compares the expression of a target gene normalized to the reference gene (Cyclophilin A). The validation of the reference gene was confirmed using the ANOVA test ($p<0.05$) and the specificity of the qPCR assays was confirmed by melting curve analyses. Sequences of the primers used in this study are shown in Table 4. To characterize the transcription pattern of both ASFV RNA helicases, Vero cells grown onto 30 mm dishes were infected (MOI=1.5) and collected at indicated time points (0, 2, 4, 6, 8, 10, 12, 16 and 20 hpi), for total RNA extraction. Results represent the mean value of two independent experiments performed in different days.

Table 4. Primers used in the present study.

Target	Primer designation	Sequence (5´- 3´)	Target coordinates*	Orientation
ASFV-QP509L	509FwE	GTGCCTGAGAAAGAGCGGTA	142562-142581	Forward
ASFV-QP509L	509FwI	GTCCCACCACAACCTTTTCC	142927-142908	Forward
ASFV-QP509L	509RvI	AATACACACAGGGCTAACGAAGT	142870-142848	Reverse
ASFV-Q706L	706FwE	TCCCCGTCCAAATAGAAGCA	142211-142192	Forward
ASFV-Q706L	706FwI	CAGGGGGAAAACACACGGG	142050-142032	Forward
ASFV-Q706L	706RvI	AAGTGAGATGGCAAGCGACA	154439-154420	Reverse
Cyclophilin A	CycloFw1	AGACAAGGTTCCAAAGACAGCAG	-	Forward
Cyclophilin A	CycloRev	AGACTGAGTGGTTGGATGGCA	-	Reverse
Cyclophilin A	CycloFw2	TGCCATCCAACCACTCAGTCT	-	Forward
ASFV-B646L	VP72Fw	ACGGCGCCCTCTAAAGGT	88273-88290	Forward
ASFV-B646L	VP72Rev	CATGGTCAGCTTCAAACGTTTC	88322-88343	Reverse
ASFV-CP204L	VP32Rev	TCTTTTGTGCAAGCATATACAGCTT	108162-108186	Forward
ASFV-CP204L	VP32Fw	TGCACATCCTCCTTTGAAACAT	108228-108249	Reverse
ASFV-QP509L	509FwSacI1	GAGCTCATGGCTTACAATAATGCAGCGTG	143213-143194	Forward
ASFV-QP509L	509RvXhoI1	CTCGAGAGGGCTAACGAAGTCAGGA	142875-142857	Reverse
ASFV-QP509L	509FwSacI2	GAGCTCATGTACGGGCGTAGAGGCA	142529-142514	Forward
ASFV-QP509L	509RvXhoI2	CTCGAGTTTGGACGGGGAAGGA	142215-142200	Reverse
ASFV-Q706L	706FwNdeI1	CATATGATGTATGAAAGATTCTACACCGCTTATG	141540-141516	Forward
ASFV-Q706L	706RvXhoI1	CTCGAGTTTTAGCATGCGCACTATTTT	141108-141088	Reverse
ASFV-Q706L	706FwNdeI2	CATATGATGTCTAAAACGGGAGCTGAGG	140742-140724	Forward
ASFV-Q706L	706RvXhoI2	CTCGAGTTCGTAAAAGGTATAGCCTAATCCTAC	140241-140215	Reverse

*Primer coordinates are relative to Ba71V sequence used has template for primer design.

2.7. Cloning, expressing and purifying recombinant fragments of ASFV-QP509L and ASFV-Q706L

In order to produce antibodies against ASFV-QP509 and ASFV-Q706L, the hydrophobicity profile of both viral proteins was analyzed to select two distinct hydrophilic regions in each ORF. Taking into account this information, specific primers were designed to include in the 5´and 3´, a restriction enzyme site to facilitate vector insertion [ASFV-Q706L, clone using NdeI (5') and XhoI (3'); ASFV-QP509L, clone using SacI (5') and XhoI (3')] and the correspondent DNA fragments were amplified by PCR. The PCR reactions were performed as follows: 1x 98ºC for 2', 30x 98ºC for 30'', 72ºC for 1'10'' plus one extension step of 72ºC for 10'. After size confirmation in agarose gel (1%), the fragments were purified and DNA concentration was quantified (NanoDrop 2000c). The DNA fragments were inserted in the pET24a expression vector (Novagen) in order to add a C-terminal 6xHis tag to allow purification. Two clones per ORF were sequenced to confirm eventual mutations and plasmids transformed into the *E.coli* strain BL21(DE3)-pLysS (Novagen) and grown in LB medium (10 g tryptone, 5 g yeast extract, 5 g NaCl, pH 7.2), supplemented with kanamycin (30 µg/ml) plus chloramphenicol (34 µg/ml), at 37 °C, with shaking at 200 rpm, until the OD_{600} reached 0.1-0.2. Protein expression was induced by adding isopropyl-β-D-1-thiogalactopyranoside (IPTG, 1 mM, 5 h). After this step, bacterial cells were harvested by centrifugation (10,000 g for 10 min, 4 °C), and washed with sterile water. The pellet was resuspended in binding buffer (20 mM sodium phosphate, 500 mM NaCl, 20 mM imidazole, pH 7.4) and cells were lysed with a lysis solution (0.2 mg/ml

lysozyme, 20 µg/ml DNAse and 1mM PMSF) and sonicated for 5x5 minutes on ice (5 cycles, 70% amplitude). Lysates were then centrifuged at 3000g for 15 minutes and pellets were discarded. The extracts were thereafter filtered (0.45 µm syringe filter Rotilabo®, CarlRoth) and incubated with Ni Sepharose 6 Fast Flow slurry (GE Healthcare) for 1 hour. The mixture was loaded onto a PD-10 column (GE Healthcare), washed with binding buffer solution (20 mM sodium phosphate, 500 mM NaCl, pH 7.4) containing increasing concentrations of imidazole (40, 60 and 80 mM), and the recombinant fragments of pQP509L and pQ706L were eluted with an elution buffer (20 mM sodium phosphate, 500 mM NaCl, 500 mM imidazole, pH 7.4). Finally, fractions were collected in low-binding tubes (Maxymum Recovery® TM tubes, Axygen, Corning Life Sciences, Amsterdam, The Netherlands), analyzed by SDS-PAGE and the recombinant proteins, purified under native conditions and stored at -80 °C until further use.

2.8. Antibody production

Briefly, young female mice (BALB/c, 4 to 6-week-old) were injected subcutaneously with 100µg of each purified fragment of ASFV-pQP509L and ASFV-pQ706L, in a mixture with Freund's complete adjuvant. Following the primary injection, two booster injections were administered at 2-week intervals. After 10 days from the date of the second booster injection, the total blood was collected and sera were aliquoted and stored at -20 °C until further use. The specificity of the polyclonal antiserum was tested against purified recombinant ASFV-pQP509L and ASFV-pQ706L and whole infected-cells extracts.

2.9. Immunofluorescence and microscopy analysis

Vero cells seeded on glass coverslips ($1x10^5/cm^2$) were mock-infected or infected with the ASFV Ba71V isolate (MOI of 1). At 8, 12, and 16 hpi, cells were fixed in 3.7% paraformaldehyde and HPEM buffer [25 mM HEPES (4-(2-hydroxyethyl)-1-piperazineethanesulfonic acid), 60 mM PIPES (piperazine-N,N′-bis 2-ethanesulfonic acid), 10 mM EGTA (ethylene glycol tetraacetic acid) and 1 mM $MgCl_2$] for 15 min, at room temperature, and permeabilized with PBS/Tx-100 (0.5%, v/v) during 5 min. Following this step, cells were washed in PBS, blocked with PBST/BSA (3%, w/v) for 30 min and incubated with the appropriate primary and secondary antibodies. The immunostaining of ASFV-pQP509L and ASFV-pQ706L and ASFV-infected cells was achieved by incubation with two in-house primary antibodies: mouse anti-ASFV-pQP509L and anti-ASFV-pQ706L (1:10 in PBST, 0.01%, overnight, 4ºC) and swine anti-ASFV polyclonal antibody (1:100, 1h, RT). Two secondary fluorescent-conjugated antibodies were used as follows: anti-mouse FITC (1:300, sc-2099, Santa Cruz Biotechnology) and anti-swine

Texas Red (1:500, ab6775, Abcam). Between each antibody incubation, cells were wash twice with PBS (5 min) and once with PBST (0.1% v/v, 5 min). All incubations were performed in a dark humidified chamber to prevent fluorochrome fading and a mounting medium with DAPI (4′,6-diamidino-2-phenylindole) was used to detect the cell nucleus and viral factories (Vectashield, Vector Laboratories, Peterborough, UK).

Fluorescence images were acquired using an epifluorescence microscope equipped with a 40X objective (Leica DMR HC model, Wetzlar, Germany) and data sets were acquired with the Adobe Photoshop CS5 software (Adobe Systems, Inc., San Jose, USA). Images were subsequently processed using the ImageJ open source software (version IJ 1.48g, National Institutes of Health, Bethesda, MD, USA).

2.10. Immunoblot analysis

Vero cells grown in 30 mm dishes were infected with the ASFV-Ba71V isolate (MOI of 5) and when indicated, exposed to cytosine arabinoside (50 µg/ml, AraC; Sigma-Aldrich), after the adsorption period (1h). Following this step and before protein extraction, mock-infected, infected and AraC-treated infected-cells were washed twice with PBS and then lysed in ice-cold modified RIPA buffer [25 mM Tris, 150 mM NaCl, 0.5% (v/v) NP40, 0.5% (w/v) sodium deoxycolate, 0.1% (w/v) SDS, pH 8.2] supplemented with a protease-inhibitor cocktail (cOmplete, Mini, EDTA-free, Roche) and a phosphatase-inhibitor cocktail (PhosStop, Roche). Clarified whole-cell lysates harvested at 4, 8, 12, 14, 16, 18 and 20 hpi, were subjected to SDS-PAGE gel electrophoresis using 8-16% (w/v) polyacrylamide separating gels (Bio-Rad), and transferred to a 0.2 µm pore diameter nitrocellulose membrane (Whatman Schleicher & Schuell) by electroblotting. Blot membranes were then blocked with phosphate-buffered saline plus 0.05% (v/v) Tween-20 (PBST), containing 5% (w/v) of BSA (Sigma-Aldrich), during 1 hour at RT, and thereafter incubated with specific primary antibodies (RT,1 h), followed by a wash step with PBST (3x 10 min). The membranes were then incubated with appropriate secondary antibodies conjugated with HRP, for 1 hour, at RT. Finally, a wash step in PBST (3x 10 min) was performed before protein detection with a chemiluminescence detection kit (Pierce® ECL Western Blotting Substrate, Thermo Scientific), on Amersham Hyperfilm ECL (GE Healthcare). α-Tubulin was used as a loading control. For blot analysis, three primary antibodies (anti-ASFV-pQP509L and ASFV-pQ706L, 1:100; anti-α-tubulin, 1:1250, #2125, Cell Signalling Technology) and two HRP-conjugated secondary antibodies were used (anti-rabbit IgG, 1:10000, 4010-05; anti-mouse IgG, 1:30000, 1010-05; both from SouthernBiotech). All antibody dilutions were performed in blocking solution and incubated according to the manufacturers' recommendations.

2.11. siRNA assays

Four double-stranded siRNAs (ON-TARGETplus, Thermo Fisher Scientific) targeting different sequence regions of the ASFV-QP509L and ASFV-Q706L transcripts were designed (siDESIGN Center, Thermo Fisher Scientific), based on the full genome sequence of ASFV Ba71V isolate (GenBank/EMBL, accession number: ASU18466). One siRNA against the GAPDH gene (siRNA-GAPDH; Silencer™ GAPDH siRNA human control number 4605; Ambion/Thermo Fisher Scientific) was used as a control in all siRNA assays. The siRNA sequences used in the study are shown in Table 5. All siRNAs duplexes were diluted at different final concentrations (10, 50 and 100 nM) in serum-free Opti-MEM (Gibco) and using 8 µl HiPerfect Transfection reagent (Qiagen). Mixtures were incubated at room temperature for 20 min to allow the formation of transfection complexes. Thereafter, 100 µl of the transfection solution was incubated with $2x10^4$ Vero cells cultured in 500 µl of DMEM supplement with 10 % FBS in a 24-well plate, during 8h. One hour before infection, the culture medium was removed and fresh medium was added to allow recovery of the cells. Next, cells were infected with ASFV Ba71V (MOI = 0.1) during one hour and harvested at 37 °C for 16 hpi for quantification of the viral transcripts or 72 h for quantification of genome copy number and viral progeny titration. Due to economic and practical reasons only the two siRNAs duplexes that showed higher inhibitory results (CPE reduction), were used for these assays. To ensure high RNA concentrations, the siRNA assays were performed in quadruplicated and the qPCR assay was performed in duplicate to improve the biological relevance of the results. The ASFV-genome copy number was estimated by measuring B646L gene using qPCR and TaqMan probes (King et al., 2003).

Table 5. siRNA sequences to knockdown ASFV-QP509L and ASFV-Q706L transcripts.

Target	siRNA designation	Sequence (5´- 3´)	Target coordinates*	Orientation
ASFV-QP509L	QP509_IF	GCAAGAAGCCUGAGCAGUUUUUU	596-614	Sense
ASFV-QP509L	QP509_IR	AAAACUGCUCAGGCUUCUUGCUU	596-614	Anti-sense
ASFV-QP509L	QP509_IIF	AGCAAGAAAUGGUCGAUAAUUUU	302-320	Sense
ASFV-QP509L	QP509_IIR	AAUUAUCGACCAUUUCUUGCUUU	302-320	Anti-sense
ASFV-Q706L	Q706_IF	GGAUAAGGCCCGAGAGGAUUUUU	1566-1584	Sense
ASFV- Q706L	Q706_IR	AAAUCCUCUCGGGCCUUAUCCUU	1566-1584	Anti-sense
ASFV-Q706L	Q706_IIF	CCGAAAUGCUAACAGUAAAUUUU	1043-1061	Sense
ASFV- Q706L	Q706_IIR	AAUUUACUGUUAGCAUUUCGGUU	1043-1061	Anti-sense

*siRNA coordinates according to the relative position in gene nucleotide sequence (start at position 1, ATG).

2.12. Statistical analysis

The GraphPad Prism software (version 7.02) was used to perform statistical analysis. The Kolmogorov-Smirnov test was used to verify the normal distribution of data from the RNAi assays (mRNA expression, ASFV genome copy number and virus titre) and differences between experimental groups were identified by the non-parametric Wilcoxon-Mann-Whitney test. *p*-values less than 0.05 were considered statistically significant.

3. Results

3.1. The ASFV DEAD-box RNA helicases QP509L and Q706L are conserved among virulent and non-virulent isolates, uncovering genotype clustering and showing partial homology with RNA helicases of other NCLDV

The sequence homology analysis among the five ASFV RNA helicases, revealed a high degree of similarity between virulent and non-virulent ASFV isolates (e.g. L60 and Ba71V, Fig.12A). Our analysis also showed that ASFV RNA helicases do not share a common ancestor, with the exception of ASFV-Q706L and ASFV-D1133L helicases that form a monophyletic group (Fig.12A). Surprisingly, no phylogenetic relation was found between ASFV-QP509L and ASFV-Q706L, although belonging to the Super family 2 and sharing a DEAD-box domain and a sequence overlap of 126 base pairs (bp) (between 3' end of ASFV-QP509L and 5' end of ASFV-Q706L, Fig.12B).

Figure 12 The ASFV-QP509L and Q706L RNA helicases are highly conserved among virulent and non-virulent isolates, sharing a distinct ancestor.

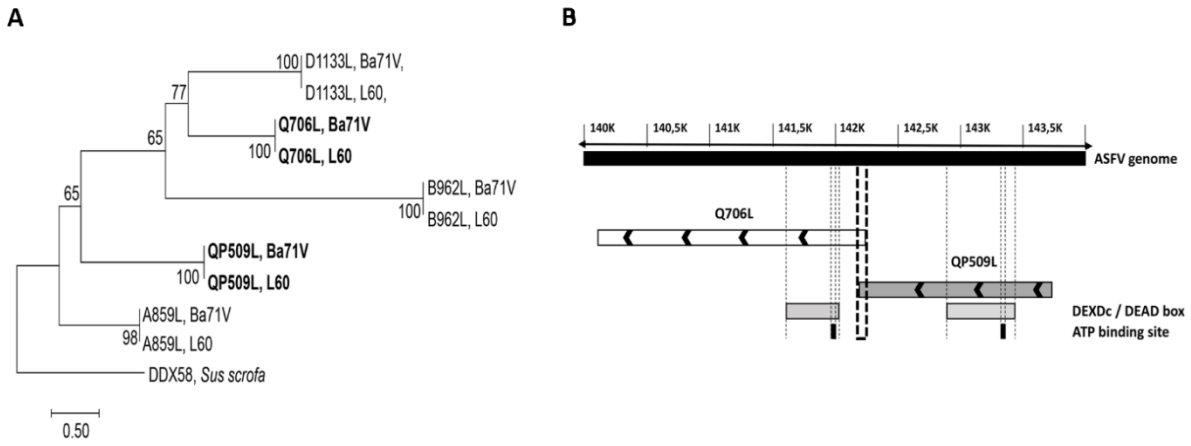

(A) Phylogenetic analysis of ASFV RNA helicases. Maximum-likelihood phylogenetic tree constructed from a multiple amino acid sequence alignment of ASFV-QP509L, Q706L, A859L, B962L, D1133L ORFs, using two different ASFV isolates (L60 – virulent and Ba71V – non-virulent). Sequence from a RNA helicase SF2 of Sus scrofa worked as outgroup. Bootstrap values are indicated. (B) Schematic representation of ASFV genome, including the localization of ASFV-QP509L and ASFV-Q706L. Relative positions of DEAD box motifs, ATP-binding sites and sequence overlap (126 bp) are represented.

Furthermore, the phylogenetic analysis of both SF2 RNA helicases among different ASFV isolates, showed a similar cluster distribution, with sequences from the West of Africa and Europe (e.g. Angola, L60, Ba71V) being separated from isolates of East Africa countries (e.g. Kenya 1950 and Malawi 1983) and also from South African isolates (e.g. Mkuzi 1979) (Fig.13 A and B). In addition, the sequence of ASFV-QP509L RNA helicase from the European isolate Georgia 2007/1 clusters with the Tengani 1962 (Malawi) isolate (Fig. 13A), whereas the ASFV-Q706L sequence from Georgia 2007/1 appears isolated (Fig. 13B). Finally, the comparison of

the amino acid sequences between the two SF2 RNA helicases encoded by ASFV and SF2 RNA helicases encoded by other NCLDV members revealed that ASFV-QP509L clusters with the A18 helicase from vaccinia virus and with ORF55 Ranavirus helicase, as ASFV-Q706L clusters with vaccinia virus D11 helicase and MAR_ORF241 helicase of Marseillevirus (Fig. 13C). This analysis also showed that ASFV-QP509L sequence is more close to other viral SF2 RNA helicases encoded by other NCLDV than ASFV-Q706L (e.g. *Bathycoccus sp*. RCC1105 virus; *Ostreococcus tauri*; *Chlorella virus* 1) (Fig. 13C).

Figure 13. ASFV-QP509L and ASFV-Q706L RNA helicases show a similar genotype cluster segregation to ASFV-B646L, sharing the same monophyletic groups with other SF2 RNA helicases from NCLDV.

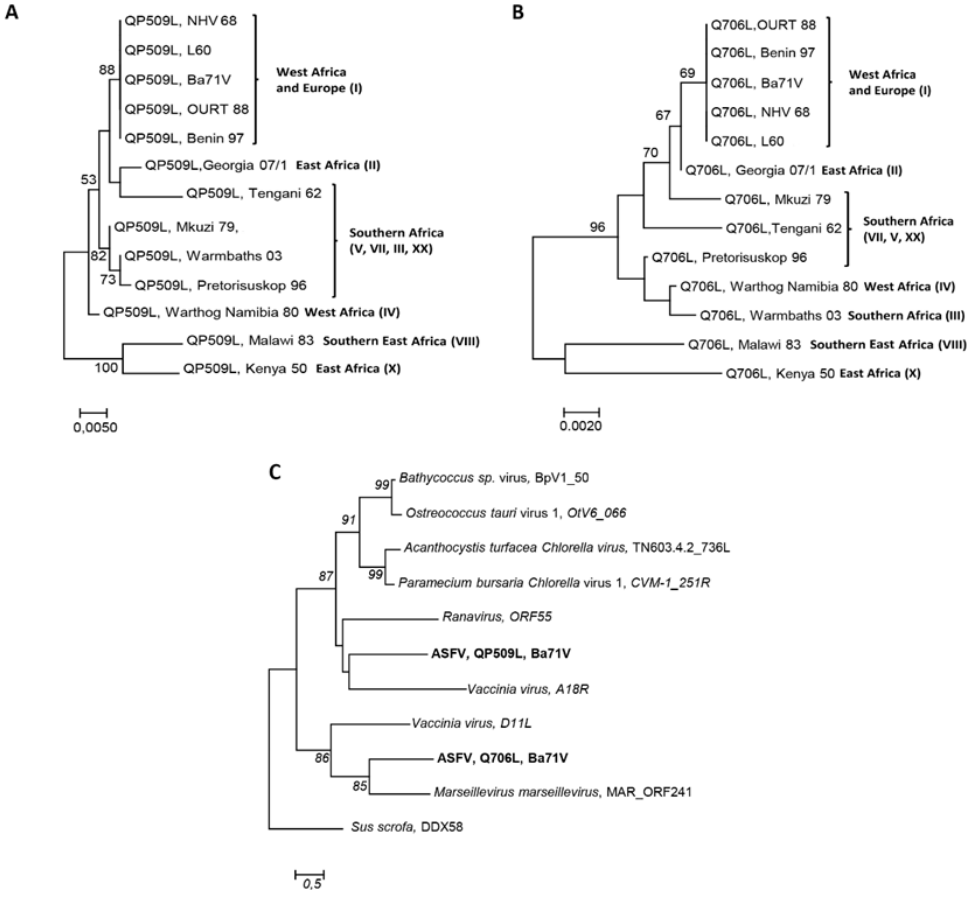

(A) The maximum-likelihood phylogenetic tree was constructed from a multiple amino acid sequence alignment of ASFV-QP509L, using 13 different ASFV isolates. (B) Maximum-likelihood phylogenetic tree was constructed from a multiple amino acid sequence alignment of ASFV-Q706L, using 13 different ASFV isolates. Geographic distribution and genotype of ASFV isolates are also indicated. (C) Phylogenetic analysis of ASFV-QP509L, ASFV-Q706L and other viral Superfamily 2 (SF2) RNA helicases. The maximum-likelihood tree was generated from a multiple amino acid sequence alignment of ASFV-QP509L and ASFV-Q706L RNA helicases with other SF2 encoded by NCLDV members. The sequence of one SF2 RNA helicase of *Sus scrofa* (DDX58) acted as outgroup. Bootstrap values are indicated.

3.2. QP509L and Q706 ASFV genes are transcribed during infection, encoding for two intermediate-late proteins with distinct localization

The detection and quantification of specific viral transcripts by qPCR revealed that QP509L gene is actively transcribed from 2 hpi onwards, reaching a maximum concentration peak at 12 hpi (Fig. 14A). Similarly, the ASFV-Q706L transcripts were detected from 2 hpi, showing a peak concentration at 10 hpi (Fig. 14B). As expected, the mRNA levels of both ASFV SF2 RNA helicases were found much lower than the transcripts of two viral genes (CP204L and B646L) which encode for two structural proteins (vp32 and vp72, Fig. 14 C and D), suggesting that expression of the two ASFV RNA helicases is highly regulated.

Figure 14.ASFV-QP509L and ASFV-Q706L are transcribed from early times of infection.

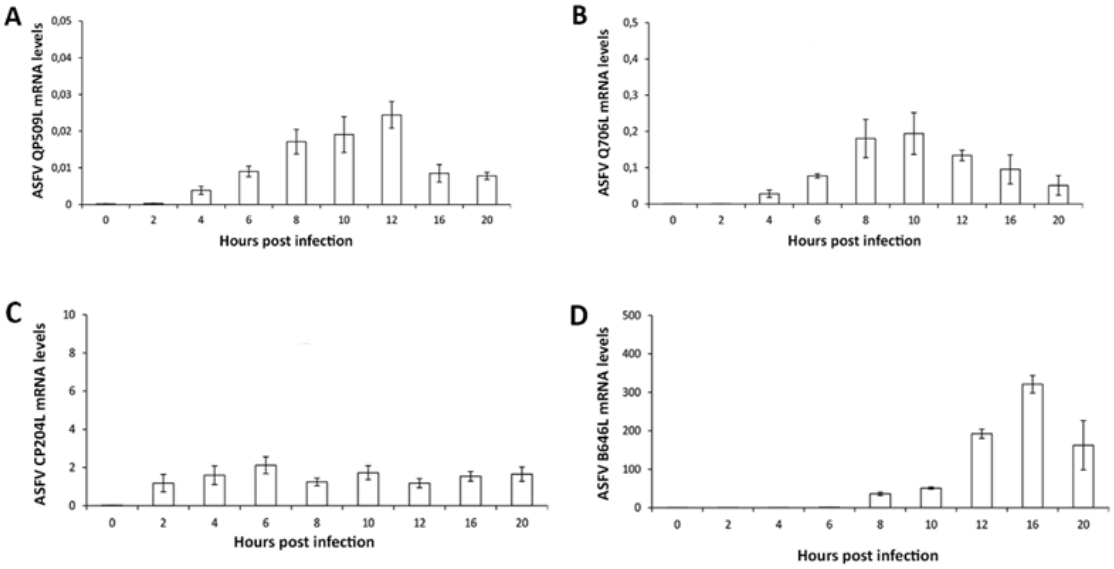

(A) ASFV-QP509L transcripts were detected from 2 hpi, showing a maximum concentration peak at 12 hpi. (B) ASFV-Q706L transcripts were detected from early times of infection (2 hpi) reaching a maximum concentration at 10 hpi. (C, D) ASFV-CP204L and ASFV-B646L mRNA were used as controls. Results are shown as mean ± standard error of the number of transcripts of each viral gene normalized with Cyclophilin A mRNA levels (reference gene). Three independent experiments were performed in duplicate.

In parallel, immunostaining studies showed that pQP509L accumulates in viral cytoplasmic factories from 12 hpi onwards, displaying a diffuse nuclear localization at later times of infection (Fig. 15A). Regarding pQ706L, results disclosed that this viral protein is also detected from 12 hpi onwards, without any nuclear staining (Fig. 15B). The immunoblot analysis unveiled that pQ706L is detectable from 12 hpi onwards, showing increased concentrations among infection course, corroborating the immunostaining results (Fig. 15C). Finally, pQ706L expression was absent in ASFV-infected cells exposed to cytosine arabinoside (AraC), an inhibitor of ASFV

DNA replication and late transcription (Fig. 15C), suggesting that ASFV-Q706L RNA helicase is synthesized before viral DNA replication.

Figure 15. ASFV-pQP509L and ASFV-pQ706L are detected at late times of infection, showing distinct distribution patterns.

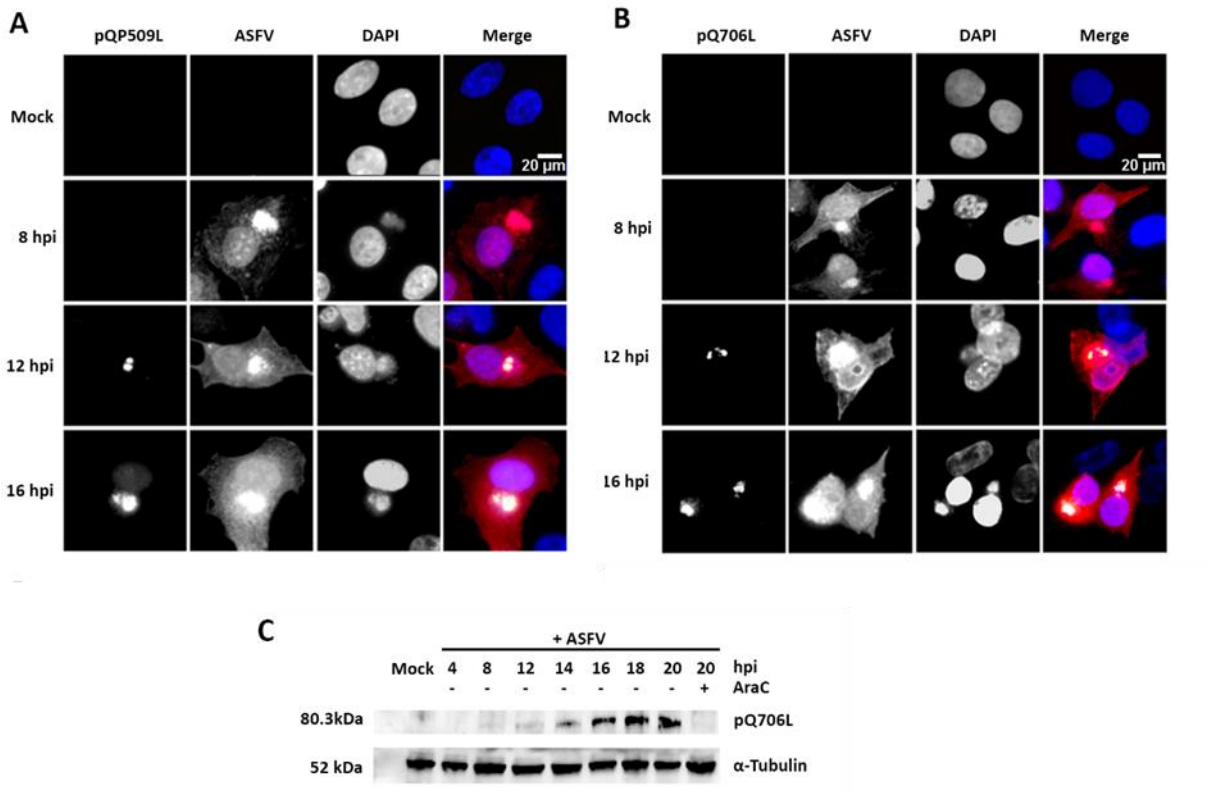

(A) ASFV-pQP509L was detected at viral factories and host nucleus from 12 hpi onwards. (B) ASFV-pQ706L was identified only within viral factories and also after 12 hpi. Vero-infected cells (MOI= 2) were fixed (4, 8, 12 and 16 hpi), stained and analyzed by fluorescence microscopy. In the merged images, ASFV-pQP509L and ASFV-pQ706L were labelled in green, infected cells in red and DNA in blue (DAPI staining). Representative images of at least three independent experiments are shown. (C) Immunoblot analysis revealed that ASFV-pQ706L is a late protein, being absence in the presence of cytosine arabinoside (AraC). Vero cells infected with ASFV/Ba71V isolate (MOI of 5) were harvested at the indicated time points. The AraC (50 µg/ml) exposure was performed after an initial viral adsorption period (1 hour) and cells were collected at 20 hpi.

3.3. QP509L and Q706L ASFV RNA helicases are required for viral infection showing non-redundant functions

Taking in the consideration, the expression patterns of both viral SF2 RNA helicases, siRNAs experiments were performed to explore the downregulation effect of ASFV-pQP509L or ASFV-pQ706L in viral replication. To achieve this goal, the efficacy of two siRNAs targeting each ASFV transcript was separately assed. A significant knockdown efficiency was found for both siRNAs targeting ASFV-QP509L transcripts (up to -41.2%, $p \leq 0.05$, Fig. 16A) and for a siRNA duplex against ASFV-Q706L transcripts (up to -41.7%, $p \leq 0.05$, Fig.16D). Additional qPCR analysis revealed lower transcription levels of ASFV B646L late gene in ASFV-QP509L

depleted cells (up to -46.2%, p≤0.05, Fig. 16C) and in ASFV-Q706L knockdown cells (up to -77.7%, p≤0.05, Fig. 5F) in comparison to control infected cells (transfected with siRNA targeting GAPDH transcripts). However, no significant reduction in the transcriptional activity of ASFV CP204L early gene was found (Fig. 16 B and E).

Figure 16. siRNAs targeting ASFV-QP509L and ASFV-Q706L transcripts disrupt late viral transcription.

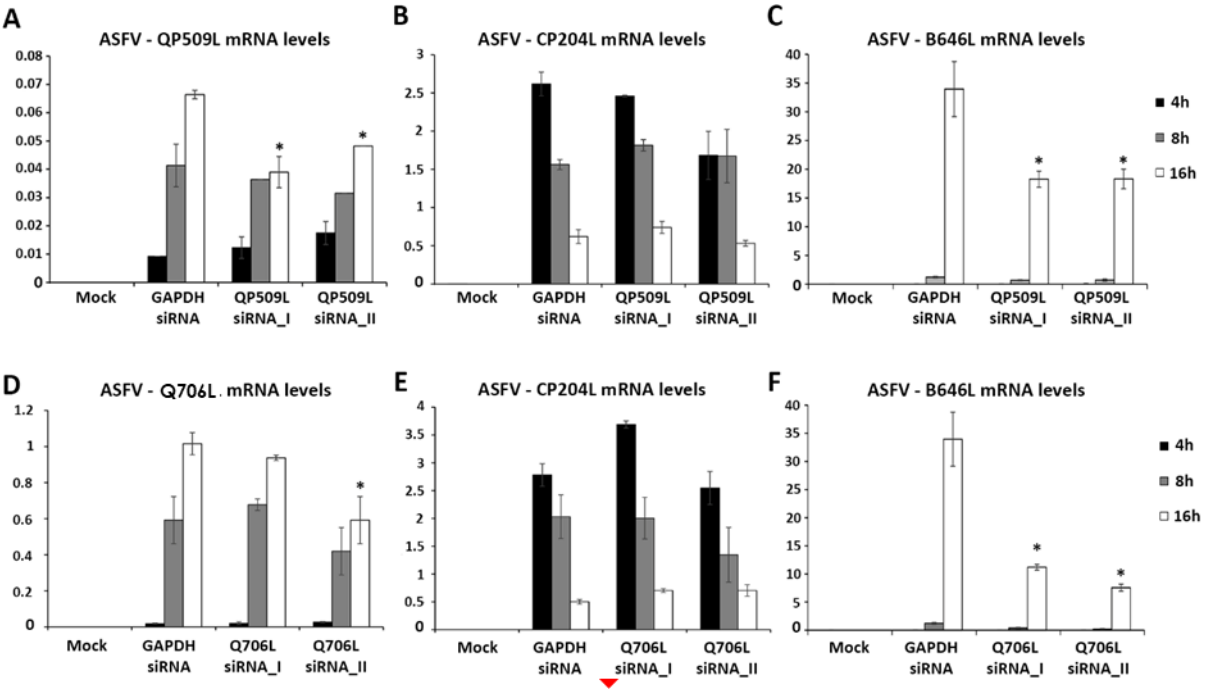

(A) siRNAs against ASFV-QP509L showed significant depletion efficacy at 16 hpi (p≤0.05). (B) Unchanged ASFV-CP204L mRNA levels between QP509L-depleted cells and control group. (C) QP509L-depleted cells showed significant lower mRNA levels of late ASFV-B646L gene (p≤0.05). (D) Q706L siRNA_II showed significant knockdown efficacy at 16 hpi (p≤0.05). (E) Unchanged ASFV-CP204L mRNA levels between Q706L- knockdown cells and control group. (F) Q706L-depleted cells showed a significantly lower mRNA levels of ASFV-B646L gene (p≤0.05). Results are shown as average ± standard error (AVG ± S.E.), between the number of molecules of each viral transcript and the number of Cyclophilin A mRNA molecules (reference gene). Three independent experiments were performed in duplicate.

Additionally, a significant decreased number of viral genomes was measured in depleted cells, ranging between -26.1% and -53.4% in ASFV-QP509L- knockdown cells (p≤0.05; Fig. 17A) and between -68.3% and -71.4% in ASFV-Q706L knockdown cells (p≤0.05; Fig. 17A). Finally, a significant reduction of viral progeny was found in ASFV-QP509L depleted cells (between -82.2 % to -99.4%; p≤0.05) and in ASFV-Q706L depleted cells (-92.5% to -98.6%) in comparison to controls (p≤0.05, Fig. 17B).

Figure 17. ASFV-QP509L and ASFV-Q706L downregulation disrupts ASFV DNA replication and progeny production.

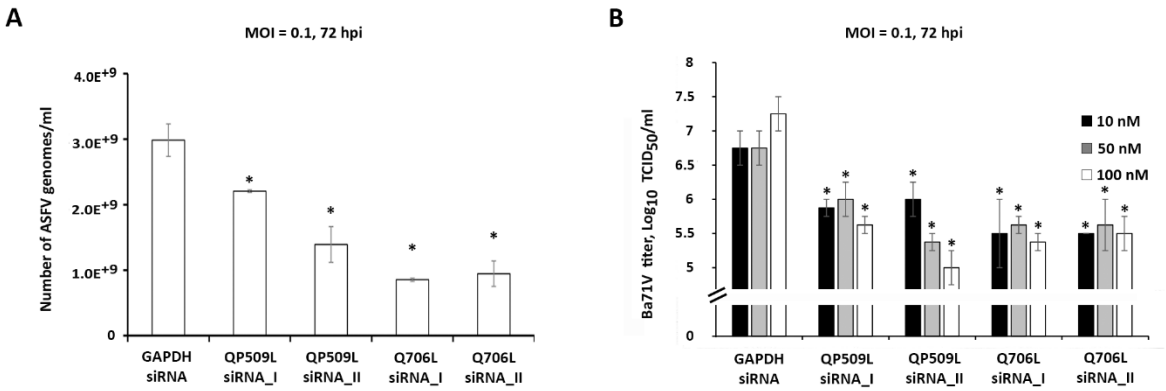

(A) QP509L and Q706L-depleted cells showed a decreased number of ASFV genomes [$2.21x10^9$ genomes/ml using QP509L siRNA_I (-26%), $1.39x10^9$ genomes/ml for QP509L siRNA_II (-53%), $8.53x10^8$ genomes/ml for Q706L siRNA_I (-71%) and $9.45x10^8$ genomes/ml using Q706L siRNA_II (-68.32%)] when compared to the control group ($2.98x10^9$ genomes/ml, $p \leq 0.05$). Results represent the mean of three independent experiments. (B) A statistically significant reduction in viral yields was observed between ASFV-infected Vero cells (MOI of 0.1) transfected with siRNAs against ASFV-QP509L and ASFV-Q706L (-82.2% and -99.4% for QP509L siRNA I and II, respectively, and -92.5% and 98.6% for Q706L siRNA I and II), in comparison with the GAPDH siRNA-transfected infected cells ($p \leq 0.05$). Results were obtained from three independent experiments. Error bars represent standard error (SE) of the mean values.

3. Discussion

RNA helicases are found in all kingdoms of life, participating in several aspects of RNA metabolism and in different events of DNA replication (Jankowsky, 2011; Jeang & Yedavalli, 2006). Although many viruses hijack cellular RNA helicases (Jeang & Yedavalli, 2006), members of some viral families encode their own, as *Herpesviridae* (Chattopadhyay et al., 2006), *Poxviridae* (Jankowsky et al., 2000), *Parvoviridae* (Christensen & Tattersall, 2002), *Flaviviridae* (Utama et al., 2000). Notably, ASFV encodes five putative RNA helicases, including the two pQP509L and pQ706L SF2 DEAD-box RNA helicases (Freije, Lain, Vinuela, Lopez Otin, & Lopez-Otin, 1993; Linder & Jankowsky, 2011). In eukaryotes, these enzymes are known to unwind duplexes formed during RNA transcription, in an ATP-dependent fashion (Bizebard et al., 2004; Yang et al., 2007; Yang & Jankowsky, 2006), with viral counterparts being involved in DNA-RNA and RNA-protein interactions that occur from the beginning of viral gene expression and culminate with the release of infectious particles (Frick & Lam, 2006; Ranji & Boris-Lawrie, 2010). Thus, these proteins are being explored as antiviral drug targets (Briguglio et al., 2011). In ASFV, and besides the initial sequence data assembly and annotation, scarce information is available about the role of viral RNA helicases in infection. In this study, we showed that ASFV RNA helicases are highly conserved among virulent and non-virulent isolates, with ASFV-QP509L and ASFV-Q706L helicases belonging to distinct monophyletic lines, despite their partial sequence overlap and common superfamily 2 motifs. An identical geographic/genotype cluster segregation was found for both viral RNA helicases, similar to the one reported for ASFV-B646L (Bastos et al., 2003; Boshoff, Bastos, Gerber, & Vosloo, 2007; Lubisi, Bastos, Dwarka, & Vosloo, 2005) and other viral genes (Michaud, Randriamparany, & Albina, 2013). However, and probably due to the recent recombination events reported in Georgia 2007/1 isolate (Rowlands et al., 2008), the QP509L sequence of this genotype II clusters with a ASFV isolate belonging to genotype V (Tengani 62), reinforcing the idea that viral phylogenetic studies should include more than one ORF (Chapman et al., 2011). In addition, the comparison between the two ASFV SF2 RNA helicases and SF2 RNA helicases encoded by other NCLDV members revealed that ASFV-QP509L shares the same monophyletic group with vaccinia virus A18R and *Ranavirus* ORF55 RNA helicases, whereas ASFV-Q706L clusters with vaccinia virus D6/D11L and *Marseillevirus marseillevirus* MAR_ORF241 RNA helicases, corroborating previous studies (Baylis et al., 1993; Duffy, Shackelton, & Holmes, 2008; Roberts et al., 1993; Rodríguez & Salas, 2013; Yáñez et al., 1993). Although these results are somehow expected, since NCLDV members share a common ancestor (Yutin & Koonin, 2012), the two genes of SF2 RNA helicases in vaccinia virus are separated approximately 20000 bp, suggesting a different evolutionary route for ASFV. Indeed, recent studies reported that ASFV presents a higher evolutionary rate than other DNA viruses (Alkhamis et al., 2018; Duffy et al., 2008; Grenfell et al., 2004), probably

due to its complex inter-species transmission (wild boars, ticks and domestic pigs), showing a diversity peak over the last 200 years (Alkhamis et al., 2018).

Regarding the expression patterns of the two ASFV SF2 RNA helicases, maximum mRNA levels were detected between 8 and 12 hpi, suggesting that both enzymes are mainly required during the intermediate and late stages of the infection cycle, when the viral DNA replication and transcription are more active. In fact, pQP509L was detected from 12 hpi within viral factories and host nucleus, whereas pQ706L was detected only at viral factories from 12 hpi onwards, indicating that both ASFV RNA helicases have different roles during replication cycle. Despite an early intranuclear phase has been proposed for ASFV (García-Beato, et al., 1992; Simões, et al., 2015), the presence of pQP509L in this cellular compartment, at later times of infection, can be related to other viral events than transcription and/or DNA replication as, for example, modulation of antiviral responses. This plethora of activities is described for other viral RNA helicase as, for example, in NS3 RNA helicase of HCV which is involved in unwinding of the double-stranded RNA intermediates (Dumont et al., 2006) and viral assembly (Ma et al., 2008), and in D6/D11 RNA helicase of vaccinia virus that unwinds RNA-RNA, RNA-DNA and RNA-protein intermediates (Jankowsky et al., 2000). Thus, these viral SF2 DEAD-box RNA helicases were described as essential for infection by HCV (Lam & Frick, 2006; Mackintosh et al., 2006), Vaccinia virus (Gross & Shuman, 1998; Shuman, 1992) and Plum pox virus (Fernández & Guo, 1997), with cellular RNA helicases being unable to rescue the activity of viral counterparts. In a very similar way, our results from siRNA experiments disclosed that QP509L- and Q706L-knockdown cells show lower levels of late viral transcripts (ASFV-B646L), although the expression of an early viral gene (ASFV-CP204L) is not affected. Depleted cells also exhibited a reduced number of viral genomes coupled with a decreased viral yield, indicating that both ASFV RNA helicases have relevant and non-redundant functions, not rescued by cellular RNA helicases. Considering our above results and the data reported on vaccinia virus counterparts, a working model for both ASFV SF2 RNA helicases is depicted in figure 18. Briefly, ASFV-Q509L and ASFV-Q706L RNA helicases are mainly involved in viral transcription events, with ASFV-Q509L assisting termination and release of late viral transcripts (as reported for vaccinia virus A18R helicase orthologous), whereas ASFV-Q706L regulates elongation and release of late viral transcripts (as vaccinia virus D6/D11 helicase).

Figure 18. Proposed working model for ASFV-QP509L and ASFV-Q706L RNA helicases.

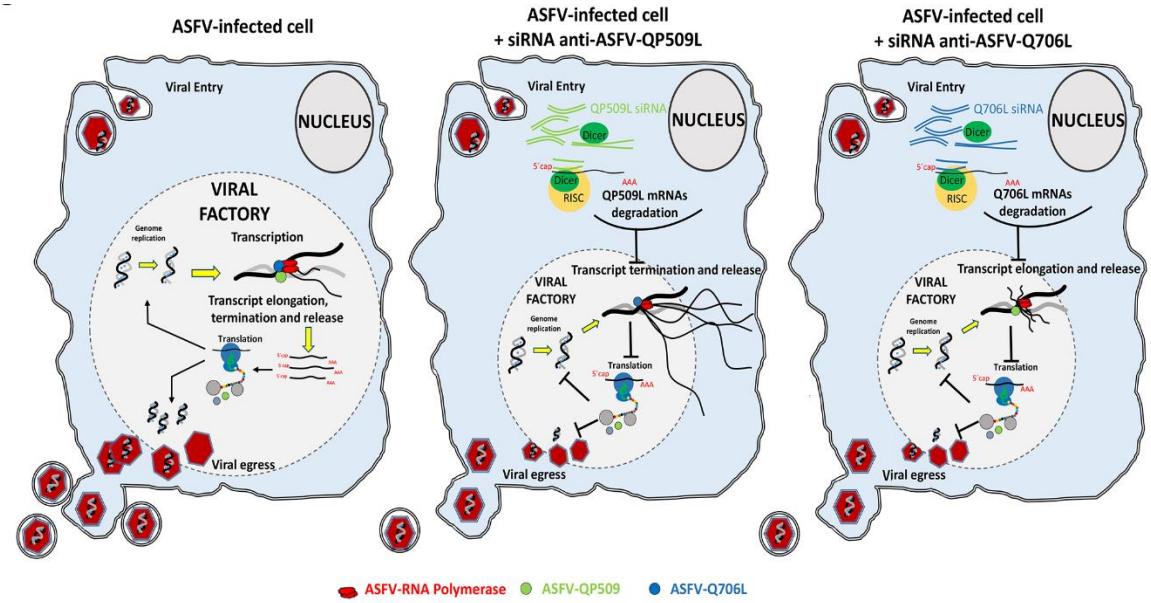

Considering the experimental data available for ASFV-QP509L and ASFV-Q706L orthologous (A18R and D6/D11 SF2 RNA helicases of Vaccinia virus, respectively), our model hypothesized that absence of ASFV-QP509L on the transcription complex will leads to continuous reading of neighbouring viral ORFs and transcriptionally silenced regions, giving rise to an accumulation of long RNAs, with its release being also affected. In parallel, our working model postulates that downregulation of ASFV-Q706L will disrupt transcription elongation and termination with serious implications in viral progeny production.

Finally, taking into consideration that there is neither a vaccine nor a treatment available against ASFV and the important roles of both ASFV SF2 RNA helicases, we hypothesized that a mutant on ASFV-QP509L or ASFV-Q706L gene can be a good candidate to generate a live attenuated vaccine. These ASFV mutants will not produce progeny, allowing the immediate-early and early viral gene expression and providing antigens that can induce a protective immune response.

Acknowlegments

This work was supported by Fundação para a Ciência e a Tecnologia (CIISA-UID/CVT/00276/2019) and by the European Union's Seventh Framework Programme (FP7/2007-2013, 311931, ASFORCE). FBF and GF were supported by doctoral scholarships from Fundação para a Ciência e a Tecnologia (SFRH/BD/89426/2012, SFRH/BD/104261/2014).

CHAPTER IV

In vitro inhibition of African swine fever virus-topoisomerase II disrupts viral replication

Ferdinando B. Freitas, Gonçalo Frouco, Carlos Martins, Alexandre Leitão, Fernando Ferreira (2016) Antiviral Research. 2016 Oct; 134:34-41. doi: 10.1016/j.antiviral.2016.08.021. Epub 2016 Aug 26

Abstract

African swine fever virus (ASFV) is the etiological agent of a highly-contagious and fatal disease of domestic pigs, leading to serious socio-economic impact in affected countries. To date, neither a vaccine nor a selective anti-viral drug are available for prevention or treatment of African swine fever (ASF), emphasizing the need for more detailed studies at the role of ASFV proteins involved in viral DNA replication and transcription. Notably, ASFV encodes for a functional type II topoisomerase (ASFV-Topo II) and we recently showed that several fluoroquinolones (bacterial DNA topoisomerase inhibitors) fully abrogate ASFV replication in vitro. Here, we report that ASFV-Topo II gene is actively transcribed throughout infection, with transcripts being detected as early as 2 hpi and reaching a maximum peak concentration around 16 hpi, when viral DNA synthesis, transcription and translation are more active. siRNA knockdown experiments showed that ASFV-Topo II plays a critical role in viral DNA replication and gene expression, with transfected cells presenting lower viral transcripts (up to 89% decrease) and reduced cytopathic effect (-66%) when compared to the control group. Further, a significant decrease in the number of both infected cells (75.5%) and viral factories per cell and in virus yields (up to 99.7%, 2.5 log) was found only in cells transfected with siRNA targeting ASFV-Topo II. We also demonstrate that a short exposure to enrofloxacin during the late phase of infection (from 15 to 16 hpi) induces fragmentation of viral genomes, whereas no viral genomes were detected when enrofloxacin was added from the early phase of infection (from 2 to 16 hpi), suggesting that fluoroquinolones are ASFV-Topo II poisons. Altogether, our results demonstrate that ASFV-Topo II enzyme has an essential role during viral genome replication and transcription, emphasizing the idea that this enzyme can be a potential target for drug and vaccine development against ASF.

Graphical Abstract

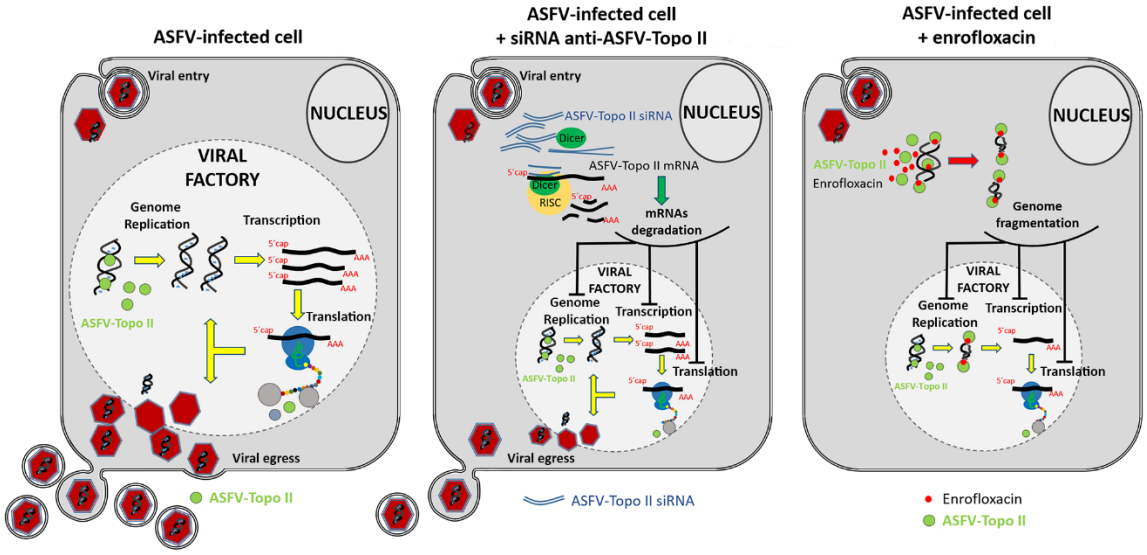

Keywords: ASFV-Topoisomerase II, qPCR, siRNA, Antiviral therapy, Vaccine development.

1. Introduction

African swine fever (ASF) is a highly contagious hemorrhagic disease that affects domestic and wild suids. Clinical signs may vary from a hyperacute form, with 100% mortality, to a less common chronic and asymptomatic forms that can turn pigs into carrier state (Costard et al., 2009; Penrith & Vosloo, 2009). Until today there is no effective vaccine or treatment for ASF and control strategies include, among others, quarantine and compulsory slaughter of affected animals (reviewed in Gallardo et al., 2015; Michaud et al., 2013). The economic losses from these measures can disrupt both the local and, in severe outbreaks, the national economy due to international trade restrictions (Costard et al., 2009; Michaud et al., 2013). Nowadays, ASF is endemic in most of the sub-Saharan countries and in the Italian island of Sardinia for more than 35 years (Costard et al., 2009; Mur et al., 2016). In 2007, it was introduced in Georgia spreading to Armenia, Azerbaijan, Russia, to Ukraine in 2012 and, to Belarus in 2013 (reviewed in Sánchez-Vizcaíno et al., 2013, 2015). In 2014, ASF reached the European Union, namely Lithuania, Poland, Estonia and Latvia (reviewed in Sánchez-Vizcaíno et al., 2015). The etiological agent of the disease is the African swine fever virus (ASFV), a large (≈200nm) enveloped icosahedral double-stranded DNA virus (170 to 190 kbp). ASFV is the only known *Asfarviridae* member and infects different species of soft ticks (*Ornithodoros spp*), wild and domestic pigs (reviewed in Boinas et al., 2014; Tulman et al., 2009). Its genome contains between 151-167 genes depending on the strain, however, about half of them lack any known or predictable function (Chapman et al., 2008; reviewed in Dixon et al., 2013). Remarkably, ASFV is the only known virus that infects mammals encoding for a protein with type II DNA topoisomerase activity (ASFV-Topo II) (Coelho et al., 2015), sharing high similarity with bacterial topoisomerases, although its sequence homology with eukaryotic type II topoisomerases is low (Baylis et al., 1992; García-Beato et al., 1992; Gadelle et al., 2003; Coelho et al., 2015). Type II topoisomerases control DNA topology during replication, transcription, chromosome condensation-decondensation and segregation by catalysing transient double-stranded breaks in one helix DNA, pass a second DNA helix, and then close the gate, in all forms of life (reviewed in Champoux, 2001; de Souza et al., 2010; Forterre et al., 2007).

Although previous studies show that several bacterial topoisomerase II inhibitors disrupt ASFV infection (Salas et al., 1983; Mottola et al., 2013), very little is known about the role of ASFV-Topo II during infection and how these drugs act. Indeed, more information about this protein, putatively involved in viral replication/transcription, is urgently needed to understand if ASFV-Topo II is a good target for drug development and/or vaccine design. In this study, qPCR was performed to investigate the transcription pattern of ASFV-Topo II gene during infection. siRNA technology was used to selectively knock down the ASFV-Topo II expression in order to analyze the role of this protein in viral replication and transcription, an approach that has been

recently described to evaluate the importance of viral genes in West Nile virus infection (Anthony et al., 2009), dengue virus (Wu et al., 2010; Ye et al., 2011), influenza virus (Hirsch, 2010) and also in ASFV (Keita, Heath, & Albina, 2010). Finally, a mechanism of action is proposed for the antiviral effects of fluoroquinolones, supported by the results obtained from the comet assay.

2. Material and methods

2.1. Cells and viruses

Vero cells from the European Collection of Cell Cultures (ECACC, Salisbury, UK) were maintained in DMEM (Dulbecco Modified Eagle's minimal essential medium) containing 10% (v/v) heat inactivated fetal calf serum, 1% of non-essential amino acids and Penicillin/Streptomycin at 100 units/ml and 100 µg/ml, respectively (all from Gibco, Life Technology, Karlsruhe, Germany). All experiments were conducted on actively replicating sub confluent cells grown at 37 °C under a 5% CO_2 humidified atmosphere (≥95%). The Vero-adapted ASFV strain (Badajoz 1971, Ba71V) was used in all infections and propagated as previously described (Carrascosa et al., 2011). Viral suspension titrations were performed by observation of cytopathic effect (CPE) at end-point dilutions, using Vero cells inoculated with 10-fold serial dilutions of supernatants during 5 days and results were expressed as TCID50/ml (Spearman-Kärber endpoint method).

2.2. Cytopathic effect (CPE) evaluation

Cells were seeded, transfected and infected (MOI = 0.025 and 0.1) as described in siRNA delivery assay (see 2.8.). Using an inverted microscope, CPE's were evaluated by two researchers at 72 hpi, based on a four grade scale: 0 (no CPE), 33 (CPE ≤ 33%), 66 (CPE > 33% and ≤ 66%) and 100 (CPE > 66%), as previously described (Servan de Almeida et al., 2007; Keita et al., 2010). CPE values were calculated as the arithmetic mean of the two individual scores.

2.3. RNA extraction and cDNA synthesis

For all qPCR quantifications total RNA was extracted using the RNeasy Mini Kit (Qiagen, Courtaboeuf, France). Possible DNA contaminants in the RNA preparation were eliminated by treatment in column with DNAse I (Qiagen). RNA concentrations and purity were measured (OD value at 260 nm and A260/A280 coefficient) using a spectrophotometer (NanoDrop, 2000c, Thermo Fisher Scientific, Waltham, USA) and only RNA samples showing high purity (A260/A280 ratio between 1.8 and 2.0) were used. 200 ng of each total RNA sample was reverse transcribed (Transcriptor First Strand cDNA Synthesis Kit, Roche, Basel, Switzerland), according to the manufacturer's instructions. The obtained cDNA was diluted (1/20) in ultra-pure water and stored at −20 °C until further use.

2.4. Recombinant plasmids

The amplified fragments were cloned into a pGEM-Teasy Vector System II (Promega, Madison, USA), and the plasmids were used to transform DH5α competent cells. The vector plasmids were isolated from bacteria using the Roche High Pure Plasmid Isolation Kit (Roche Applied Science, Germany), according to the manufacturer's manual. To determine whether the cloned DNA fragments (ASFV-Topo II, VP32, VP72 and Cyclophilin A) were incorporated into isolated vectors, the inserts were amplified by PCR and their sequences were confirmed. Following this step, the concentration of each plasmid preparation was determined by spectrophotometric absorbance (NanoDrop, model 2000c). Their corresponding copy number was calculated using the equation: pmol (dsDNA) = µg (dsDNA) × 1515/DNA length in pb (pmol = picomoles, dsDNA = double-strand DNA, DNA length in pb = number of base pairs from the amplified fragment; 1 mol = 6022 × 1023 molecules).

2.5. Standard curves optimization

A ten-fold serial dilutions of each plasmid (ASFV-Topo II, VP32, VP72 and Cyclophilin A), ranging from $1x10^{-1}$ to $1x10^{-9}$ were initially used in duplicate to construct the standard curves in two different days. Threshold cycle (Ct) values obtained from each dilution were plotted against the logarithm of their initial template copy numbers and corresponding standard curves were generated by linear regression of the plotted points. From the slope of each standard curve, PCR amplification efficiency (E) was calculated according to the equation: E (%) = (10–1/slope– 1) x 100% (Pfaffl, 2001).

2.6. Quantitative PCR

ASFV-Topo II, VP32, VP72 and Cyclophilin A mRNA levels were quantified by qPCR using Maxima SYBR Green PCR Master Mix (Thermo Fisher) according to the manufacturer's instructions [12.5 µl of master mix, 2.5 µl of forward and reverse primers (50 nM each), 5 µl of water and 2.5 µl of cDNA)]. All qPCR reactions were performed in Applied Biosystems 7300 Real Time PCR system (Thermo Fisher) with the following thermal profile: 10 min at 95 °C for initial denaturation; 40 cycles of 15 s at 95 °C and 60 s at 60 °C, followed by a final denaturation step of 5 s at 65 °C with a 20 °C/s ramp rate and subsequent heating of the samples to 95 °C with a ramp rate of 0.1 °C/s. Quantification of ASFV-Topo II, VP32, VP72 and Cyclophilin A mRNA levels were determined by the intersection between the fluorescence amplification curve and the threshold line. The crossing point values of each plasmid obtained from different known concentrations were plotted in a standard curve used to determine the copy number of

each transcript. The values were determined using the comparative threshold cycle method, which compares the expression of a target gene normalized to the reference gene (Cyclophilin A). The validation of the reference gene was confirmed using the ANOVA test. The specificity of the qPCR assays was confirmed by melting curve analyses. The sequences of all primers used in this study are shown in Table 6.

Table 6. List of used primers.

Target	Primer designation	Sequence (5´- 3´)	Coordinates*	Orientation
ASFV-Topo II	TOPOup	TTGCCGCTTGCTATTATGGA	133242-133261	Foward
ASFV-Topo II	TOPOlow	CGGGCCCAAGTGGTGTAC	133292-133309	Reverse
Cyclophilin A	CycloFw1	AGACAAGGTTCCAAAGACAGCAG	-	Foward
Cyclophilin A	CycloRev	AGACTGAGTGGTTGGATGGCA	-	Reverse
Cyclophilin A	CycloFw2	TGCCATCCAACCACTCAGTCT	-	Foward
VP72	VP72Fw	ACGGCGCCCTCTAAAGGT	88273-88290	Foward
VP72	VP72Rev	CATGGTCAGCTTCAAACGTTTC	88322-88343	Reverse
VP32	VP32Rev	TCTTTTGTGCAAGCATATACAGCTT	108162-108186	Foward
VP32	VP32Fw	TGCACATCCTCCTTTGAAACAT	108228-108249	Reverse

*Primer coordinates are relative to Ba71V sequence used has template for primer design.

2.7. Quantification of ASFV-Topo II, VP32, VP72 mRNA levels

To quantify the ASFV-Topo II mRNA expression levels during infection, Vero cells (5×10^5) were seeded onto 30 mm dishes and infected with a multiplicity of infection (MOI) of 1.5 (ASFV-Ba71V isolate). After 1 h of adsorption, the virus inoculum was removed, the cells were washed twice and fresh DMEM was added. Total RNA was extracted at indicated time points after infection (2, 4, 6, 8, 10, 12, 14, 16, and 20 hpi). The extraction protocol, cDNA synthesis and qPCR amplifications were performed as previous described (see 2.3 RNA extraction and cDNA synthesis, 2.6 Quantitative PCR). Three independent experiments were performed to verify the reliability of the results.

2.8. siRNA assays

Four double-stranded siRNAs (ON-TARGETplus, Thermo Fisher Scientific) targeting different sequence regions of the ASFV-Topo II transcript were designed (siDESIGN Center, Thermo Fisher Scientific), based on the full genome sequence of ASFV Ba71V isolate (GenBank/EMBL, accession number: ASU18466). One siRNA against the GAPDH gene (siRNA-GAPDH; Silencer™ GAPDH siRNA human control number 4605; Ambion/Thermo Fisher Scientific) was used as a control in all siRNA assays. The siRNA sequences used in the study are shown in Table 7. All siRNAs duplexes were diluted at different final concentrations (10, 50 and 100 nM) in serum-free Opti-MEM (Gibco, Life Technology, Karlsruhe, Germany) and using 8 µl HiPerfect Transfection reagent (Qiagen, Courtaboeuf, France). Mixtures were incubated at room temperature for 20 min to allow the formation of

transfection complexes. Thereafter, 100 µl of the transfection solution was incubated with 2×10^4 Vero cells cultured in 500 µl of DMEM supplement with 10% FBS in a 24-well plate during 8 h. One hour before infection, the culture medium was removed and fresh medium was added to allow recovery of the cells. Next, cells were infected with ASFV Ba71V (MOI = 0.025 and 0.1), the viral inoculum was removed 1 h after and further incubated at 37 °C for 72 h. The viability of transfected cells was assessed every 8 h until 72 h by phase-contrast microscopy. The different siRNAs were used individually or in combination (50 + 50 nM) and their antiviral effects were evaluated by titrating viral progeny, quantifying the number of infected cells, the CPE and mRNA levels (ASFV-Topo II, VP32 and VP72). Due to economic and practical reasons only the two siRNAs duplexes (including combinations) that showed higher inhibitory results (CPE reduction) were used in further assays.

Table 7. siRNA used in this work.

Target	siRNA designation	Sequence (5´- 3´)	Target coordinates*	Orientation
ASFV-Topo II	ASFV_TOPOII_I	CCUAAUAGCACGAUACAUAUU	790-808	Sense
ASFV-Topo II	ASFV_TOPOII_I	PUAUGUAUCGUGCUAUUAGGUU	790-808	Antisense
ASFV-Topo II	ASFV_TOPOII_II	CCAUUAAGGCCGAUGCAAAUU	815-833	Sense
ASFV-Topo II	ASFV_TOPOII_II	PUUUGCAUCGGCCUUAAUGGUU	815-833	Antisense
ASFV-Topo II	ASFV_TOPOII_III	GGGCGGAACCAGAGUACUAUU	2492-2510	Sense
ASFV-Topo II	ASFV_TOPOII_III	PUAGUACUCUGGUUCCGCCCUU	2492-2510	Antisense
ASFV-Topo II	ASFV_TOPOII_IV	GGGCCUACGUCGAUAAGAAUU	2618-2636	Sense
ASFV-Topo II	ASFV_TOPOII_IV	PUUCUUAUCGACGUAGGCCCUU	2618-2636	Antisense

*siRNA coordinates according to the relative position in gene nucleotide sequence (start at position 1, ATG).

2.9. Immunofluorescence and microscopy analysis

Cells were seeded onto glass coverslips (2×10^4), in 24-well plates, transfected with ASFV-Topo II siRNA_III + IV, and infected with ASFV Ba71V isolate (MOI = 1). At 12 hpi, cells were fixed in 3.7% paraformaldehyde and HPEM buffer [25 mM HEPES (4-(2-hydroxyethyl)-1-piperazineethanesulfonic acid), 60 mM PIPES (piperazine-N,N′-bis 2-ethanesulfonic acid), 10 mM EGTA (ethylene glycol tetraacetic acid), 1 mM MgCl2] for 15 min at room temperature and permeabilized in PBS/Tx-100 1% for 5 min. Following this step, cells were washed in PBS, blocked with PBS/BSA 1% for 30 min and incubated with an anti-ASFV conjugated FITC serum (1:50). A mounting medium with DAPI (4′,6-diamidino-2-phenylindole), was used (Vectashield, Vector Laboratories, Peterborough, UK). All incubations were performed in a dark humidified chamber to prevent fluorochrome fading. Immunofluorescence analysis was performed using an epifluorescence microscope (Leica DMR HC model, Wetzlar, Germany), data sets were acquired by Adobe Photoshop CS5 software (Adobe Systems, Inc., San Jose, USA) and images were subsequently processed using the ImageJ open source software (version 1.46r).

2.10. Quantification of ASFV-Topo II, VP32 and VP72 transcripts after the siRNA treatments

Vero cells (2×10^4) were transfected with the most efficient siRNA during 8 h. At 1 h post-transfection, cells were infected with Ba71V (MOI = 1) and at 16 hpi total RNA was extracted. To ensure high RNA concentrations, the siRNA assays were performed in quadruplicated. The extraction protocol, cDNA synthesis and qPCR amplifications were performed as previous described (see 2.3 RNA extraction and cDNA synthesis, 2.6 Quantitative PCR). The qPCR assay was performed in triplicate to ensure the biological relevance of the results.

2.11. Comet assay

Comet assay was performed using the alkaline technique (Singh, McCoy, Tice, & Schneider, 1988). In brief, Vero cells ($2x10^5$) infected with Ba71V (MOI = 1) were exposed to enrofloxacin (100 µg/ml) from 0 to 12 hpi or from 15 to 16 hpi. In addition, infected and non-exposed, non-infected exposed and non-exposed to enrofloxacin were used as controls. At indicated time points, cells were gently washed twice in PBS, trypsinized and embedded in 60 µL of low-melting-point agarose (0.7%, Lonza, Rockland, USA) prewarmed at 37°C. The mixture was immediately pipetted onto frosted microscope slides precoated with a layer of 1% normal melting point agarose diluted in PBS (Sigma, St. Louis, USA), and allowed to jellify (4°C, 10 min). Slides were then immersed in an alkaline lysis solution (2.5 M NaCl, 100 mM EDTA, 10 mM Tris-HCl, 1% Triton X-100, pH 10), for 1 hour at 4°C. Before electrophoresis, slides were incubated with a fresh cold electrophoresis buffer (1 mM EDTA, 300 mM NaOH) during 10 min to allow unwinding of DNA. Electrophoresis was performed at 0.83 V/cm on ice for 20 min. After the electrophoresis, slides were washed in neutralization buffer (0.4 M Tris-HCl, pH 7.5) during 15 min. All steps described above were carried out in the absence of light to avoid DNA damage. For DNA staining, slides were incubated with a nucleic acid staining solution (RedSafe Nucleic Acid Staining Solution, 0.02 µl/mL, iNtRON Biotechnology, Gyeonggi-do, South Korea), and visualized in an epifluorescence microscope (Leica DM R HC model, Wetzlar, Germany). For each sample, 5 randomly selected microscopic fields were captured using Adobe Photoshop CS5 software (Adobe Systems, Inc., San Jose, USA) and DNA damage was evaluated by comparing the intensity of the comet tails between the experimental groups.

2.12. Effect of enrofloxacin on ASFV transcription

To evaluate the effect of enrofloxacin on ASFV transcription, Vero cells ($2x10^5$) were seeded into a 24-well plate, incubated at 37°C and infected with ASFV-Ba71V isolate (MOI of 1). After 1 hour of adsorption, the virus inoculum was removed, the cells were gently washed and then exposed to enrofloxacin (100 µg/ml) during 6, 12 and 24 hours followed by extraction of total RNA. The extraction protocol, cDNA synthesis and qPCR amplifications were performed as previous described (see 2.3. and 2.6). Results represent the mean value of three independent experiments performed in different days.

3. Results

3.1. ASFV-topoisomerase II gene is transcribed from the early phase of infection

Our results showed that ASFV-Topo II transcripts are detected as early as 2 hpi, gradually increasing throughout the infection and reaching a maximum peak at 16 hpi (Fig.19). Additionally, ASFV-Topo II viral gene is less transcribed than the two viral structural genes used as controls (VP32 and VP72). In order to ensure that the normalized mRNA levels of different viral genes are comparable, only qPCR reactions with efficiency values ranged from 90 to 91% and showing R^2 values>0.987 were considered.

Figure 19. ASFV-Topo II is a late gene.

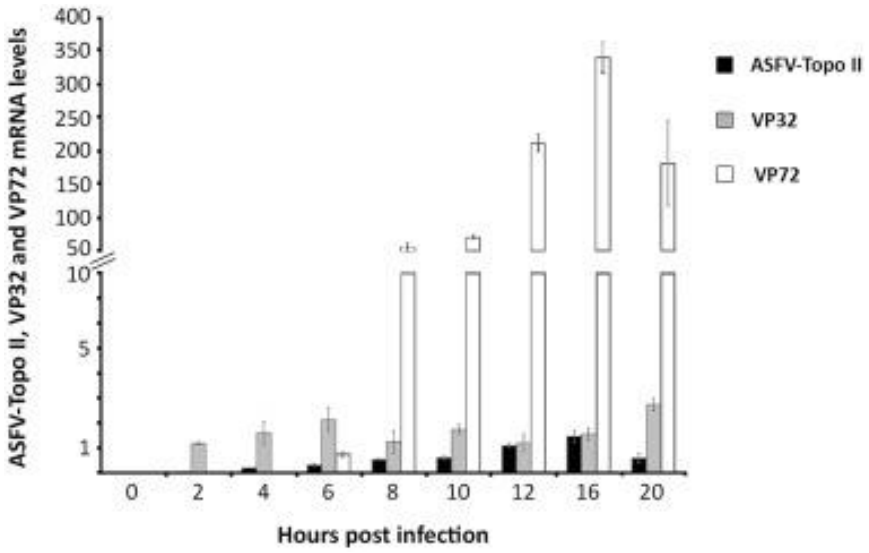

ASFV-Topo II transcripts were detected from 2 hpi onwards, reaching a maximum concentration at 16 hpi. Transcription levels were compared with VP32/VP72 mRNA levels and normalized to Cyclophilin A (reference gene). Error bars represent standard error of the mean from three independent experiences. (MOI of 1.5).

3.2. siRNAs targeting ASFV-Topo II impairs viral infection

The inhibitory activity of four siRNA duplex targeting ASFV-Topo II mRNA was initially screened by visualizing the viral-induced cytopathic effect (CPE). When Vero cells were transfected individually with siRNA III or IV (100 nM) or in combination between them (50 + 50 nM) prior to infection (MOI = 0.025) the induced CPE was reduced in 66%, whereas when siRNA oligos were individually used at 10 and 50 nM, a decrease of 33% was found. No additional inhibitory effects were seen with increasing concentration beyond 100 nM (data not shown). In contrast, siRNA I or II did not showed any antiviral effects. As expected, the siRNA against GAPDH did not alter the viral CPE (Fig. 20A). Although similar results were observed when cells were infected with a MOI of 0.1, the reduction of CPE induced by ASFV was less obvious reaching a maximum value of 33% for the siRNA III or IV at 100 nM (data not shown).

Considering the CPE inhibition observed in siRNA experiments, the supernatants harvested from the controls and from infected Vero cells transfected with siRNA III, IV (alone and combined) or siRNA GAPDH were used to infect new cells cultures, in order to assess the siRNAs effects on viral progeny. A virus titer reduction of 1.25–2.50 log was observed in infected cells transfected with siRNA III and IV (a decrease of 94.3–99.7%) in comparison with control groups (Fig. 20b).

Figure 20. siRNAs against ASFV-Topo II inhibit ASFV replication.

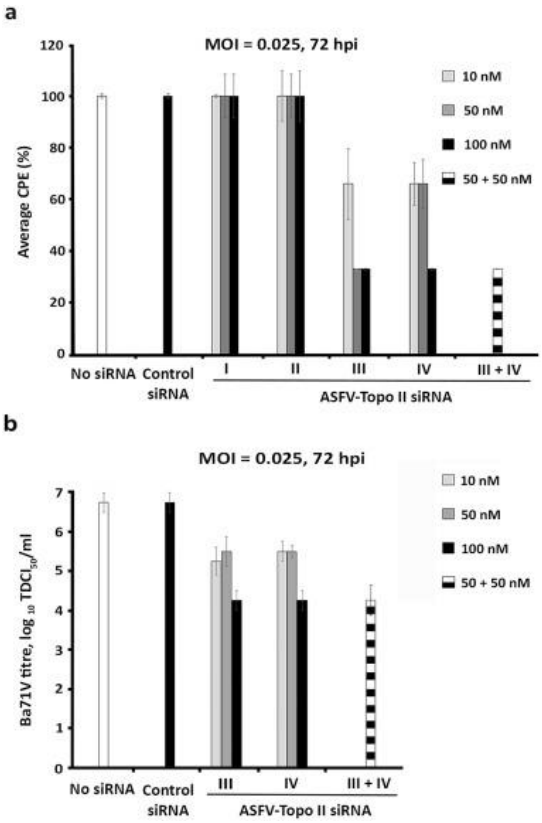

(a) A significant inhibition of CPE was observed when infected cells (MOI of 0.025) were transfected with siRNA_III or/and siRNA_IV. The CPE assay was performed as described previously (Keita et al., 2010) Error bars represent standard error of the mean from three independent experiences. (b) A reduction in virus yield was also found in infected cells transfected with siRNA_III and/or siRNA_IV (up to 99.9%). Error bars represent standard error of the mean from three independent experiences.

Considering the role of type II topoisomerases in DNA synthesis and transcription and given our results, we assessed if siRNA III + IV against ASFV-Topo II had an effect in these processes by evaluating the number of infected cells and viral factories in Vero cells transfected with siRNA using immunofluorescence. Due to economical and practical reasons only this siRNA combination was used in this assay. A significant reduction (75.5%, $P < 0.002$) in the average number of infected cells was found between the group of transfected cells and the control group (7.30 ± 1.22, 29.80 ± 5.28, respectively), at 12 hpi (Fig. 21a and b). Regarding the number of ASFV factories per cell, a decrease was found in transfected cells when

compared to control group (one factory: 5.30 ± 1.01, 19.50 ± 3.97, P = 0.006; two factories: 0.70 ± 0.33, 4.30 ± 0.94, P = 0.004 and three factories: 1.30 ± 0.42, 6.00 ± 1.25, P = 0.005), (Fig. 21c), with the number of each morphological type (circular or irregular) being significantly lower on transfected cells (circular P = 0.010; asymmetrical P = 0.006; data not shown). Although the above results suggest that ASFV-Topo II plays a key role during infection it remains to verify the efficiency of siRNA against the ASFV-Topo II mRNA and the impact in the viral transcription. For these propose, the mRNA levels of ASFV-Topo II and two viral structural genes were measured by qPCR. Results show a repression of the specific target transcript (up to 89%) but also a reduction in mRNA levels of VP32 (73%) and VP72 (77%) when compared with the infection control (Fig. 22).

Figure 21. siRNAs anti-ASFV-Topo II inhibit the viral protein synthesis and the formation of viral factories sites.

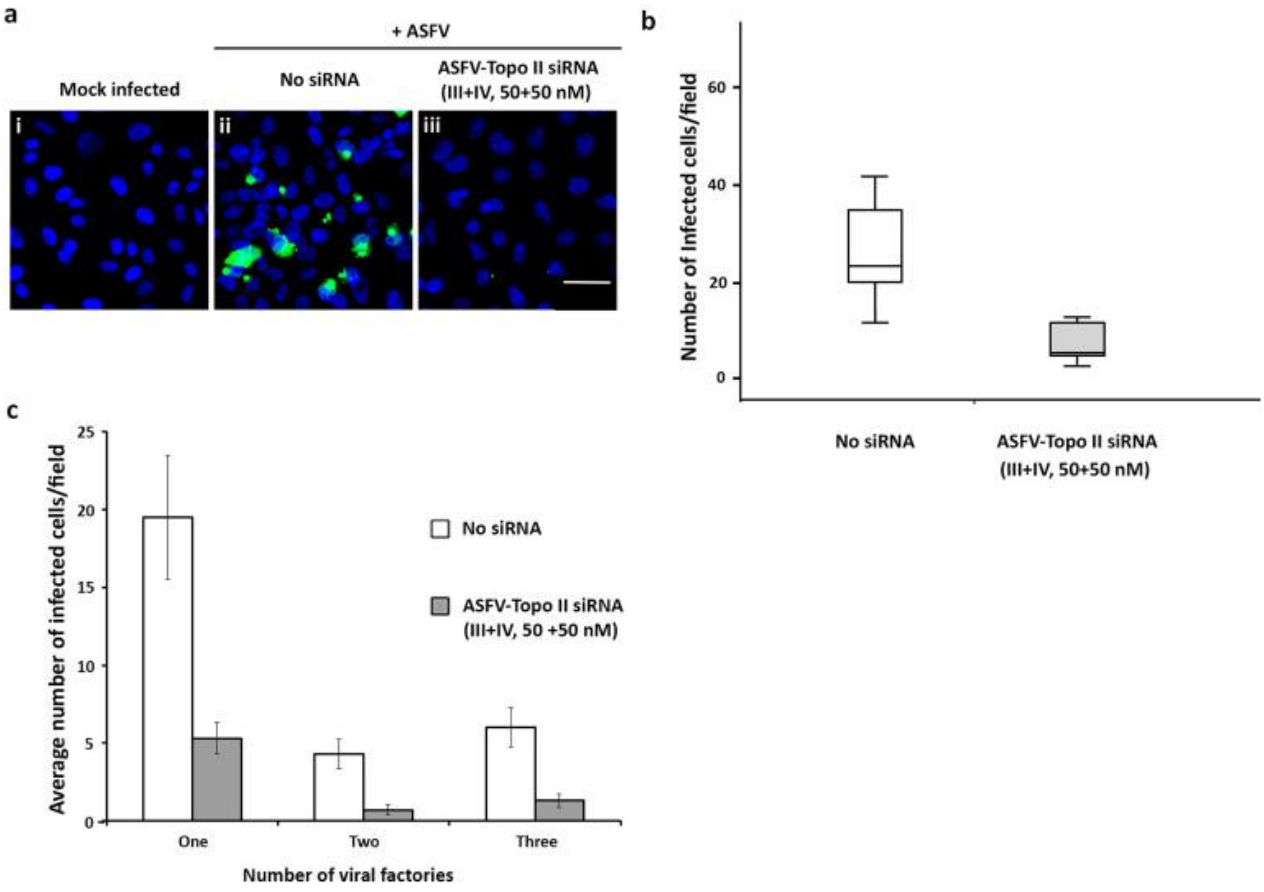

(a,b)- A significant reduction in the number of infected cells was observed between the transfected group (siRNA_III + IV, 50 nM each) and the non-transfected group (, P = 0.001). (c) The average number of viral factories per cell was also lower in the transfected group than in control group (P = 0.002 for one factory and, P = 0.003 for two and three factories). Error bars represent standard error (±SE) of the mean of three independent experiments. Scale bar, 60 μm.

Figure 22. ASFV-Topo II siRNAs disrupt viral transcription.

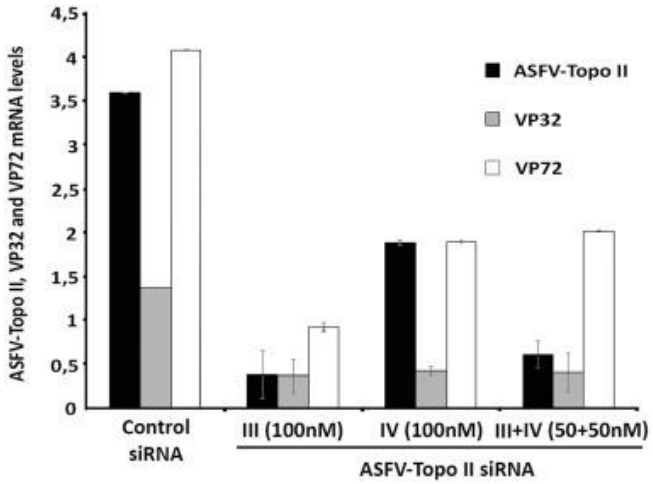

The most effective siRNAs (III and IV) were able to reduce ASFV-Topo II mRNA levels up to 89%, VP32 mRNA levels up to 73% and VP72 gene transcription up to 77%. Transcripts levels were normalized to Cyclophilin A mRNA levels (reference gene) and error bars represent standard error of the mean from three independent experiences.

3.3. Enrofloxacin acts as an ASFV-Topo II poison during infection

In previous studies it was shown that fluoroquinolones inhibit ASFV genome replication (Mottola et al., 2013), however the mechanism of action remains unknown, leading us to clarify the inhibitory effects of enrofloxacin during infection using a single cell electrophoresis analysis (comet assay). When ASFV-infected Vero cells were exposed to enrofloxacin from 15 to 16 hpi, a tail of fragmented DNA (comet) was observed (Fig. 23c), in contrast to infected cells exposed from the early phase of infection (0 to 12 hpi, Fig. 23f). As expected, no DNA fragmentation was identified in both infection control groups without any treatment (Fig. 23be) as in negative infection controls (Fig.23ad). Although effects of enrofloxacin upon viral DNA were detected by comet assay, it remains to be verified whether this drug interferes with transcription. For this purpose, ASFV-Topo II, VP32 and VP72 mRNA levels were compared between the infection control and infected Vero cells exposed to enrofloxacin. In early phase of infection (6 hpi), no changes were found in the viral transcript levels (ASFV-Topo II and VP32) between the non-exposed and exposed infected groups. At later times (12 and 24 hpi), ASFV-infected Vero cells exposed to enrofloxacin showed lower viral mRNA levels than control, while the transcript of the late gene VP72 was not detected at all (Fig. 24). This outcome strongly suggest that the fluoroquinolones are able to interfere with gene transcription by completely blocking the expression of later genes (e.g. VP72).

Figure 23. Enrofloxacin induces viral DNA breaks, thus acting as an ASFV-topoisomerase poison.

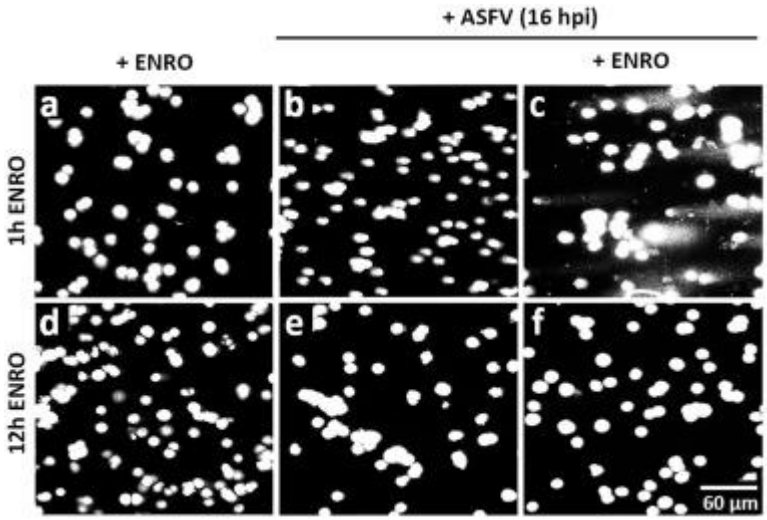

Although the ASFV-infected Vero cells (MOI = 1) exposed to enrofloxacin from the early phase of infection (0–12 hpi) did not show viral DNA breaks or viral genomes (f), ASFV-infected Vero cells (MOI = 1) treated with enrofloxacin (100 µg/ml, 1 h) showed a tail of fragmented DNA (c). As expected, no DNA fragmentation was identified in both infected (b and e) and non-infected treated controls (a and d). Representative images of at least three independent experiments are shown. Scale bar, 60 µm.

Figure 24. Enrofloxacin disrupts ASFV transcription activity.

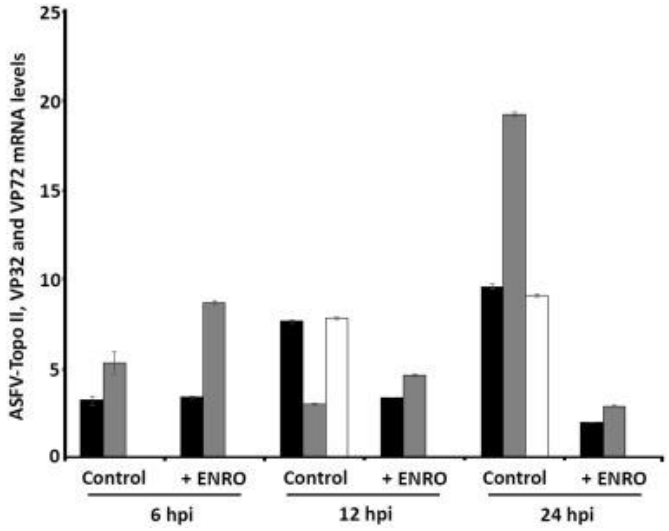

Despite the fact that, at 6 hpi, ASFV-infected Vero cells (Ba71V, MOI = 1) exposed to enrofloxacin (100 µg/ml) showed similar ASFV-Topo II (black bars) and VP32 (grey bars) mRNA levels to infected control, at 12 hpi the mRNA levels of these genes become reduced and the transcripts of the late VP72 gene were not detectable (white bars). At 24 hpi, when a second infection cycle was already initiated, the ASFV-infected cells exposed to enrofloxacin showed a clear reduction in VP32 and ASFV-Topo II mRNA levels, in comparison to untreated cells, as the VP72 mRNA levels still absent. Transcripts levels were normalized to Cyclophilin A mRNA levels and error bars represent standard error of the mean from three independent experiences.

4. Discussion

It was recently shown that ASFV encodes for a protein (ORF P1192R) that co-localizes with cytoplasmic viral factories at intermediate and late phases of infection, being able to complement a *Saccharomyces cerevisiae* Top2A temperature-sensitive mutant (Coelho et al., 2015). Although phylogenetic studies revealed that ORF P1192R shares high sequence homology (Forterre et al., 2007) and functional motifs and domains with bacterial topoisomerases (Coelho et al., 2015), no further studies have been conducted to explore the role of ASFV-Topo II in ASFV infection. Using a well-established *in vitro* model of infection we showed that ASFV-Topo II mRNA levels continuously increase from 2 hpi to 16 hpi, similarly to other late ASFV genes (reviewed in Rodríguez and Salas, 2013). Most probably, The transcription kinetics of ASFV-Topo II indicates it is most likely needed during the stage of accumulation of viral genomes that serve as templates for DNA replication and transcription, thus showing an increasing number of topological complexities (e. g. knots, tangles and catenanes) that must be solved (reviewed in Rodríguez and Salas, 2013). Still, we cannot reject the possibility that ASFV-Topo II activity may also be required for other mechanisms like genome unpacking after virus entry or genome compaction before viral egress. Furthermore, our siRNA experiments show that a partial depletion of transcripts encoding ASFV-Topo II reduces the viral-induced CPE, the ASFV progeny, the number of infected cells and also the number of viral factories per cell, suggesting that viral transcription activity is diminished. Indeed, Vero cells transfected with siRNAs showed a reduction in mRNA levels of ASFV genes VP32 and VP72, early and late transcripts, respectively (Gil et al., 2008; Zhang et al., 2010). Even though viral transcription is repressed, we cannot exclude that depletion of ASFV-Topo II mRNA levels is in fact inhibiting viral DNA replication, avoiding the synthesis of an enough number of transcription templates to support viral progression. It is also important to refer that some of the siRNA did not induce a higher repression effect, although several siRNA combinations were used to prevent an eventual misbinding like described in other studies (Boden et al., 2003; Gitlin et al., 2005; Keita et al., 2010). In the present study enrofloxacin was found to induce ASFV DNA fragmentation when added at the intermediate-late phase of infection. This phase is characterized by a high rate of viral DNA replication (reviewed in Rodríguez and Salas, 2013) probably when ASFV-Topo II DNA relaxation activity is more needed for viral genome segregation. In contrast, when ASFV-infected Vero cells are exposed to enrofloxacin from the early phase of infection, no viral genomes are detected, suggesting that viral DNA synthesis was completely abolished. Although the mechanism of action of fluoroquinolones in bacteria is not fully understood, it is well known that these drugs target DNA gyrase and topoisomerase IV, blocking the replication machinery and inducing irreversible chromosome fragmentation (Drlica & Malik, 2003; Drlica et al., 2008; Malik et al., 2007). In a similar way, our results strongly suggest that enrofloxacin blocks the activity of

ASFV-Topo II in infected cells, reinforcing previous *in vitro* studies (Mottola et al., 2013; Coelho et al., 2016), and further supporting that the mechanism of action is conserved between ASFV and bacteria.Enrofloxacin most likely acts as a poison by trapping ASFV-Topo II on DNA and stabilizing cleavage complexes which leads to viral DNA fragmentation. When infected cells were exposed to enrofloxacin from 2 hpi onwards, no VP72 transcripts were detected, whereas the early transcription of VP32 and ASFV-Topo II genes seems to be unaffected. These results corroborate a previous research in which enrofloxacin only disrupts late ASFV protein synthesis (Mottola et al., 2013). Overall our results suggest that ASFV-Topo II plays a major role in the intermediate-late phase of infection, probably by unwinding the viral DNA ahead of the transcription and replication machineries. Moreover, it also unlikely that ASFV-Topo II is carried in the virion, since no changes in the transcription of early genes were found. Overall, our results strongly suggest that ASFV-Topo II plays a key role both at intermediate and late stages of viral infection, when viral DNA replication and transcription events are increased. However, we cannot exclude the possibility that this enzyme may also be involved in other early viral mechanisms (e.g unpacking of viral genomes, processing and control of genome concatemerization), since ASFV-Topo II transcripts were detected immediately after infection, reinforcing the idea that ASFV-Topo II could be a good candidate for the development of an effective vaccine or used as target for antiviral therapy. A shematic representation of ASFV TopoII inhibition is represented in figure.

Acknowledgments

This research was supported by the project grant (CIISA-UID/CVT/00276/2013), by the PhD fellowship from the Fundação para a Ciência e Tecnologia (SFRH/BD/104261/2014), and by the European Union's Seventh Framework Programme (FP7/2007-2013) under grant agreement nº 311931, ASFORCE.

CHAPTER V

Discussion, conclusion and future perspectives

1. Discussion

Since its discovery African swine fever virus is considered one of the most puzzling and enigmatic disease agents in veterinary virology. The virus genome contains more than 150 ORFs, some of them characterized as being involved in replication, transcription and virus assembly (Dixon et al., 2013). However, and besides the continuous efforts, most of these ORFs lack any known biological function. The complexity of the virus and the lack of knowledge on ASFV biology and on viral-host interactions have precluded so far the generation of an effective vaccine against this infection (Rock, 2016). Although several studies point out that a vaccine against ASFV must stimulate antibody responses and cytotoxic activity by T cell lymphocytes, so far, either traditional approaches or advanced strategies using recombinant DNA/protein procedures failed to obtain efficient and safe vaccines (Sunwoo et al., 2019). Nevertheless, the basis of vaccine development is supported by the evidence that pigs recovering from ASFV infection develop protection against homologous viral isolates (Boinas et al., 2004; Hamdy & Dardiri, 1984; Mebus & Dardiri, 1980). Moreover, previous studies have also shown that pigs are protected against virulent isolates after initial infection with natural low virulence isolates, with virus attenuated by passage in tissue culture or with mutant virus (in genes involved in virulence) (King et al., 2011; Lacasta et al., 2015; Leitão et al., 2001; Lewis et al., 2000; O'Donnell et al., 2015; Reis et al., 2016). These methodologies have, however, failed to confer protection against heterologous virus and have also shown safety concerns preventing them to be used as vaccines. The current epidemiological scenario of ASF and the devastating socio–economic impacts of the disease in the affected areas highlight the need to fill the knowledge gaps in ASFV critical mechanisms, in order to uncover possible candidates for vaccine development or to be used as drug targets (Arias et al., 2017, 2018). Under this context, the objectives of the studies here described were to characterize the role of ASFV I215L, QP509L, Q706L and P1192R during the infection, aiming at interfering with ASFV replication cycle.

1.1. Characterization of ASFV I215L during the infection

In the present study, it was shown that ASFV pI215L has the capacity to bind to one or two pre-activated ubiquitin molecules in the catalytic residue 85 (Cys 85), as reported in other E2-conjugating enzymes (Randow & Lehner, 2009), that are capable to transfer pre-activated ubiquitin to an E3 enzyme. In other words, these E2 ubiquitin-conjugating enzymes are key players in the proteasome signaling pathway (Randow & Lehner, 2009). Previous studies revealed the presence of ASFV pI215L in extracellular particles (Hingamp et al.,1995), suggesting that this protein is needed for the early steps of infection. Our studies revealed the presence of pI215L conjugation complexes in a wide range of pH values (4-9) suggesting that

this viral enzyme remains active during cell entry via low-pH-dependent endosomal pathway and in the mid gut of the tick where the pH is very low (Sojka et al., 2013). Indeed, a recent study showed that the ubiquitin proteasome system is required for the ASFV early infection, supporting our data and the idea that ASFV subverts this post-transcriptional mechanism for its own benefit (Barrado-Gil et al., 2017). Moreover, ASFV pI215L is able to bind free ubiquitin at distinct temperatures (from 4 to 42 °C) suggesting its participation in different aspects of the viral replication cycle including the infection of the vector under distinct environmental temperatures and during high fever episodes of pigs as previous described (Lvov et al., 2015). Interestingly, mono- di- and poly- ubiquitinated forms were detected in detergent soluble protein fractions of infected cells suggesting that during infection pI215L can be involved in the regulation of a plethora of mechanisms. On the other hand, the detection of di-ubiquitinated forms in detergent-insoluble extracts is probably due to the fact that pI215L binds to host proteins containing an ARID DNA-binding domain like initially reported (Bulimo et al., 2000). The involvement of pI215L in different stages and mechanisms during the infection is corroborated by the detection of two main peaks of I215L mRNA levels (at 2 and 16 hpi), similarly to other viruses (Fukuyo et al., 2011). Moreover, pI215L was earlier detected by immunoblotting studies from 4 hpi throughout infection even in the presence of AraC, a strong transcription inhibitor. Immunolocalization studies also revealed that pI215L is recruited to viral factories (suggesting its involvement in viral transcription and/or DNA replication), presenting a diffuse distribution throughout the cytoplasm that may be related to its role in the ubiquitination of different viral proteins and/or host proteins. Finally, the downregulation assays conducted by siRNA, showed that pI215L i) is crucial for the late viral transcription as identified by a reduction of the transcripts of the late B646L gene, ii) affects the genome replication, since a reduction in the number of ASFV genomes up to 68 % was detected, and iii) induces a decrease of the viral progeny around 94%. Altogether, these results strongly suggest that ASFV subverts the cellular ubiquitin-proteasome pathway being important for viral entry, genome replication, late viral transcription and progeny production similarly to other human and swine viruses (Calistri et al., 2014; Feng et al., 2018; van de Weijer et al., 2017). Although more studies are needed to identify the viral ubiquitination targets during infection, the essential role of pI215L suggests that this mechanism and, this particular protein, can be used to design antiviral strategies such as vaccines and also be an interesting target for drugs.

1.2. ASFV QP509L and Q706L; phylogenetic analysis and activity characterization during the infection

ASFV encodes several putative RNA helicases, suggesting a high degree of independence from the cellular transcription machinery (Rodríguez & Salas, 2013). Previous studies hypothesized that QP509L is orthologous to the vaccinia virus A18R helicase (Baylis et al., 1993; Roberts et al., 1993; Rodríguez & Salas, 2013) and Q706L to the vaccinia virus

D6/D11 helicase (Rodríguez & Salas, 2013; Yáñez et al., 1993). However, no functional characterization studies were previously performed to uncover their involvement in ASFV transcription or in other viral or cellular regulatory processes. QP509L and Q706L share a sequence overlap in ASFV genome, whereas, in vaccinia virus, their counterparts are separated by approximately 20000 bp. Our phylogenetic analysis showed that ASFV-QP509L and Q706L helicases belong to distinct monophyletic clades being highly conserved among virulent and non-virulent isolates. Although the geographic/genotype cluster segregation was found to be very similar for both viral RNA helicases, as reported for ASFV-B646L (Bastos et al., 2003; Boshoff et al., 2007; Lubisi et al., 2005) and for other viral genes (Michaud et al., 2013), some exceptions were identified in our analysis. Namely, the QP509L from the isolate Georgia 2007/1 clusters with Tengani 62 isolate (belonging to distinct genotype) reinforcing the recombination events, recently reported (Rowlands et al., 2008). Indeed, several studies point out that ASFV presents a higher evolutionary rate compared with other DNA virus (Alkhamis et al., 2018; Duffy et al., 2008; Grenfell et al., 2004) probably due its complex inter-species transmission routes between wild boars, ticks and domestic pigs. Besides this, when the phylogenetic analyses was performed between ASFV-QP509L, Q706L and among other RNA helicases belonging to other NCLDV members, a high degree of homology was found corroborating the previous studies and the idea of a common ancestor (Baylis et al., 1993; Duffy et al., 2008; Roberts et al., 1993; Rodríguez & Salas, 2013; Yáñez et al., 1993). Our experiments also revealed that the maximum peak of mRNA transcripts of the two ASFV SF2 RNA helicases was detected between 8 and 12 hpi, corresponding to the intermediate and late stages of the infection, when the viral DNA replication and, in particular the transcription, are more active. pQP509L was detected from 12 hpi in viral factories and host nucleus, whereas pQ706L was detected only at viral factories from 12 hpi onwards, indicating different roles during replication cycle. In particular, the presence of pQP509L in the nucleus at later times of infection suggests its participation in other viral processes besides transcription and/or DNA replication as, for example, modulation of antiviral responses and viral assembly (Dumont et al., 2006; Fairman-Williams et al., 2010; Gross & Shuman, 1998; Lam & Frick, 2006; Ma et al., 2008; Mackintosh et al., 2006; Shuman, 1992). siRNA assays against ASFV-QP509L and Q706L transcripts revealed the essential role of both proteins as showed by the reduction in late viral transcripts (ASFV-B646L), decreased number of viral genomes and viral progeny. These data also support the idea of non-redundant functions for both ASFV RNA helicases and the incapacity of cellular RNA helicases to rescue their function. Although more studies are needed to precisely identify the biological activity of these RNA helicases, our results and the known role of their counterparts in vaccinia virus, suggest that those proteins are involved in viral transcription. The QP509L is probably crucial in termination and release of late viral transcripts (as reported for vaccinia virus A18R helicase ortholog), whereas ASFV-Q706L regulates elongation and release of late viral transcripts (like vaccinia virus D6/D11 helicase).

In eukaryotes, these enzymes are typically associated with the unwind of RNA duplexes in an ATP-dependent fashion (Bizebard et al., 2004; Yang et al., 2007; Yang & Jankowsky, 2006). On the other hand, and during viral infections, they are involved in DNA-RNA and RNA-protein interactions, interfering with gene expression and with the release of infectious particles (Frick & Lam, 2006; Ranji & Boris-Lawrie, 2010). Not surprisingly the essential role of this type of enzymes has also been explored as antiviral drug target (Briguglio et al., 2011). Finally, taking into consideration that there is neither a vaccine nor a treatment available against ASFV and the essential roles of both ASFV SF2 RNA helicases, it can be hypothesized that a mutant on ASFV-QP509L or ASFV-Q706L gene can be a good candidate to generate a live attenuated vaccine. These ASFV mutants will not produce progeny, allowing the immediate-early and early viral gene expression, providing antigens that can induce a protective immune response.

1.3. ASFV-ORF P1192R activity characterization studies during infection

Although some information is available regarding ASFV replication, due to its complexity and to its degree of independence from the host cell, several aspects are still unclear, as the role of ASFV-pP1192R (Dixon et al., 2013). Similarly to eukaryotes and prokaryotes, the ASFV DNA molecule needs to undergo conformational changes before DNA replication takes place. Type II topoisomerases are the type of enzymes that traditionally solve DNA constraints during replication, transcription, chromosome condensation-decondensation and segregation by catalysing transient double-stranded breaks in one DNA helix. In addition, in prokaryotes these proteins are also targets for clinically important antibacterial molecules (fluoroquinolones) and, in eukaryotes, for anticancer drugs (Drlica et al., 2009; Nitiss, 2009a; Vos et al., 2011). ASFV encodes a type II DNA topoisomerase and, interestingly, this viral ORF shares around 20% sequence identity with bacterial topoisomerases (Baylis et al., 1992; García-Beato et al., 1992; Gadelle et al., 2003). Besides this first evidence, only recently it was shown that fluoroquinolones disrupt ASFV infection (Mottola et al., 2013). In this thesis, the role of ASFV-topo II during infection and the anti-viral effect of fluoroquinolones were clarified. The quantification of ASFV-Topo II mRNAs showed an expression dynamic that mimics other well studied late viral transcripts, being detected from 2 hpi but increasing continuously up to 16 hpi (reviewed in Rodríguez and Salas, 2013). This data suggests that this enzyme is important in the intermediate-late phase of infection, when most of DNA replication occurs and when conformation complexities must be solved (reviewed in Rodríguez and Salas, 2013). Moreover, ASFV topo II expression pattern seems to be in accordance with the previous data showing that ASFV topo II co-localizes with cytoplasmic viral factories at intermediate and late phases of infection (Coelho et al., 2016, 2015). However, the role of this enzyme during ASFV infection remained to be clarified. Our siRNA assays revealed that ASFV topo II depletion leads to a reduction in i) viral progeny, ii) the number of infected cells and iii) the number of viral

factories per cell. In parallel, the early and late transcription were also found to be disrupted. However, we cannot exclude that this could be due to a viral DNA replication inhibition that prevents the synthesis of an enough number of transcription templates to support viral progression. Our studies also suggest a similar mechanism of action of fluoroquinolones between ASFV and prokaryotes. Indeed, the exposure to enrofloxacin during the intermediate-late phase of infection induced ASFV DNA fragmentation. This phase of infection is characterized by a high rate of viral DNA replication (reviewed in Rodríguez and Salas, 2013), probably when ASFV-Topo II DNA relaxation activity is more relevant for viral genome segregation. Interestingly, when ASFV-infected Vero cells are exposed to enrofloxacin from early times of infection, the viral DNA synthesis is completely abrogated. Fluoroquinolones are widely used in clinical practice, still, their mechanism of action in bacteria is not fully understood. Some studies state that fluoroquinolones interfere with DNA resealing at the DNA cleavage gate (Bax et al., 2010; Chan et al., 2015; Laponogov et al., 2009, 2010), thus blocking the replication machinery and inducing irreversible chromosome fragmentation (Drlica & Malik, 2003; Drlica et al., 2008; Malik et al., 2007). Indeed, when infected cells were exposed to enrofloxacin from 2 hpi onwards, no VP72 transcripts (late) were detected at all, whereas the early transcription of VP32 seems to be unaffected, suggesting that enrofloxacin is indeed blocking ASFV topo II activity after early gene expression, when the viral DNA replication is increased. Since no changes in the transcription of early genes were found it is unlikely that ASFV-Topo II is carried in the virion; however, its expression from 2 hpi raises the possibility that this enzyme may also be involved in other early viral processes including genome unpacking. Previous studies have also shown a disruption of late ASFV protein synthesis when infected cells were exposed to enrofloxacin (Mottola et al., 2013). Our results suggest that ASFV-Topo II plays a major role in the intermediate-late phase of infection, probably by unwinding the viral DNA ahead of the transcription and replication machineries, similarly to other topoisomerases. *In vitro* studies revealed that ASFV topo II is functional in yeast complementation assays and, capable to catenate, decatenate and relax DNA *in vitro* (Coelho et al., 2016, 2015). Altogether, the results published by our lab suggest that ASFV pP1192R maybe a good candidate to design effective strategies to block the viral infection or even to generate deleted or attenuated viruses to be used as a vaccine (s).

1.4. Future perspectives

The present work reveals that ASFV I215L, QP509, Q706L and P1192R are essential for the viral replication cycle, being involved in DNA replication, RNA transcription and other key regulatory processes. These characterization studies uncover new pathways that may interfere with ASFV infection, either by directly targeting these proteins or the mechanisms they are involved with. Taking into consideration the results obtained and the data available from similar

proteins in other biological systems, including viruses, it is expected that ASFV infectious virions lacking ASFV pI215L will result on an interference with viral protein regulation, crucial for viral cycle progression, during virus entry, viral early/late transcription and DNA replication. Regarding the viral particles deleted in RNA helicases pQP509L and pQ706L, the absence of these proteins will lead to a deficient viral transcription, in elongation and/or release phases. In a similar way, viral particles deleted in P1192R will infect host cells, but viral genome replication will be blocked inducing an irreversible genome fragmentation, thus preventing the release of infectious progeny. It is expected that in the absence of the proteins described above, related to relevant steps in transcription and replication, the expression of other of viral proteins at earlier stages of infection may allow the induction of host protective immune responses that may be silenced upon full viral replication. To further explore this possibility, recombinant particles lacking ASFV I215L, QP509L and Q706L genes were generated. In brief, a selection marker β-glucuronidase (GUS) gene was inserted in a vector (pJET 1.2 Thermo Scientific), flanked by the left and right homology arms (500bp) of each specific ORF, under the control of a strong viral promotor B646L (p72). In the 5´end of the right arm, a restriction (EcoRV- New England Biolabs) site was inserted to facilitate the insertion of the central region of the construct. The vector was used to transfect previously infected Vero cells where by homologous recombination the target gene was replaced by the selection maker like previously described (Abrams & Dixon, 2012) (Figure 25). Primers used to generate these constructs are presented in table 8. To further isolate and expand these viruses deleted in essential genes it is mandatory to generate a complementary cell line expressing the corresponding viral proteins. A complementary helper cell line was also engineered.

Figure 25. Schematic diagram representing the generation recombinant ASF viruses expressing GUS reporter gene.

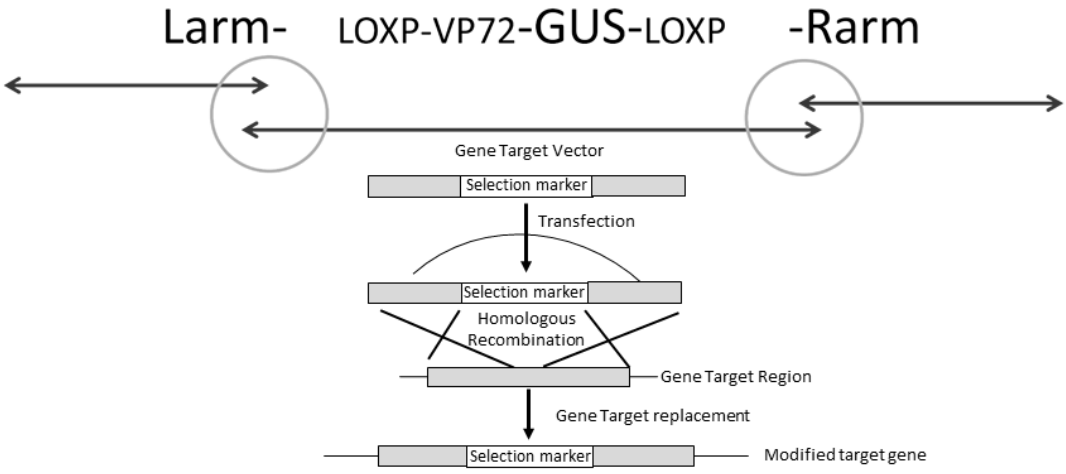

Schematic representation of the strategy to generate ASF recombinant virus. The target gene will be excise by homologous recombination and replaced by the selection marker. The selection marker will allow the identification and isolation of recombinant virus in infected cells.

In our preliminary results, the strategy to obtain the recombinant virus (deleted in ASFV I215L and QP509L or Q706L) seems to be a successful approach since the recombinant viruses expressing the reported GUS gene were identified by the presence of blue plaques when X-Gluc (5-bromo-4-chloro-3-indolyl-b-D-glucuronic acid, Sigma-Aldrich) was added (Figure 26A). In addition, the target replacement by the selection marker was confirmed by PCR for each target gene under study. However, the unsuccessful attempts to isolate and replicate these recombinant viruses, suggest that the generated complementary Vero cell lines do not support the replication of recombinant mutants (Figure 26B).

The main issue in the generation of virus lacking essential genes is the production of a helper cell line expressing the corresponding viral gene, being able to rescue the original function of the protein. So far, these difficulties preclude our strategy to obtain an ASFV DISC. However, further studies should be done to generate a stable cell line. At the time of writing this thesis, new approaches to generate complementary cell lines are being performed using the CRISPR/Cas9. This strategy aims to introduce the viral ORF in specific regions of the cell genome (non-essential but actively transcribed regions), and to tightly regulate the expression of heterologous protein. Moreover, once isolated, these DISC particles must be characterized in terms of transcript expression, genome replication and viral progeny production.

Figure 26. Isolation of recombinant virus using the plaque method.

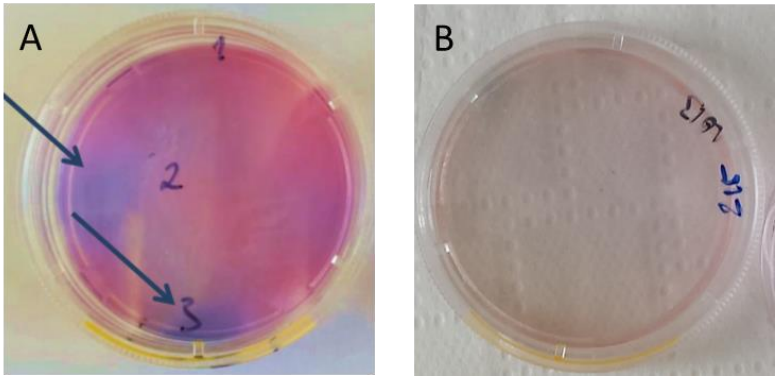

Supernatants of the recombination step were used to infect new Vero-cells expressing pI215L, pQP509L and pQ706L. A layer of agarose and X-Gluc was added after infection (A). Recombinant virus detected by a blue infection plaques, (B). The blue plaques formed were picked and used to infect new cell cultures. No blue plaques were visible in a third passage.

Table 8. Primers used to generate the constructs for viral gene deletion.

Target	Primer designation	Sequence (5´- 3´)	Orientation
ASFV-I215L	215LarmFw	GGTACCCTTTAAATGTATAACGACAACTA AAACCCCT	Forward
ASFV-I215L	215LarmRv	CGCGGATCCATCGGTCCCACGGTTATTT AATATTAATTAAATTCCCTGGTTTATTCC	Forward
ASFV-I215L	215RarmFw	TGGATCCAGCGGCCCGACGTACGTTTAC ATTTTAGTGTTGATTTTAGTTACTTAGATT TTAGTG	Reverse
ASFV-I215L	215RarmRv	TCTAGATGCATGAAATGCCAGCAG	Forward
ASFV-QP509L	509LarmFw	GGTACCGATAAACAAGCTCACTCACTTCT GAGTG	Forward
ASFV-QP509L	509LarmRv	CGCGGATCCATCGGTCCCACATGGCCTC CATTCTCGC	Reverse
ASFV-QP509L	509RarmFw	TGGATCCAGCGGCCCGACGTACGATGTC TTGCGTGCACAACAA	
ASFV-QP509L	509RarmRv	TCTAGAGGCGCTATTGATAATTCCTCTAA AGAG	
ASFV-Q706L	706LarmFw	GGTACCCGATGAGCCGTATGGCATC	
ASFV-Q706L	706LarmRv	CGCGGATCCATCGGTCCCACCTCTTTAT ATTTTTCATATACCTCTTTTAGGTATGCTT	Forward
ASFV-Q706L	706RarmFw	TGGATCCAGCGGCCCGACGTACGATGTC CAGGCCGGAACA	Reverse
ASFV-Q706L	706RarmRv	TCTAGACAGCGCTTCCAAAGTCAATG	Forward
GUS-gene	GUSFw	ATTTAATAAAAACAATAAATTATTTTTATA ACATTATATATGTTACGTCCTGTAGAAAC CCCAACC	Reverse
GUS-gene	GUSRV	TCATTGTTTGCCTCCCTGCTG	Forward

1.5. General conclusion

ASF is a major threat to pig husbandry at global scale. Following the transcontinental introduction of the disease in Georgia (2007) and due to existing poor biosecurity conditions, complex transmission routes and the lack of a vaccine or treatment, the continuous spread of ASF to non-endemic areas of Europe and Asia constitutes one of the major concerns for national and international animal health authorities. Despite the efforts in the last decades, ASFV complexity and the gaps on the knowledge of its biology thwart the development of an efficient vaccine to control the disease. Under these circumstances, this work aimed at characterizing the ASFV I215L, QP509L, Q706L and P1192R proteins during the infection. These studies contribute to increase the knowledge on ASFV biology, by uncovering the expression dynamics, cellular distribution and biologic role of each of those proteins, in key steps of the viral infection, which open new insights for the rational design of efficient vaccines against ASF.

References

Abrams, C. C., & Dixon, L. K. (2012). Sequential deletion of genes from the African swine fever virus genome using the cre/loxP recombination system. *Virology*, 433 (1), 142-148.

Abrams, C. C., Goatley, L., Fishbourne, E., Chapman, D., Cooke, L., Oura, C. A., Netherton, C. L.,Takamatsu, H. H., & Dixon, L. K. (2013). Deletion of virulence associated genes from attenuated African swine fever virus isolate OUR T88/3 decreases its ability to protect against challenge with virulent virus. *Virology*, 443 (1), 99-105.

Ahmad, S., & Hur, S. (2015). Helicases in Antiviral Immunity: Dual Properties as Sensors and Effectors. *Trends in Biochemical Sciences*. 40 (10), 576-585.

Alcamí, A., Angulo, A., López-Otín, C., Muñoz, M., Freije, J. M., Carrascosa, A. L., & Viñuela, E. (1992). Amino acid sequence and structural properties of protein p12, an African swine fever virus attachment protein. *Journal of Virology*, 66 (6), 3860-8.

Alcamí, A., Carrascosa, A. L., & Viñuela, E. (1989). The entry of African swine fever virus into Vero cells. *Virology*, 171 (1), 68-75.

Alkhamis, M. A., Gallardo, C., Jurado, C., Soler, A., Arias, M., & Sánchez-Vizcaíno, & J. M. (2018). Phylodynamics and evolutionary epidemiology of African swine fever p72-CVR genes in Eurasia and Africa. *PloS One* 13 (2), e0192565.

Almazán, F., Rodríguez, J. M., Andrés, G., Perez, R., Viñuela, E., & Rodríguez, J. F. (1992). Transcriptional analysis of multigene family 110 of African swine fever virus. *Journal of Virology*, 66 (11), 6655-6667.

Almazán, F., Rodríguez, J. M., Angulo, A., Viñuela, E., & Rodriguez, J. F. (1993). Transcriptional mapping of a late gene coding for the p12 attachment protein of African swine fever virus. *Journal of Virology*, 67 (1), 553-556.

Alonso, C., Galindo, I., Cuesta-Geijo, M. A., Cabezas, M., Hernaez, B., & Muñoz-Moreno, R., (2013) African swine fever virus-cell interactions: From virus entry to cell survival. *Virus Research,* 173 (1), 42-57.

Andrés, G., Alejo, A., Salas, J., & Salas, M. L. (2002). African Swine Fever Virus Polyproteins pp220 and pp62 Assemble into the Core Shell. *Journal of Virology*, 76 (24), 12473-12482.

Andrés, G., García-Escudero, R., Viñuela, E., Salas, M. L., & Rodríguez, J. M. (2001). African swine fever virus structural protein pE120R is essential for virus transport from assembly sites to plasma membrane but not for infectivity. *Journal of Virology*, 75 (15), 6758-6768.

Angulo, A., Viñuela, E., & Alcamí, A. (1993). Inhibition of African swine fever virus binding and infectivity by purified recombinant virus attachment protein p12. *Journal of Virology*, 67 (9), 5463-5471.

Anthony, K. G., Bai, F., Krishnan, M. N., Fikrig, E., & Koski, R. A. (2009). Effective siRNA targeting of the 3' untranslated region of the West Nile virus genome. *Antiviral Research*, 82 (3), 166-168.

Argilaguet, J. M., Pérez-Martín, E., López, S., Goethe, M., Escribano, J. M., Giesow, K., Keil, J. M., & Rodríguez, F. (2013). BacMam immunization partially protects pigs against sublethal challenge with African swine fever virus. *Antiviral Research*, 98 (1), 61-65.

Arias, M., de la Torre, A., Dixon, L., Gallardo, C., Jori, F., Laddomada, A., Martins, C., Parkhouse, R. M., Revilla, Y., Rodriguez, F., & Sanchez-Vizcaino, J. M. (2017). Approaches and Perspectives for Development of African Swine Fever Virus Vaccines. *Vaccines*, 5 (4), e35.

Arias, M., Jurado, C., Gallardo, C., Fernández-Pinero, J., & Sánchez-Vizcaíno, J. M. (2018). Gaps in African swine fever: Analysis and priorities. *Transboundary and Emerging Diseases*, 65 (1), 235-247.

Backes, S., Shapiro, J. S., Sabin, L. R., Pham, A. M., Reyes, I., Moss, B., Cherry, S., TenOever, B. R. (2012). Degradation of host microRNAs by poxvirus poly(A) polymerase reveals terminal RNA methylation as a protective antiviral mechanism. *Cell Host & Microbe*, 12 (2), 200-210.

Ballester, M., Rodríguez-Cariño, C., Pérez, M., Gallardo, C., Rodríguez, J. M., Salas, M. L., & Rodriguez, F. (2011). Disruption of nuclear organization during the initial phase of African swine fever virus infection. *Journal of Virology*, 85 (16), 8263-8269.

Barrado-Gil, L., Galindo, I., Martínez-Alonso, D., Viedma, S., & Alonso, C. (2017). The ubiquitin-proteasome system is required for African swine fever replication. *PloS One*. 12 (12), e0189741.

Basta, S., Gerber, H., Schaub, A., Summerfield, A., & McCullough, K. C. (2010). Cellular processes essential for African swine fever virus to infect and replicate in primary macrophages. *Veterinary Microbiology*, 140 (1–2), 9-17.

Bastos, A. D. S., Penrith, M. L., Crucière, C., Edrich, J. L., Hutchings, G., Roger, F., Couacy-Hymann, E., & Thomson, G. R. (2003). Genotyping field strains of African swine fever virus by partial p72 gene characterisation. *Archives of Virology*, 148 (4), 693-706.

Bax, B. D., Chan, P. F., Eggleston, D. S., Fosberry, A., Gentry, D. R., Gorrec, F., Giordano, I., Hann, M. M., Hennessy, A., Hibbs, M., Huang, J., Jones, E., Jones, J., Brown, K. K., Lewis, C. J., May, E. W., Saunders, M. R., Singh, O., Spitzfaden, C. E., Shen, C., Shillings, A., Theobald, A.J., Wohlkonig, A. Pearson, N. D., & Gwynn, M. N. (2010). Type IIA topoisomerase inhibition by a new class of antibacterial agents. *Nature*, 466, 935-940.

Baylis, S. A., Dixon, L. K., Vydelingum, S., & Smith, G. L. (1992). African swine fever virus encodes a gene with extensive homology to type II DNA topoisomerases. *Journal of Molecular Biology*, 228 (3), 1003-1010.

Baylis, S. A., Twigg, S. R. F., Vydelingum, S., Dixon, L. K., & Smith, G. L. (1993). Three African swine fever virus genes encoding proteins with homology to putative helicases of *vaccinia virus*. *Journal of General Virology*, 74 (9), 1969-1974.

Belon, C. A., & Frick, D. N. (2009). Helicase inhibitors as specifically targeted antiviral therapy

for hepatitis C. *Future Virology*, 4 (3), 277-293.

Bishop, R. P., Fleischauer, C., De Villiers, E. P., Okoth, E. A., Arias, M. L., & Gallardo, C. (2015). Comparative analysis of the complete genome sequences of Kenyan African swine fever virus isolates within p72 genotypes IX and X. *Virus Genes*, 50 (2), 303-309.

Bizebard, T., Ferlenghi, I., Iost, I., & Dreyfus, M. (2004). Studies on three *E. coli* DEAD-box helicases point to an unwinding mechanism different from that of model DNA helicases. *Biochemistry*, 43 (24), 7857-7866.

Blome, S., Gabriel, C., & Beer, M. (2013). Pathogenesis of African swine fever un domestic pigs and European wild boar. *Virus Research*, 173 (1), 122-30.

Blome, S., Gabriel, C., & Beer, M. (2014). Modern adjuvants do not enhance the efficacy of an inactivated African swine fever virus vaccine preparation. *Vaccine*, 32 (31), 3879-82.

Boden, D., Pusch, O., Lee, F., Tucker, L., & Ramratnam, B. (2003). Human Immunodeficiency Virus Type 1 Escape from RNA Interference. *Journal of Virology*, 77 (21), 11531-11535.

Boinas, F. S., Hutchings, G. H., Dixon, L. K., & Wilkinson, P. J. (2004). Characterization of pathogenic and non-pathogenic African swine fever virus isolates from *Ornithodoros erraticus* inhabiting pig premises in Portugal. *Journal of General Virology*, 85, 2177-2187.

Boinas, F. S., Ribeiro, R., Madeira, S., Palma, M., de Carvalho, I. L., Núncio, S., & Wilson, A. J. (2014). The medical and veterinary role of *Ornithodoros erraticus* complex ticks (Acari: Ixodida) on the Iberian Peninsula. *Journal of Vector Ecology: Journal of the Society for Vector Ecology*, 39 (2), 238-248.

Boinas, F. S., Wilson, A. J., Hutchings, G. H., Martins, C., & Dixon, L. J. (2011). The persistence of African swine fever virus in field-infected Ornithodoros erraticus during the ASF endemic period in Portugal. *PloS One*, 6 (5), e20383.

Borca, M. V., Irusta, P. M., Kutish, G. F., Carrillo, C., Afonso, C. L., Burrage, T., Neilan, J. G., & Rock, D. L. (1996). A structural DNA binding protein of African swine fever virus with similarity to bacterial histone-like proteins. *Archives of Virology*, 141 (2), 301-13

Boshoff, C. I., Bastos, A. D., Gerber, L. J., & Vosloo, W. (2007). Genetic characterisation of African swine fever viruses from outbreaks in southern Africa (1973-1999). *Veterinary Microbiology*, 121 (1–2), 45-55.

Breese, S. S., & DeBoer, C. J. (1966). Electron microscope observations of African swine fever virus in tissue culture cells. *Virology*, 28, (3), 420-428.

Briguglio, I., Piras, S., Corona, P., & Carta, A. (2011). Inhibition of RNA Helicases of ssRNA+ Virus Belonging to *Flaviviridae*, *Coronaviridae* and *Picornaviridae* Families. *International Journal of Medicinal Chemistry*, 54 (5), 1-22.

Brookes, S. M., Hyatt, A. D., Wise, T., & Parkhouse, R. M. E. (1998). Intracellular virus DNA distribution and the acquisition of the nucleoprotein core during African swine fever virus particle assembly: ultrastructural *in situ* hybridisation and DNase-gold labelling. *Virology*, 249 (1), 175-88.

Broyles, S. S. (2003). Vaccinia virus transcription. *Journal of General Virology*. 84, 2293-2303.

Bulimo, W. D., Miskin, J. E., & Dixon, L. K. (2000). An ARID family protein binds to the African swine fever virus encoded ubiquitin conjugating enzyme, UBCv1. *FEBS Letters*, 471 (1), 17-22.

Calistri, A., Munegato, D., Carli, I., Parolin, Parolin, C., G., & Palù, G. (2014). The ubiquitin-conjugating system: Multiple roles in viral replication and infection. *Cells*, 3 (2), 386-417.

Carrascosa, A. L., Bustos, M. J., & de Leon, P. (2011). Methods for growing and titrating african swine fever virus: Field and laboratory samples. *Current Protocols in Cell Biology*, 53 (1), 26141-261425.

Caruthers, J. M., & McKay, D. B. (2002). Helicase structure and mechanism. *Current Opinion in Structural Biology*, 12 (1), 123-133.

Champoux, J. J. (2001). DNA topoisomerases: structure, function, and mechanism. *Annual Review of Biochemistry*, 70, 369-413.

Chan, P. F., Srikannathasan, V., Huang, J., Cui, H., Fosberry, A. P., Gu, M., Hann, M.M., Hibbs, M., Homes, P., Ingraham, K., Pizzollo, J., Shen, C., Shillings, A. J., Spitzfaden, C. E., Tanner, R., Theobald, A.J., Stavenger, R. A. Bax, B. D., & Gwynn, M. N. (2015). Structural basis of DNA gyrase inhibition by antibacterial QPT-1, anticancer drug etoposide and moxifloxacin. *Nature Communications*, 6, 10048.

Chapman, D. A., Darby, A. C., Da Silva, M., Upton, C., Radford, A. D., & Dixon, L. K. (2011). Genomic analysis of highly virulent Georgia 2007/1 isolate of African swine fever virus. *Emerging Infectious Disease*, 17 (4), 599-605.

Chapman, D. A. G., Tcherepanov, V., Upton, C., & Dixon, L. K. (2008). Comparison of the genome sequences of nonpathogenic and pathogenic African swine fever virus isolates. *Journal of General Virology*, 89 (2), 397-408.

Chattopadhyay, S., Chen, Y., & Weller, S. K. (2006). The two helicases of herpes simplex virus type 1 (HSV-1). *Frontiers in Bioscience*, 11*,* 2213-2223.

Christensen, J., & Tattersall, P. (2002). Parvovirus initiator protein NS1 and RPA coordinate replication fork progression in a reconstituted DNA replication system. *Journal of Virology*, 76 (13), 6518-6531.

Cobbold, C., Windsor, M., & Wileman, T. (2001). A virally encoded chaperone specialized for folding of the major capsid protein of African swine fever virus. *Journal of Virology*, 75 (16), 7221-7229.

Coelho, J., Ferreira, F., Martins, C., & Leitão, A. (2016). Functional characterization and inhibition of the type II DNA topoisomerase coded by African swine fever virus. *Virology*, 493, 209-216.

Coelho, J., Martins, C., Ferreira, F., & Leitão, A. (2015). African swine fever virus ORF P1192R codes for a functional type II DNA topoisomerase. *Virology*, 474, 82–93.

Colson, P., De Lamballerie, X., Yutin, N., Asgari, S., Bigot, Y., Bideshi, D. K., Cheng, X.

W., Federici, B. A., Van Etten, J.L., Koonin, E. V., La Scola, B., & Raoult, D. (2013). 'Megavirales', a proposed new order for eukaryotic nucleocytoplasmic large DNA viruses. *Archives of Virology*, 158 (12), 2517-2521.

Corbett, K. D., & Berger, J. M. (2004). Structure, Molecular Mechanisms, and Evolutionary Relationships in DNA Topoisomerases. *Annual Review of Biophysics and Biomolecular Structure*, 3 (1), 95-118.

Corbett, K. D., Schoeffler, A. J., Thomsen, N. D., & Berger, J. M. (2005). The structural basis for substrate specificity in DNA topoisomerase IV. *Journal of Molecular Biology*, 351 (3), 545-561.

Cordin, O., & Beggs, J. D. (2013). RNA helicases in splicing. *RNA Biology*, 10 (1), 83-95.

Cordin, O., Hahn, D., & Beggs, J. D. (2012). Structure, function and regulation of spliceosomal RNA helicases. *Current Opinion in Cell Biology*, 24 (3), 431-438.

Correia, S., Ventura, S., & Parkhouse, R. M. (2013). Identification and utility of innate immune system evasion mechanisms of ASFV. *Virus Research*, 173 (1), 87-100.

Costard, S., Mur, L., Lubroth, J., Sanchez-Vizcaino, J. M., & Pfeiffer, D. U. (2013). Epidemiology of African swine fever virus. *Virus Research*, 173 (1), 191-197.

Costard, S., Wieland, B., de Glanville, W., Jori, F., Rowlands, R., Vosloo, W., Roger, F., Pfeiffer, D.U., & Dixon, L. K. (2009). African swine fever: How can global spread be prevented? *Philosophical Transactions of the Royal Society B: Biological Sciences*, 364 (1530), 2683-2696.

Cuesta-Geijo, M. A., Galindo, I., Hernáez, B., Quetglas, J. I., Dalmau-Mena, I., & Alonso, C. (2012). Endosomal Maturation, Rab7 GTPase and Phosphoinositides in African Swine Fever Virus Entry. *PloS One*, 7 (11), e48853.

David, Y., Ziv, T., Admon, A., & Navon, A. (2010). The E2 ubiquitin-conjugating enzymes direct polyubiquitination to preferred lysines. *Journal of Biological Chemistry*, 285 (12), 8595-8604.

De Silva, F. S., Lewis, W., Berglund, P., Koonin, E. V., & Moss, B. (2007). Poxvirus DNA primase. *Proceedings of the National Academy of Sciences*, 104 (47), 18724-18729

de Souza, R. F., Iyer, L. M., & Aravind, L. (2010). Diversity and evolution of chromatin proteins encoded by DNA viruses. *Biochimica et Biophysica Acta*, 1799 (3-4), 302-318.

De Villiers, E. P., Gallardo, C., Arias, M., Da Silva, M., Upton, C., & Martin, R. (2010). Phylogenomic analysis of 11 complete African swine fever virus genome sequences. *Virology*, 400 (1), 128-136.

Deng, L., Wang, C., Spencer, E., Yang, L., Braun, A., You, J., Slaughter, C., Pickart, C., Chen, Z. J. (2000). Activation of the IkappaB kinase complex by TRAF6 requires a dimeric ubiquitin-conjugating enzyme complex and a unique polyubiquitin chain. *Cell*, 103 (2), 351-361.

Detray, D. E. (1957). Persistence of viremia and immunity in African swine fever. *American*

Journal of Veterinary Research, 18 (69), 811-816.

Dixon, L. K., Alonso, C., Escribano, J. M., Martins, C., Revilla, Y., Salas, M. L., & Takamatsu, H. (2012). *Family Asfarviridae. In A. M.Q. King, M.J. Adams, E. B. Carstens, and E. J. Lefkowitz (*Eds*.) Virus Taxonomy: Classification and Nomenclature of Viruses. Ninth Report of the International Committee on Taxonomy of Viruses.* San Diego: Academic Press. pp1338.

Dixon, L. K., Chapman, D. A. G., Netherton, C. L., & Upton, C. (2013). African swine fever virus replication and genomics. *Virus Research*, 173 (1), 3-14.

Dixon, L. K., Twigg, S. R. F., Baylis, S. A., Vydelingum, S., Bristow, C., Hammond, J. M., & Smith, G. L. (1994). Nucleotide sequence of a 55 kbp region from the right end of the genome of a pathogenic African swine fever virus isolate (Malawi LIL20/1). *Journal of General Virology*, 75 (7), 1655-1684.

Drlica, K., Hiasa, H., Kerns, R., Malik, M., Mustaev, A., & Zhao, X. (2009). Quinolones: Action and Resistance Updated. *Current Topics in Medicinal Chemistry*, 9 (11), 981-998.

Drlica, K., & Malik, M. (2003). Fluoroquinolones: action and resistance. *Current Topics in Medicinal Chemistry*, 3 (3), 249-282.

Drlica, K., Malik, M., Kerns, R. J., & Zhao, X. (2008). Quinolone-Mediated Bacterial Death. *Antimicrobial Agents and Chemotherapy*, 52 (2), 385-392.

Dudek, T., & Knipe, D. M. (2006). Replication-defective viruses as vaccines and vaccine vectors. *Virology*, 344 (1), 230-239.

Duffy, S., Shackelton, L. A., & Holmes, E. C. (2008). Rates of evolutionary change in viruses: Patterns and determinants. *Nature Reviews Genetics*, 9, 267-276.

Dumont, S., Cheng, W., Serebrov, V., Beran, R. K., Tinoco, I., Pyle, A. M., & Bustamante, C. (2006). RNA translocation and unwinding mechanism of HCV NS3 helicase and its coordination by ATP. *Nature*, 439 (7072), 105-108.

EFSA Panel. (2014). EFSA Scientific opion on African Swine Fever 2014. *EFSA Journal*, 12 (4), 1-77.

Epifano, C., Krijnse-Locker, J., Salas, M. L., Salas, J., & Rodríguez, J. M. (2006). Generation of filamentous instead of icosahedral particles by repression of African Swine Fever Virus structural protein pB438L. *Journal of Virology*, 80 (23), 11456-11466.

Fairman-Williams, M. E., Guenther, U. P., & Jankowsky, E. (2010). SF1 and SF2 helicases: Family matters. *Current Opinion in Structural Biology*, 20 (3), 313-324.

Feenstra, F., Pap, J. S., & van Rijn, P. A. (2015). Application of Bluetongue Disabled Infectious Single Animal (DISA) vaccine for different serotypes by VP2 exchange or incorporation of chimeric VP2. *Vaccine*, 33 (6), 812-818.

Feng, T., Deng, L., Lu, X., Pan, W., Wu, Q., & Dai, J. (2018). Ubiquitin-conjugating enzyme UBE2J1 negatively modulates interferon pathway and promotes RNA virus infection. *Virology Journal*, 15 (132), 1-9.

Fernández, A., & Guo, H. (1997). The motif V of plum pox potyvirus CI RNA helicase is involved in NTP hydrolysis and is essential for virus RNA replication. *Nucleic Acids*, 25 (22), 4474-4480.

Ferreira, C. (1996). Expression of ubiquitin, actin, and actin-like genes in African swine fever virus infected cells. *Virus Research*, 44 (1), 11-21.

Forman, A. J., Wardley, R. C., & Wilkinson, P. J. (1982). The immunological response of pigs and guinea pigs to antigens of African swine fever virus. *Archives of Virology*, 74 (2–3), 91-100.

Forterre, P., Gribaldo, S., Gadelle, D., & Serre, M.-C. (2007). Origin and evolution of DNA topoisomerases. *Biochimie*, 89 (4), 427-46.

Fouraux, M. A., Kolkman, M. J. M., Van Der Heijden, A., De Jong, A. S., Van Venrooij, W. J., & Pruijn, G. J. M. (2002). The human La (SS-B) autoantigen interacts with DDX15/hPrp43, a putative DEAH-box RNA helicase. *RNA*, 8 (11), 1428-1443.

Freije, J. M., Lain, S., Vinuela, E., Lopez Otin, C., & Lopez-Otin, C. (1993). Nucleotide sequence of a nucleoside triphosphate phosphohydrolase gene from African swine fever virus. *Virus Research*, 30, 63-72.

Freitas, F. B. F. B., Frouco, G., Martins, C., Leitão, A., & Ferreira, F. (2016). *In vitro* inhibition of African swine fever virus-topoisomerase II disrupts viral replication. *Antiviral Research*, 134, 34-41.

Frick, D. N., & Lam, A. M. (2006). Understanding helicases as a means of virus control. *Current Pharmaceutical Design*, 12 (11), 1315-1338.

Fukuyo, Y., Horikoshi, N., Ishov, A. M., Silverstein, S. J., & Nakajima, T. (2011). The herpes simplex virus immediate-early ubiquitin ligase ICP0 induces degradation of the ICP0 repressor protein E2FBP1. *Journal of Virology*, 85 (7), 3356-3366.

Gabriel, C., Blome, S., Malogolovkin, A., Parilov, S., Kolbasov, D., Teifke, J. P., & Beer, M. (2011). Characterization of African swine fever virus Caucasus isolate in European wild boars. *Emerging Infectious Diseases*, 17 (12), 2342-2345.

Gadelle, D., Filée, J., Buhler, C., & Forterre, P. (2003). Phylogenomics of type II DNA topoisomerases. *BioEssays : News and Reviews in Molecular, Cellular and Developmental Biology*, 25 (3), 232-242.

Galindo-Cardiel, I., Ballester, M., Solanes, D., Nofrarías, M., López-Soria, S., Argilaguet, J. M., Lacasta, A., Accensi, F., Rodríguez, F., & Segalés, J. (2013). Standardization of pathological investigations in the framework of experimental ASFV infections. *Virus Research*, 173 (1), 180-190.

Galindo, I., & Alonso, C. (2017). African swine fever virus: A review. *Viruses*, 9 (5), 103.

Galindo, I., Cuesta-Geijo, M. A., Hlavova, K., Muñoz-Moreno, R., Barrado-Gil, L., Dominguez, J., & Alonso, C. (2015). African swine fever virus infects macrophages, the natural host cells, via clathrin- and cholesterol-dependent endocytosis. *Virus Research*, 200, 45-55.

Gallardo, C., Reoyo, A. de la T., Fernández-Pinero, J., Iglesias, I., Muñoz, M. J., & Arias, M. (2015). African swine fever: a global view of the current challenge. *Porcine Health Management*, 1 (1), 21.

Gallardo, C., Sánchez, E. G., Pérez-Núñez, D., Nogal, M., de León, P., Carrascosa, Á. L., Soler, A., Arias, M. L., & Revilla, Y. (2018). African swine fever virus (ASFV) protection mediated by NH/P68 and NH/P68 recombinant live-attenuated viruses. *Vaccine*, 36 (19), 2694-2704.

García-Beato, R., Freije, J. M., López-Otín, C., Blasco, R., Viñuela, E., & Salas, M. L. (1992). A gene homologous to topoisomerase II in African swine fever virus. *Virology*, 188 (2), 938-947.

García-Beato, R., Salas, M. L., Viñuela, E., & Salas, J. (1992). Role of the host cell nucleus in the replication of African swine fever virus DNA. *Virology*, 188 (2), 637-649.

García-Escudero, R., & Viñuela, E. (2000). Structure of African swine fever virus late promoters: requirement of a TATA sequence at the initiation region. *Journal of Virology*, 74 (17), 8176-8182.

Gellert, M., Mizuuchi, K., O'Dea, M. H., & Nash, H. A. (1976). DNA gyrase: an enzyme that introduces superhelical turns into DNA. *Proceedings of the National Academy of Sciences*, 73 (11), 3872-3876.

Gil, S., Sepúlveda, N., Albina, E., Leitão, A., & Martins, C. (2008). The low-virulent African swine fever virus (ASFV/NH/P68) induces enhanced expression and production of relevant regulatory cytokines (IFNalpha, TNFalpha and IL12p40) on porcine macrophages in comparison to the highly virulent ASFV/L60. *Archives of Virology*, 153 (10), 1845-1854.

Gitlin, L., Stone, J. K., & Andino, R. (2005). Poliovirus escape from RNA interference: short interfering RNA-target recognition and implications for therapeutic approaches. *Journal of Virology*, 79 (2), 1027-1035.

Gogin, A., Gerasimov, V., Malogolovkin, A., & Kolbasov, D. (2013). African swine fever in the North Caucasus region and the Russian Federation in years 2007-2012. *Virus Research*, 173 (1), 198-203.

Gómez-Puertas, P., Rodríguez, F., Oviedo, J. M., Brun, A., Alonso, C., & Escribano, J. M. (1998). The African swine fever virus proteins p54 and p30 are involved in two distinct steps of virus attachment and both contribute to the antibody-mediated protective immune response. *Virology*, 243 (2), 461-471.

González-Santamaría, J., Campagna, M., García, M. A., Marcos-Villar, L., González, D., Gallego, P., Lopitz-Otsoa, F., Guerra, S., Rodríguez, M. S., Esteban, M., & Rivas, C. (2011). Regulation of *Vaccinia virus* E3 protein by small ubiquitin-like modifier proteins. *Journal of Virology*, 85 (24), 12890-12900.

Gorbalenya, A. E., & Koonin, E. V. (1993). Helicases: amino acid sequence comparisons and

structure-function relationships. *Current Opinion in Structural Biology*, 3 (3), 419-429.

Grenfell, B. T., Pybus, O. G., Gog, J. R., Wood, J. L. N., Daly, J. M., Mumford, J. A., & Holmes, E. C. (2004). Unifying the epidemiological and evolutionary dynamics of pathogens. *Science*, 303 (5656), 327-332.

Gross, C. H., & Shuman, S. (1998). The nucleoside triphosphatase and helicase activities of vaccinia virus NPH-II are essential for virus replication. *Journal of Virology*, 72 (6), 4729-4736.

Grue, P., Gräßer, A., Sehested, M., Jensen, P. B., Uhse, A., Straub, T., Ness, W., & Boege, F. (1998). Essential mitotic functions of DNA topoisomerase IIα are not adopted by topoisomerase IIβ in human H69 cells. *Journal of Biological Chemistry*, 273, 33660-33666.

Guinat, C., Gogin, A., Blome, S., Keil, G., Pollin, R., Pfeiffer, D. U., & Dixon, L. (2016). Transmission routes of African swine fever virus to domestic pigs: current knowledge and future research directions. *The Veterinary Record*, 178 (11), 262-267.

Gulenkin, V. M., Korennoy, F. I., Karaulov, A. K., & Dudnikov, S. A. (2011). Cartographical analysis of African swine fever outbreaks in the territory of the Russian Federation and computer modeling of the basic reproduction ratio. *Preventive Veterinary Medicine*, 102 (3), 167-174.

Gustin, J. K., Moses, A. V., Früh, K., & Douglas, J. L. (2011). Viral takeover of the host Ubiquitin system. *Frontiers in Microbiology*, 2, 161.

Haglund, K., & Dikic, I. (2005). Ubiquitylation and cell signaling. *The EMBO Journal*, 24 (19), 3353–3359.

Hamdy, F. M., & Dardiri, A. H. (1984). Clinical and immunologic responses of pigs to African swine fever virus isolated from the Western Hemisphere. *American Journal of Veterinary Research*, 45 (4), 711-714.

He, Y., Andersen, G. R., & Nielsen, K. H. (2010). Structural basis for the function of DEAH helicases. *EMBO Reports*, 11 (3), 180-186.

Hernáez, B., & Alonso, C. (2010). Dynamin- and clathrin-dependent endocytosis in African swine fever virus entry. *Journal of Virology*, 84 (4), 2100-2109.

Hernáez, B., Guerra, M., Salas, M. L., & Andrés, G. (2016). African Swine Fever Virus undergoes outer envelope disruption, capsid disassembly and inner envelope fusion before core release from multivesicular endosomes. *PLoS Pathogens*, 12 (4), e1005595.

Hershko, A., & Ciechanover, A. (1998). The ubiquitin system. *Annual Review of Biochemistry*, 67, 425-79.

Hingamp, P. M., Arnold, J. E., Mayer, R. J., & Dixon, L. K. (1992). A ubiquitin conjugating enzyme encoded by African swine fever virus. The *EMBO Journal*, 11 (1), 361-366.

Hingamp, P. M., Leyland, M. L., Webb, J., Twigger, S., Mayer, R. J., & Dixon, L. K. (1995). Characterization of a ubiquitinated protein which is externally located in African swine

fever virions. *Journal of Virology*, 69 (3), 1785-1793.

Hirsch, A. J. (2010). The use of RNAi-based screens to identify host proteins involved in viral replication. *Future Microbiology*, 5 (2), 303-311.

Hochstrasser, M. (2006). Lingering mysteries of ubiquitin-chain assembly. *Cell*, 124 (1), 27-34.

Hoeller, D., Crosetto, N., Blagoev, B., Raiborg, C., Tikkanen, R., Wagner, S., Kowanetz, K., Breitling, R., Mann, M., Stenmark, H., & Dikic, I. (2006). Regulation of ubiquitin-binding proteins by monoubiquitination. *Nature Cell Biology*, 8 (2), 163-169.

Isaacs, R. J., Davies, S. L., Sandri, M. I., Redwood, C., Wells, N. J., & Hickson, I. D. (1998). Physiological regulation of eukaryotic topoisomerase II. *Biochimica et Biophysica Acta - Gene Structure and Expression,* 1400 (1-3), 121-137.

Isaacson, M. K., & Ploegh, H. L. (2009). Ubiquitination, ubiquitin-like modifiers, and deubiquitination in viral infection. *Cell Host and Microbe*, 5 (6), 559-570.

Iyer, L. M., Aravind, L., & Koonin, E. V. (2001). Common Origin of Four Diverse Families of Large Eukaryotic DNA Viruses. *Journal of Virology*, 75 (23), 11720-11734.

Iyer, L. M., Balaji, S., Koonin, E. V., & Aravind, L. (2006). Evolutionary genomics of nucleo-cytoplasmic large DNA viruses. *Virus Research*, 117 (1), 156-184.

Jankowsky, E. (2000). The DExH/D protein family database. *Nucleic Acids Research*, 28 (1), 333-334.

Jankowsky, E. (2011). RNA helicases at work: Binding and rearranging. *Trends in Biochemical Sciences*, 36 (1), 19-29.

Jankowsky, E., & Bowers, H. (2006). Remodeling of ribonucleoprotein complexes with DExH/D RNA helicases. *Nucleic Acids Research*, 34 (15), 4181-4188.

Jankowsky, E., Gross, C. H., Shuman, S., & Pyle, A. M. (2000). The DExH protein NPH-II is a processive and directional motor for unwinding RNA. *Nature*, 403 (6768), 447-451.

Jeang, K.-T., & Yedavalli, V. (2006). Role of RNA helicases in HIV-1 replication. *Nucleic Acids Research*, 34 (15), 4198-4205.

Jori, F., & Bastos, A. D. S. (2009). Role of wild suids in the epidemiology of African swine fever. *EcoHealth*, 6 (2), 296-310.

Jouvenet, N., Monaghan, P., Way, M., & Wileman, T. (2004). Transport of African swine fever virus from assembly sites to the plasma membrane is dependent on microtubules and conventional kinesin. *Journal of Virology*, 78 (15), 7990-8001.

Jouvenet, N., Windsor, M., Rietdorf, J., Hawes, P., Monaghan, P., Way, M., & Wileman, T. (2006). African swine fever virus induces filopodia-like projections at the plasma membrane. *Cellular Microbiology*, 8 (11), 1803-1811.

Kärber, G. (1931). Beitrag zur kollektiven behandlung pharmakologischer reihenversuche. naunyn-schmiedebergs archiv fur experimentelle*. Pathologie Und Pharmakologie*, 162 (4), 480-483.

Käs, E., & Laemmli, U. K. (1992). *In vivo* topoisomerase II cleavage of the Drosophila histone

and satellite III repeats: DNA sequence and structural characteristics. *The EMBO Journal,* 11 (2)*,* 705-716.

Katoh, K., Rozewicki, J., & Yamada, K. D. (2017). MAFFT online service: multiple sequence alignment, interactive sequence choice and visualization. *Briefings in Bioinformatics*, 1-7.

Keita, D., Heath, L., & Albina, E. (2010). Control of African swine fever virus replication by small interfering RNA targeting the A151R and VP72 genes. *Antiviral Therapy*, 15 (5), 727-736.

King, D. P., Reid, S. M., Hutchings, G. H., Grierson, S. S., Wilkinson, P. J., Dixon, L. K., Bastos, A. D., & Drew, T. W. (2003). Development of a TaqMan® PCR assay with internal amplification control for the detection of African swine fever virus. *Journal of Virological Methods*, 107 (1), 53-61.

King, K., Chapman, D., Argilaguet, J. M., Fishbourne, E., Hutet, E., Cariolet, R., Hutchings, G., Oura, C. A., Netherton, C.L., Moffat, K., Taylor, G., Le Potier, M. F., Dixon, L. K., & Takamatsu, H. H. (2011). Protection of European domestic pigs from virulent African isolates of African swine fever virus by experimental immunisation. *Vaccine*, 29 (28), 4593-4600.

Koonin, E. V., & Yutin, N. (2010). Origin and evolution of eukaryotic large nucleo-cytoplasmic DNA viruses. *Intervirology*, 53 (5), 284-292.

Kreuzer, K. N. (1998). Bacteriophage T4, a model system for understanding the mechanism of type II topoisomerase inhibitors. *Biochimica et Biophysica Acta - Gene Structure and Expression*, 1400 (1-3), 339-347.

Kumar, S., Stecher, G., & Tamura, K. (2016). MEGA7: Molecular Evolutionary Genetics Analysis Version 7.0 for Bigger Datasets. *Molecular Biology and Evolution*, 33 (7), 1870-1874.

Kuraku, S., Zmasek, C. M., Nishimura, O., & Katoh, K. (2013). aLeaves facilitates on-demand exploration of metazoan gene family trees on MAFFT sequence alignment server with enhanced interactivity. *Nucleic Acids Research*, 41, (1), 22-28.

Lacasta, A., Monteagudo, P. L., Jiménez-Marín, Á., Accensi, F., Ballester, M., Argilaguet, J., Galindo-Cardiel, I., Segalés, J., Salas M. L., Domínguez, J., Moreno, A., Garrido, J. J., & Rodríguez, F. (2015). Live attenuated African swine fever viruses as ideal tools to dissect the mechanisms involved in viral pathogenesis and immune protection. *Veterinary Research*, 46 (135), 1-16.

Lam, A. M. I., & Frick, D. N. (2006). Hepatitis C virus subgenomic replicon requires an active NS3 RNA helicase. *Journal of Virology*, 80 (1), 404-411.

Laponogov, I., Pan, X. S., Veselkov, D. A., Mcauley, K. E., Fisher, L. M., & Sanderson, M. R. (2010). Structural basis of gate-DNA breakage and resealing by type II topoisomerases. *PloS One*, 5(6), e11338.

Laponogov, I., Sohi, M. K., Veselkov, D. A., Pan, X. S., Sawhney, R., Thompson, A. W.,

McAuley, K. E., Fisher, L. M., & Sanderson, M. R. (2009). Structural insight into the quinolone-DNA cleavage complex of type IIA topoisomerases. *Nature Structural and Molecular Biology*, 16, 667-669.

Le, S. Q., & Gascuel, O. (2008). An improved general amino acid replacement matrix. *Molecular Biology and Evolution*, 25 (7), 1307-1320.

Leitão, A., Cartaxeiro, C., Coelho, R., Cruz, B., Parkhouse, R. M. E., Portugal, F. C., Vigário, J. D., & Martins, C. L. V. (2001). The non-haemadsorbing African swine fever virus isolate ASFV/NH/P68 provides a model for defining the protective anti-virus immune response. *Journal of General Virology*, 82 (3), 513-523.

Lewis, T., Zsak, L., Burrage, T. G., Lu, Z., Kutish, G. F., Neilan, J. G., & Rock, D. L. (2000). An African swine fever virus ERV1-ALR homologue, 9GL, affects virion maturation and viral growth in macrophages and viral virulence in swine. *Journal of Virology*, 74 (3), 1275-1285.

Li, W., Tu, D., Brunger, A. T., & Ye, Y. (2007). A ubiquitin ligase transfers preformed polyubiquitin chains from a conjugating enzyme to a substrate. *Nature*, 446 (7133), 333-337.

Li, W., Tu, D., Li, L., Wollert, T., Ghirlando, R., Brunger, A. T., & Ye, Y. (2009). Mechanistic insights into active site-associated polyubiquitination by the ubiquitin-conjugating enzyme Ube2g2. *Proceedings of the National Academy of Sciences of the United States of America*, 106 (10), 3722-3727.

Linder, P., & Jankowsky, E. (2011). From unwinding to clamping - the DEAD box RNA helicase family. *Nature Reviews Molecular Cell Biology*, 12, 505-516.

Liu, L. F. (1994). *DNA topoisomerases: biochemistry and molecular biology*. J. August, M. Anders, F. Murad, J.Coyle (Eds.) Academic Press. pp320.

Lokhandwala, S., Waghela, S., Bray, J., Martin, C., Sangewar, N., Charendoff, C., Shetti, R., Ashley, C., Chen, C. H., Berghman, L. R., Mwangi, D., Dominowski, P. J., Foss, D. L., Rai, S., Vora, S., Gabbert, L., Burrage, T. G., Brake, D., Neilan, J., & Mwangi, W. (2016). Induction of robust immune responses in swine using a cocktail of adenovirus-vectored African Swine Fever Virus Antigens. *Clinical and Vaccine Immunology*, 23 (11), 888-900.

Lokhandwala, S., Waghela, S. D., Bray, J., Sangewar, N., Charendoff, C., Martin, C. L., Hassan, W. S., Koynarski, T., Gabbert, L., Burrage, T.G., Brake, D., Neilan, J., & Mwangi, W. (2017). Adenovirus-vectored novel African Swine Fever Virus antigens elicit robust immune responses in swine. *PloS One*, 12 (5), e0177007.

Louza, A. C., Boinas, F. S., Caiado, J. M., Vigario, J. D., & Hess, W. R. (1989). Role of vectors and animal reservoirs in the persistence of African swine fever in Portugal. *Epidemiologie et Sante Animale,* 15, 89-102.

Lubisi, B. A., Bastos, A. D. S., Dwarka, R. M., & Vosloo, W. (2005). Molecular epidemiology of African swine fever in East Africa. *Archives of Virology*, 150 (12), 2439-2452.

Lvov, D. K., Shchelkanov, M. Y., Alkhovsky, S. V., & Deryabin, P. G. (2015). *Single-Stranded RNA Viruses*. *Zoonotic Viruses in Northern Eurasia*. (Eds.) *Academic Press*. pp452.

Ma, Y., Yates, J., Liang, Y., Lemon, S. M., & Yi, M. (2008). NS3 Helicase domains involved in infectious intracellular hepatitis C virus particle assembly. *Journal of Virology*, 82 (15), 7624-7639.

Mackintosh, S. G., Lu, J. Z., Jordan, J. B., Harrison, M. K., Sikora, B., Sharma, S. D., Cameron, C. E., Raney, K. D., & Sakon, J. (2006). Structural and biological identification of residues on the surface of NS3 helicase required for optimal replication of the hepatitis C virus. *Journal of Biological Chemistry*, 281 (6), 3528-3535.

Malik, M., Hussain, S., & Drlica, K. (2007). Effect of anaerobic growth on quinolone lethality with *Escherichia coli*. *Antimicrobial Agents and Chemotherapy*, 51(1), 28-34.

Malmquist, W. A. (1963). Serologic and immunologic studies with African swine fever virus. *American Journal of Veterinary Research*, 24, 450-459.

Manso Ribeiro, J. (1962). Attenuation of African swine fever virus by tissue culture. *Bulletin de l'Office Internationale Des Épizooties*, 58, 1031-1040.

Manso Ribeiro, J., & Azevedo, J. A. (1961). La peste porcine africaine au Portugal. *Bulletin de l'Office Internationale Des Épizooties,* 56, 1212-1214.

Manso Ribeiro, J., Nunes Petisca, J. L., Lopes Frazão, F., & Sobral, M. (1963). African swine fever immunization. *l'Office Internationale Des Épizooties*, 60, 921-937.

Matsuo, E., Celma, C. C. P., Boyce, M., Viarouge, C., Sailleau, C., Dubois, E., Bréard, E., Thiéry, R., Zientara, S., & Roy, P. (2011). Generation of replication-defective virus-based vaccines that confer full protection in sheep against virulent *Bluetongue Virus* challenge. *Journal of Virology*, 85 (19),10213-10221.

McClendon, A. K., Rodriguez, A. C., & Osheroff, N. (2005). Human Topoisomerase IIα Rapidly Relaxes Positively Supercoiled DNA. *Journal of Biological Chemistry*, 280, 39337-39345.

Mebus, C. A., & Dardiri, A. H. (1980). Western Hemisphere isolates of African swine fever virus: asymptomatic carriers and resistance to challenge inoculation. *American Journal of Veterinary Research*, 41 (11),1867-1869.

Mebus, C. A., Dardiri, A. H., Hamdy, F. M., Ferris, D. H., Hess, W. R., & Callis, J. J. (1978). Some characteristics of African swine fever viruses isolated from Brazil and the Dominican Republic. *Proceedings, Annual Meeting of the United States Animal Health Association*, 82, 232-236.

Michaud, V., Randriamparany, T., & Albina, E. (2013). Comprehensive phylogenetic reconstructions of African swine fever virus: proposal for a new classification and molecular dating of the virus. *PloS One*, 8 (7), e69662.

Mirski, S. E. L., Gerlach, J. H., & Cole, S. P. C. (1999). Sequence determinants of nuclear localization in the α and β isoforms of human topoisomerase II. *Experimental Cell Research*, 251 (2), 329-339.

Mizuuchi, K., Fisher, L. M., O'Dea, M. H., & Gellert, M. (1980). DNA gyrase action involves the introduction of transient double-strand breaks into DNA. *Proceedings of the National Academy of Sciences*, 77 (4) 1847-1851.

Montgomery, R. E. (1921). A form of swine fever occurring in British East Africa (Kenya Colony). *Journal of Comparative Pathology*, *34*, 159-191.

Morrison, L. A, & Knipe, D. M. (1996). Mechanisms of immunization with a replication-defective mutant of herpes simplex virus 1. *Virology*, 220 (2), 402-413.

Mosesson, Y., Shtiegman, K., Katz, M., Zwang, Y., Vereb, G., Szollosi, J., & Yarden, Y. (2003). Endocytosis of receptor tyrosine kinases is driven by monoubiquitylation, not polyubiquitylation. *The Journal of Biological Chemistry*, 278 (24), 21323-21326.

Mottola, C., Freitas, F. B., Simões, M., Martins, C., Leitão, A., & Ferreira, F. (2013). *In vitro* antiviral activity of fluoroquinolones against African swine fever virus. *Veterinary Microbiology*, 165 (1-2), 86-94.

Moussa, M., Arrode-Brusés, G., Manoylov, I., Malogolovkin, A., Mompelat, D., Ishimwe, H., Smaoune, A., Ouzrout, B., Gagnon, J., & Chebloune, Y. (2015). A novel non-integrative single-cycle chimeric HIV lentivector DNA vaccine. *Vaccine*, 33 (19), 2273-2282.

Munoz, M., Freije, J. M., Salas, M. L., Vinuela, E., & Lopez-Otin, C. (1993). Structure and expression in *E. coli* of the gene coding for protein p10 of African swine fever virus. *Archives of Virology*, 130 (1-2), 93-107.

Mur, L., Iscaro, C., Cocco, M., Jurado, C., Rolesu, S., De Mia, G. M., Feliziani, F., Pérez-Sánchez, R., Oleaga, A., & Sánchez-Vizcaíno, J. M. (2016). Serological surveillance and direct field searching reaffirm the absence of *Ornithodoros Erraticus* ticks role in African Swine Fever cycle in Sardinia. *Transboundary and Emerging Diseases*, 64 (4), 1322-1328.

Mur, L., Martínez-López, B., & Sánchez-Vizcaíno, J. M. (2012). Risk of African swine fever introduction into the European Union through transport-associated routes: returning trucks and waste from international ships and planes. *BMC Veterinary Research,* 8, 149.

Nandi, D., Tahiliani, P., Kumar, A., & Chandu, D. (2006). The ubiquitin-proteasome system. *Journal of Biosciences*, 31 (1), 137–55.

Nei, M., & Kumar, S. (2000). *Molecular Evolutionand Phylogenetics*. *Archives of Virology* (Vol. 154) Oxford University Press, New York. pp333.

Neilan, J. G., Zsak, L., Lu, Z., Burrage, T. G., Kutish, G. F., & Rock, D. L. (2004). Neutralizing antibodies to African swine fever virus proteins p30, p54, and p72 are not sufficient for antibody-mediated protection. *Virology*, 319 (2), 337-342.

Nitiss, J. L. (2009a). DNA topoisomerase II and its growing repertoire of biological functions. *Nature Reviews Cancer*, 9, 327-337.

Nitiss, J. L. (2009b). Targeting DNA topoisomerase II in cancer chemotherapy. *Nature Reviews, Cancer*, 9 (5), 338-350.

O'Donnell, V., Holinka, L. G., Gladue, D. P., Sanford, B., Krug, P. W., Lu, X., Arzt, J., Reese, B., Carrillo, C., Risatti, G. R., & Borca, M. V. (2015). African Swine Fever Virus Georgia isolate harboring deletions of MGF360 and MGF505 genes is attenuated in swine and confers protection against challenge with virulent parental virus. *Journal of Virology*, 89 (11), 6048-6056.

Onisk, D. V., Borca, M. V., Kutish, S., Kramer, E., Irusta, P., & Rock, D. L. (1994). Passively Transferred African Swine Fever Virus Antibodies Protect Swine against Lethal Infection. *Virology*, 198 (1), 350-354.

Ortin, J., Enjuanes, L., & Vinuela, E. (1979). Cross-links in African swine fever virus DNA. *Journal of Virol*ogy, 31 (3), 579-583.

Ortin, J., & Viñuela, E. (1977). Requirement of cell nucleus for African swine fever virus replication in Vero cells. *Journal of Virology*, 21 (3), 902-905

Oura, C. A. L., Denyer, M. S., Takamatsu, H., & Parkhouse, R. M. E. (2005). *In vivo* depletion of CD8+ T lymphocytes abrogates protective immunity to African swine fever virus. *The Journal of General Virology*, 86 (9), 2445-2450.

Oura, C. A. L., Powell, P. P., Anderson, E., & Parkhouse, R. M. (1998). The pathogenesis of African swine fever in the resistant bushpig. *The Journal of General Virology*, 79 (6), 1439-1443.

Parrish, S., Hurchalla, M., Liu, S.-W. W., & Moss, B. (2009). The African swine fever virus g5R protein possesses mRNA decapping activity. *Virology*, 393 (1), 177-182.

Passmore, L. A, & Barford, D. (2004). Getting into position: the catalytic mechanisms of protein ubiquitylation. *The Biochemical Journal*, 379 (3), 513-525.

Pena, L., Yáñez, R. J., Revilla, Y., Viñuela, E., & Salas, M. L. (1993). African swine fever virus guanylyltransferase. *Virology*, 193 (1), 319-328.

Penrith, M. L., & Vosloo, W. (2009). Review of African swine fever: transmission spread and control. *Journal of the South African Veterinary Association*, 80 (2), 58-62.

Petroski, M. D., & Deshaies, R. J. (2005). Mechanism of lysine 48-linked ubiquitin-chain synthesis by the cullin-RING ubiquitin-ligase complex SCF-Cdc34. *Cell*, 123 (6), 1107-1120.

Pfaffl, M. W. (2001). A new mathematical model for relative quantification in real-time RT–PCR. *Nucleic Acids Research*, 29 (9), e45.

Piccininni, S., Varaklioti, A., Nardelli, M., Dave, B., Raney, K. D., & McCarthy, J. E. G. (2002). Modulation of the hepatitis C virus RNA-dependent RNA polymerase activity by the Non-Structural (NS) 3 helicase and the NS4b membrane protein. *Journal of Biological Chemistry*, 277, 45670-45679.

Portugal, R., Leitão, A., & Martins, C. (2009). Apoptosis in porcine macrophages infected *in vitro* with African swine fever virus (ASFV) strains with different virulence. *Archives of Virology*, 154 (9), 1441-1450.

Randow, F., & Lehner, P. J. (2009). Viral avoidance and exploitation of the ubiquitin system. *Nature Cell Biology*, 11 (5), 527-534.

Ranji, A., & Boris-Lawrie, K. (2010). RNA helicases: emerging roles in viral replication and the host innate response. *RNA Biology*, 7 (6), 775-787.

Reis, A. L., Abrams, C. C., Goatley, L. C., Netherton, C., Chapman, D. G., Sanchez-Cordon, P., & Dixon, L. K. (2016). Deletion of African swine fever virus interferon inhibitors from the genome of a virulent isolate reduces virulence in domestic pigs and induces a protective response. *Vaccine*, 34 (39), 4698-4705.

Roberts, P. C., Lu, Z., Kutish, G. F., & Rock, D. L. (1993). Three adjacent genes of African swine fever virus with similarity to essential poxvirus genes. *Archives of Virology*, 132 (3-4), 331-342.

Roca, J. (2004). The path of the DNA along the dimer interface of topoisomerase II. *Journal of Biological Chemistry*, 279, 25783-25788.

Roca, J., Berger, J. M., Harrison, S. C., & Wang, J. C. (1996). DNA transport by a type II two-gate mechanism topoisomerase : Direct evidence for a two-gate mechanism. *Proceedings of the National Academy of Science of the United States of America,* 93 (9) 4057-4062.

Rock, D. L. (2016). Challenges for African swine fever vaccine development—"… perhaps the end of the beginning." *Veterinary Microbiology*, 206, 52-58.

Rodríguez, I., Nogal, M. L., Redrejo-Rodríguez, M., Bustos, M. J., & Salas, M. L. (2009). The African swine fever virus virion membrane protein pE248R is required for virus infectivity and an early postentry event. *Journal of Virology*, 83 (23), 12290-12300.

Rodríguez, J. M., García-Escudero, R., Salas, M. L., & Andrés, G. (2004). African swine fever virus structural protein p54 is essential for the recruitment of envelope precursors to assembly sites. *Journal of Virology*, 78 (8), 4299-1313.

Rodríguez, J. M., Moreno, L. T., Alejo, A., Lacasta, A., Rodríguez, F., & Salas, M. L. (2015). Genome sequence of african swine fever virus BA71, the virulent parental strain of the nonpathogenic and tissue-culture adapted BA71V. *PloS One*, 10 (11), e0142889.

Rodríguez, J. M., & Salas, M. L. (2013). African swine fever virus transcription. *Virus Research*, 173 (1), 15-28.

Rodriguez, J. M., Salas, M. L., & Viñuela, E. (1992). Genes homologous to ubiquitin-conjugating proteins and eukaryotic transcription factor SII in African swine fever virus. *Virology*, 186 (1), 40-52.

Rojo, G., García-Beato, R., Viñuela, E., Salas, M. L., & Salas, J. (1999). Replication of African swine fever virus DNA in infected cells. *Virology*, 257 (2), 524-536.

Rouiller, I., Brookes, S. M., Hyatt, A. D., Windsor, M., & Wileman, T. (1998). African swine fever virus is wrapped by the endoplasmic reticulum. *Journal of Virology*, 72 (3), 2373-2387.

Rowlands, R. J., Michaud, V., Heath, L., Hutchings, G., Oura, C., Vosloo, W., Dwarka, R., Onashvili, T., Albina, E., & Dixon, L. K. (2008). African swine fever virus isolate, Georgia, 2007. *Emerging Infectious Diseases*, 14 (12), 1870-1874.

Sadowski, M., & Sarcevic, B. (2010). Mechanisms of mono- and poly-ubiquitination: Ubiquitination specificity depends on compatibility between the E2 catalytic core and amino acid residues proximal to the lysine. *Cell Division*, 5 (1), 19.

Salas, M. L., & Andrés, G. (2013). African swine fever virus morphogenesis. *Virus Research*, 173 (1), 29-41.

Salas, M. L., Kuznar, J., & Viñuela, E. (1981). Polyadenylation, methylation, and capping of the RNA synthesized *in vitro* by African swine fever virus. *Virology*, 113 (2), 484-491.

Salas, M. L., Kuznar, J., & Viñuela, E. (1983). Effect of rifamycin derivatives and coumermycin A1 on *in vitro* RNA synthesis by African swine fever virus. *Archives of Virology*, 77 (1), 77-80.

Salas, M. L., Rey-Campos, J., Almendral, J. M., Talavera, A., & Viñuela, E. (1986). Transcription and translation maps of african swine fever virus. *Virology*, 152 (1), 228-240.

Sánchez-Torres, C., Gómez-Puertas, P., Gómez-Del-Moral, M., Alonso, F., Escribano, J. M., Ezquerra, A., & Domínguez, J. (2003). Expression of porcine CD163 on monocytes/macrophages correlates with permissiveness to African swine fever infection. *Archives of Virology*, 148 (12), 2307-2323.

Sánchez-Vizcaíno, J. M., Arias, M., Zimmerman, J., Karriker, L. A., Ramirez, A., & Schwartz, K. J. (2012). *African Swine Fever. Diseases of swine*. United States of America: John Wiley and Sons.

Sánchez-Vizcaíno, J. M., Martínez-López, B., Martínez-Avilés, M., Martins, C., Boinas, F. S., Vial, L., Michaud, V., Jori, F., Etter, E., Albina, E., Roger, F. (2009). Scientific review on African Swine Fever. *EFSA Journal*, 6 (8), 1-141.

Sánchez-Vizcaíno, J. M., Mur, L., Gomez-Villamandos, J. C., & Carrasco, L. (2015). An update on the epidemiology and pathology of African Swine Fever. *Journal of Comparative Pathology*, 152 (1), 9-21.

Sánchez-Vizcaíno, J. M., Mur, L., & Martínez-López, B. (2013). African swine fever (ASF): five years around Europe. *Veterinary Microbiology*, 165 (1-2), 45-50.

Sánchez, E. G., Pérez-Núñez, D., & Revilla, Y. (2017). Mechanisms of entry and endosomal pathway of African Swine Fever Virus. *Vaccines*, *5* (4), 42.

Sánchez, E. G., Quintas, A., Pérez-Núñez, D., Nogal, M., Barroso, S., Carrascosa, Á. L., & Revilla, Y. (2012). African swine fever virus uses macropinocytosis to enter host cells. *PLoS Pathogens*, 8 (6), e1002754.

Schneider, S., & Schwert, B. (2001). Functional Domains of the Yeast Splicing Factor Prp22p. *Journal of Biological Chemistry*, 276, 21184-21191.

Schoeffler, A. J., & Berger, J. M. (2005). Recent advances in understanding structure-function relationships in the type II topoisomerase mechanism. *Biochemical Society Transactions*, 33 (6), 1465-1470.

Schoeffler, A. J., & Berger, J. M. (2008). DNA topoisomerases: harnessing and constraining energy to govern chromosome topology. *Quarterly Reviews of Biophysics*, 41 (1), 41-101.

Seissler, T., Marquet, R., & Paillart, J.-C. (2017). Hijacking of the ubiquitin/proteasome pathway by the HIV auxiliary proteins. *Viruses,* 9 (11), 322.

Servan de Almeida, R., Keita, D., Libeau, G., & Albina, E. (2007). Control of ruminant morbillivirus replication by small interfering RNA. *The Journal of General Virology*, 88 (8), 2307–2311.

Showalter, A. K., Byeon, I. J. L., Su, M. I., & Tsai, M. D. (2001). Solution structure of a viral DNA polymerase X and evidence for a mutagenic function. *Nature Structural Biology*, 8 (11), 942-946.

Shuman, S. (1992). Vaccinia virus RNA helicase: an essential enzyme related to the DE-H family of RNA-dependent NTPases. *Proceedings of the National Academy of Sciences of the United States of America*, 89 (22), 10935-10939.

Silva, G. M., Finley, D., & Vogel, C. (2015). K63 polyubiquitination is a new modulator of the oxidative stress response. *Nature Structural & Molecular Biology*, 22 (2), 116-123.

Simões, M., Martins, C., & Ferreira, F. (2015). Early intranuclear replication of African swine fever virus genome modifies the landscape of the host cell nucleus. *Virus Research*, 210, 1-7.

Simões, M., Rino, J., Pinheiro, I., Martins, C., & Ferreira, F. (2015). Alterations of nuclear architecture and epigenetic signatures during African swine fever virus infection. *Viruses*, 7 (9), 4978-4996.

Singh, N. P., McCoy, M. T., Tice, R. R., & Schneider, E. L. (1988). A simple technique for quantitation of low levels of DNA damage in individual cells. *Experimental Cell Research*, 175 (1), 184-91.

Sojka, D., Franta, Z., Horn, M., Caffrey, C. R., Mareš, M., & Kopáček, P. (2013). New insights into the machinery of blood digestion by ticks. *Trends in Parasitology*, 29 (6), 276-285.

Stokstad, E. (2017). Deadly virus threatens European pigs and boar: African swine fever outbreak alarms wildlife biologists and veterinarians. *Science*, 358 (6370), 1516-1517.

Stone, S., & Hess, W. (1967). Antibody response to inactivated preparations of African swine fever virus. *American Journal of Veterinary Research*, 28 (123), 475-481.

Suárez, C., Gutiérrez-Berzal, J., Andrés, G., Salas, M. L., & Rodríguez, J. M. (2010). African Swine Fever Virus protein p17 is essential for the progression of viral membrane precursors toward icosahedral intermediates. *Journal of Virology*, 84 (15), 7484-7499.

Sunwoo, S.Y., Pérez-Núñez, D., Morozov, I., Sánchez, G. E., Gaudreault, N. N., Trujillo, D. J., Mur, L., Nogal, M., Madden, D., Urbaniak, K., Kim, I. J., Ma, W., Revilla, Y., & Richt, A. J.

(2019). DNA-Protein Vaccination Strategy Does Not Protect from Challenge with African Swine Fever Virus Armenia 2007 Strain. *Vaccines,* 7 (1), 12.

Tabares, E., & Sánchez Botija, C. (1979). Synthesis of DNA in cells infected with African swine fever virus. *Archives of Virology*, 61 (1-2),49-59.

Takamatsu, H. H., Denyer, M. S., Lacasta, A., Stirling, C. M., Argilaguet, J. M., Netherton, C. L., Oura, C.A., Martins, C., & Rodríguez, F. (2013). Cellular immunity in ASFV responses. *Virus Research*, 173 (1),110-121.

Thomson, G. R. (1985). The epidemiology of African swine fever: the role of free-living hosts in Africa. *The Onderstepoort Journal of Veterinary Research*, 52 (3), 201-209.

Tulman, E. R., Delhon, G. A., Ku, B. K., & Rock, D. L. (2009). African swine fever virus. *Current Topics in Microbiology and Immunology*, 328, 43-87.

Utama, A., Shimizu, H., Hasebe, F., Morita, K., Igarashi, A., Shoji, I., Matsuura, Y., Hatsu, M.,Takamizawa, K.,Hagiwara, A., & Miyamura, T. (2000). Role of the DExH motif of the Japanese encephalitis virus and hepatitis C virus NS3 proteins in the ATPase and RNA helicase activities. *Virology*, 273 (2), 316-324.

Van de Weijer, M. L., Schuren, A. B. C., van den Boomen, D. J. H., Mulder, A., Claas, F. H. J., Lehner, P. J., Lebbink, R.J., & Wiertz, E. J.(2017). Multiple E2 ubiquitin-conjugating enzymes regulate human cytomegalovirus US2-mediated immunoreceptor downregulation. *Journal of Cell Science*, 130 (17), 2883-2892.

Vial, L., Wieland, B., Jori, F., Etter, E., Dixon, L., & Roger, F. (2007). African swine fever virus DNA in soft ticks, Senegal. *Emerging Infectious Diseases*, 13 (12), 1928-1931.

Vos, S. M., Tretter, E. M., Schmidt, B. H., & Berger, J. M. (2011). All tangled up: How cells direct, manage and exploit topoisomerase function. *Nature Reviews Molecular Cell Biology*, 12 (12), 827-841.

WAHID (2019). WAHID. WAHID database. Disease information. Retrieved from https://www.oie.int/wahis_2/public/wahid.php/Diseaseinformation/Immsummary.

Weissman, A. M. (2001). Themes and variations on ubiquitylation. *Nature Reviews Molecular Cell Biology*, 2 (3), 169-178.

Wieland, B., Dhollander, S., Salman, M., & Koenen, F. (2011). Qualitative risk assessment in a data-scarce environment: a model to assess the impact of control measures on spread of African Swine Fever. *Preventive Veterinary Medicine*, 99 (1), 4-14.

Wilkinson, P. J. J. (1984). The persistence of African swine fever in Africa and the Mediterranean. *Preventive Veterinary Medicine*, 2 (1-4), 71-82.

Wu, C. C., Li, T. K., Farh, L., Lin, L. Y., Lin, T. S., Yu, Y. J., Yen, T. J., Chiang, C. W., & Chan, N. L. (2011). Structural basis of type II topoisomerase inhibition by the anticancer drug etoposide. *Science*, 333 (6041), 459-462.

Wu, C. C., Li, Y. C., Wang, Y. R., Li, T. K., & Chan, N. L. (2013). On the structural basis and design guidelines for type II topoisomerase-targeting anticancer drugs. *Nucleic Acids*

Research, 41 (22), 10630-10640.

Wu, X., Hong, H., Yue, J., Wu, Y., Li, X., Jiang, L., Li, L., Li, Q., Gao, G., Yang, X. (2010). Inhibitory effect of small interfering RNA on dengue virus replication in mosquito cells. *Virology Journal*, 7 (270), 1-8.

Yáñez, R. J., Rodríguez, J. M., Boursnell, M., Rodriguez, J. F., & Viñuela, E. (1993). Two putative African swine fever virus helicases similar to yeast 'DEAH' pre-mRNA processing proteins and vaccinia virus ATPases D11L and D6R. *Gene*, 134 (2), 161-174.

Yáñez, R. J., Rodríguez, J. M., Nogal, M. L., Yuste, L., Enríquez, C., Rodriguez, J. F., & Viñuela, E. (1995). Analysis of the complete nucleotide sequence of African swine fever virus. *Virology*, 208 (1), 249-278.

Yang, Q., Del Campo, M., Lambowitz, A. M., & Jankowsky, E. (2007). DEAD-Box Proteins Unwind Duplexes by Local Strand Separation. *Molecular Cell*, 28 (2), 253-263.

Yang, Q., & Jankowsky, E. (2006). The DEAD-box protein Ded1 unwinds RNA duplexes by a mode distinct from translocating helicases. *Nature Structural and Molecular Biology*, 13 (11), 981-986.

Ye, C., Abraham, S., Wu, H., Shankar, P., & Manjunath, N. (2011). Silencing early viral replication in macrophages and dendritic cells effectively suppresses flavivirus encephalitis. *PloS One*, 6 (3), e17889.

Yutin, N., Colson, P., Raoult, D., & Koonin, E. V. (2013). Mimiviridae: Clusters of orthologous genes, reconstruction of gene repertoire evolution and proposed expansion of the giant virus family. *Virology Journal*, 10, 106.

Yutin, N., & Koonin, E. V. (2012). Hidden evolutionary complexity of Nucleo-Cytoplasmic Large DNA viruses of eukaryotes. *Virology Journal*, 9, 161.

Zanetti, G., Pahuja, K. B., Studer, S., Shim, S., & Schekman, R. (2011). COPII and the regulation of protein sorting in mammals. *Nature Cell Biology*, 14 (1), 20-28.

Zechiedrich, E. L., & Cozzarelli, N. R. (1995). Roles of topoisomerase IV and DNA gyrase in DNA unlinking during replication in *Escherichia coli*. *Genes and Developmen*t, 9 (22), 2859-2869

Zhang, F., Moon, A., Childs, K., Goodbourn, S., & Dixon, L. K. (2010). The African swine fever virus DP71L protein recruits the protein phosphatase 1 catalytic subunit to dephosphorylate eIF2alpha and inhibits CHOP induction but is dispensable for these activities during virus infection. *Journal of Virology*, 84 (20), 10681-1089.